

Methods for Considering the Effect of Non-uniformity Induced by Consolidation Process

September 2017

Department of Science and Advanced Technology
Graduate School of Science and Engineering
Saga University, Japan

YANG ZHOU

Methods for Considering the Effect of Non-uniformity Induced by Consolidation Process

*A dissertation submitted in partial fulfillment of the requirement for the degree of Doctor of
Philosophy in Geotechnical Engineering*

By

YANG ZHOU

Examination Committee: Prof. Jinchun Chai (Supervisor)
Prof. Takenori Hino
Associate Prof. Akira Sakai
Associate Prof. Daisuke Suetsugu

External Examiner: Prof. Jagdish Telangrao Shahu
(Department of Civil Engineering, IIT, Delhi)

Nationality: Chinese

Previous Degrees: Bachelor of Civil Engineering
Zhengzhou University, Zhengzhou, P.R. China

Master of Geotechnical Engineering
Hohai University, Nanjing, P.R. China

Scholarship Donor: SIPOP (Strategic International Postgraduate
Program)



Department of Science and Advanced Technology
Graduate School of Science and Engineering
Saga University, Japan
September 2017

ACKNOWLEDGEMENT

First and foremost I would like to express my appreciation and sincere gratitude to my advisor Professor Dr. Jinchun Chai for his continuous support and insightful suggestions throughout my 3-years' research. He has been a tremendous mentor for me and impressed on me the standard of work and the way of thinking deeply. Without him, I could not imagine how I can accomplish my PhD study.

Besides my advisor, I also would like to express my thanks to the examination committee members, Prof. Takenori Hino, Associate Prof. Akira Sakai, Associate Prof. Daisuke Suetsugu and external examiner, Prof. Jagdish Telangrao Shahu (Department of Civil Engineering, IIT, Delhi) for their valuable advice on the research work. I am grateful to Graduate School of Science and Engineering, Saga University for providing the SIPOP (Strategic International Postgraduate Program) scholarship to pursue this doctoral work. I would like to thank to the staff members of Department of Civil Engineering and Architecture, Mr. Akinori Saito and Mrs. Yasuko Kanada (former secretary of Prof. Chai) for their enthusiastic assistance on laboratory experiments and daily campus life, and staffs in International Division for their helps.

Furthermore, I want to express gratitude to my seniors, Dr. Fang Xu, Dr. Gaily Rondonuwu Steeva, Dr. Apichat Suddeepong, and Dr. Sailesh Shrestha for their patient help on academic problems. I would like to thank my friends, Mr. Haiqiang Liu, Mr. Pengxiang Huang, Mr. Nachanok Chanmee, Mr. Yitian Lu, Dr. Peng Wang and Mr. Nutthachai Prongmanee for bringing me precious joys and funs.

Finally, I am grateful to and my sister for always being there as a friend encouraging me over and over again and my fiancée, Xinyi Zhao for being by my side all the time. I would like to express special thanks to my father and my mother for their endless love, unconditional support and all of the sacrifices that they have made on my behalf. I am forever indebted to my parents for giving me the opportunities and experiences that have made me who I am. I dedicate this work to them.

ABSTRACT

Consolidation problem is an essential issue for geotechnical engineering. The current consolidation theories for both prefabricated vertical drains (PVD) induced horizontal radial consolidation and one-dimensional (1D) consolidation assumed that the coefficient of consolidation, c (c_v in vertical direction and c_h in the horizontal direction) of soil is a constant. However, for all soft clay deposits, c_v and/or c_h vary during the consolidation process. To consider this phenomenon, some researchers analyzed the consolidation problems incorporating the variation in compressibility and permeability (k) with void ratio (e), but assumed the soil domain is uniform. While for any consolidation problem, the consolidation is not uniform and the existing solutions are not able to consider this effect of non-uniform consolidation on the average degree of consolidation DOC. New methods are proposed to predict the average DOC considering the effect of non-uniform consolidation.

The variation of the void ratio and permeability in a soil domain under consolidation have been studied based on the results of laboratory model tests and Finite element analysis (FEA). The results indicated that the consolidation in the zone near the drainage boundary is much faster than that in the zone away from the drainage boundary.

It has been confirmed that the non-uniform consolidation has a considerable effect on the rate of consolidation. The effect is more significant in the earlier stage of consolidation. The factors influencing the effect of non-uniform consolidation are (a) initial void ratio (e_0), (b) compression index (C_c), (c) loading conditions and (d) the rate of variation of permeability with void ratio, and they were investigated quantitatively.

In the method for PVD induced consolidation, a concept of equivalent 'smear' effect, has been proposed to consider the effect of non-uniform consolidation. The value of $k_h/k_s)_e$ (k_h and k_s are the horizontal permeability in the undisturbed and smear zone of a PVD unit cell) can be evaluated quantitatively by a term, $\Delta e/C_k$. Δe is the stress increment induced reduction of void ratio calculated using basic soil properties and loading conditions, and C_k is a constant in Taylor's permeability (k) versus void ratio (e) relationship. In the method for 1D consolidation, the effect of non-uniform consolidation can be represented by a reduction factor, α and β for one soil layer system and two-soil layer system, respectively. α and β can be calculated using $\Delta e/C_k$ and $\Delta e_1/C_k$ respectively. And Δe_1 is the stress induced reduction of void ratio in soil layer-1 which contains the drainage boundary. The proposed

methods yielded very good predictions of measured DOCs when applied to some reported cases. It is recommended the proposed method can be used to analysis the average degree of consolidation considering the effect of non-uniform consolidation.

TABLE OF CONTENTS

ACKNOWLEDGEMENT	III
ABSTRACT	IV
TABLE OF CONTENTS	VI
LIST OF TABLES	X
LIST OF FIGURES	XI
LIST OF NOTATIONS	XIV
1 INTRODUCTION	1
1.1 Background	1
1.2 Objectives and scopes of the research	1
1.3 Organization of dissertation	2
2 REVIW ON PHENOMENON OF NON-UNIFORM CONSOLIDATION	4
2.1 Introduction	4
2.2 Theories for PVD induced consolidation	5
2.2.1 Parameters related to PVD induced consolidation	6
2.2.2 Average degree of consolidation	10
2.3 One dimensional consolidation	10
2.4 Consolidation theory for two-soil layer system	11
2.4.1 Effect of order of soil layer	11
2.4.2 Average degree of consolidation	13
2.5 Variation of coefficient of consolidation during consolidation process	15
2.5.1 Permeability changing with void ratio	15
2.5.2 Variation of coefficient of volume compressibility with stress	16
2.6 Non-uniform consolidation	16
2.6.1 Characteristics of PVD induced non-uniform consolidation	16
2.6.2 Characteristics of one-dimensional non-uniform consolidation	17
2.7 Researches needed	18
3 EFFECT OF NON-UNIFORM CONSOLIDATION ON PVD UNIT CELL	22
3.1 Introduction	22
3.2 Laboratory model tests	22
3.2.1 Test devices	22
3.2.2 Materials used in test	24

3.2.3 Test procedures	26
3.3 Test results and analysis	29
3.3.1 Settlement-time curves	29
3.3.2 Excess pore water pressure	31
3.3.3 Variation of water content and permeability ratio	32
3.3.4 Reduction of water content induced by installation of PVD	35
3.3.5 Summary and comments	36
3.4 Numerical investigation	36
3.4.1 Simulating model test	36
3.4.1.1 Model used	36
3.4.1.2 Evaluation of skin friction	39
3.4.1.3 Simulation results	39
3.4.1.4 Equivalent ‘smear’ effect due to non-uniform consolidation	41
3.4.2 Numerical experiments	43
3.4.2.1 Cases analysed	43
3.4.2.2 Effect of compressibility on non-uniform consolidation	45
3.4.2.3 Effect of stress ratio on non-uniform consolidation	46
3.4.2.4 Equivalent ‘smear’ effect and $\Delta e/C_k$	47
3.4.2.5 Summary and comments	48
3.5 Equivalent ‘smear’ effect approach	48
3.5.1 Proposed method	48
3.5.2 Application of proposed method	53
3.6 Summary	55
4 EFFECT OF NON-UNIFORM CONSOLIDATION ON ONE-DIMENSIONAL PROBLEM	56
4.1 Introduction	56
4.2 Experimental investigation	56
4.2.1 Test device and soil	56
4.2.2 Test procedure	58
4.2.3 Test results	60
4.3 Numerical investigation	61
4.3.1 Simulating model test	61
4.3.1.1 Model used	61

4.3.1.2 Simulation results	62
4.3.1.3 Analysis of average degree of consolidation	64
4.3.2 Influence of drainage length	65
4.3.3 Numerical simulation of incremental load oedometer test	67
4.3.4 Numerical experiments	70
4.3.4.1 Cases analysed	70
4.3.4.2 Effect of compressibility on non-uniform consolidation	72
4.3.4.3 Effect of stress ratio on non-uniform consolidation	73
4.3.4.4 Reduction for coefficient of consolidation and $\Delta e/C_k$	73
4.4 Experimental investigation on two-soil layer system	74
4.4.1 Test device and soil	75
4.4.2 Test procedure	76
4.4.3 Test results	77
4.5.1 Simulating the test	79
4.5.2 Simulation results	80
4.5.3 Analysis of the average degree of consolidation	81
4.5 Numerical Experiments	79
4.5.1 Cases analyzed	82
4.5.2 Effect of non-uniform consolidation	87
4.5.3 $\beta_1 \sim \Delta e_1/C_k$ relationship	88
4.6 Variation of the effect of non-uniform consolidation with DOC	91
4.6.1 One layer system	91
4.5.2 Two-layer system	93
4.7 Application of proposed method	95
4.7.1 One layer system	95
4.7.2 Two-soil layer system	99
4.8 Summary	101
4.8.1 One layer system	101
4.8.2 Two-soil layer system	102
5 CONCLUSIONS AND RECOMMENDATIONS	103
5.1 Conclusions	103
5.1.1 Effect of non-uniform consolidation on the rate of consolidation	103
5.1.2 Proposed method to predict the average degree of consolidation	104

5.2 Recommendations	106
REFERENCES	107

LIST OF TABLES

Table No.	Caption	Page
3.1	Properties of remoulded soil in PVD unit cell test	25
3.2	Parameters used for numerical simulations for Series 1	44
3.3	Parameters used for numerical simulations for Series 2a	44
3.4	Parameters used for numerical simulations for Series 2b	45
3.5	Parameters used for numerical simulations for Series 2c	45
3.6	Parameters used for numerical simulations for Series 3	45
3.7	Summary of case histories analysed	54
4.1	Properties of remoulded soil in model test	58
4.2	Parameters used for numerical simulations	66
4.3	The assumed conditions and results of two numerical oedometer tests	67
4.4	Parameters used for numerical simulations for Series 1	71
4.5	Parameters used for numerical simulations for Series 2	71
4.6	Properties of soil and loading conditions used in simulation	80
4.7	Parameters used in simulation for Series 1	83
4.8	Parameters used in simulation for Series 2	84
4.9	Parameters used in simulation for Series 3	86
4.10	Parameters used for the cases analyzed	99
4.11	Parameters used in FEA and theoretical analysis	100

LIST OF FIGURES

Figure No.	Caption	Page
1.1	Flowchart of this study	3
2.1	Unit cell of a PVD (after Xu 2015)	5
2.2	Drain patterns of PVD installation	6
2.3	Typical commercial band shaped PVDs (after Myint Win Bo et al.)	7
2.4	Assumed cases for two-layer system	12
2.5	Excess pore water pressure at impervious boundary (after Pyrah, 1996)	12
2.6	Soil profile for a two-layer system	13
2.7	Schematic layout of the test system (a) illustration of consolidometer and (b) photograph of consolidometers in a series (by Watabe et al. 2008)	17
2.8	Void ratio variation with elapsed time for each subspecimen (After Imai and Tang 1992)	18
2.9	Illustration of typical models for PVD induced consolidation	20
2.10	Illustration of typical models for 1D consolidation	21
3.1	Devices for model tests	23
3.2	Pore pressure transducer used in model test	24
3.3	Relationships between void ratio and permeability of soils tested	25
3.4	Picture of mini-PVD used in model tests	26
3.5	Photo of test device	27
3.6	Illustration of sampling points	28
3.7	Settlement-time curve for Case 1	30
3.8	Settlement-time curve for Case 2	30
3.9	Measured pore water pressure variation for Case 1	31
3.10	Measured pore water pressure variation for Case 2	32
3.11	Variations of water content with radial distance for Case 1	33
3.12	Variations of water content with radial distance for Case 2	34
3.13	Variations of permeability ratio with radial distance for Case 1	34
3.14	Variations of permeability ratio with radial distance for Case 2	35
3.15	Reduction of water content induced by installation of PVD	36

3.16	Model used in FEA	38
3.17	Comparison of settlement-time curve for Case 1	40
3.18	Comparison of settlement-time curve for Case 2	40
3.19	Comparison of average degrees of consolidation for Case 1	41
3.20	Comparison of average degrees of consolidation for Case 2	42
3.21	Relationship between $(k_h/k_s)_{e0}$ and C_c	46
3.22	Relationship between $(k_h/k_s)_{e0}$ and SR	43
3.23	Relationship between $(k_h/k_s)_{e0}$ and C_k	48
3.24	$(k_h/k_s)_{e1}/(k_h/k_s)_{e0}$ variation with D_e/d_w of unit cell	49
3.25	Variations of $(k_h/k_s)_e$ with T_h/μ	50
3.26	Comparison of average DOC for Case 1	52
3.27	Comparison of average DOC for Case 2	52
4.1	Illustration of device used in model test	57
4.2	Variation of permeability with void ratio	58
4.3	Photo of the model test	59
4.4	Measured settlement-time curve of model test	60
4.5	Measured pore water pressure at bottom for consolidation test	61
4.6	Model used in FEA	62
4.7	Comparison of settlement from FEA and model test	63
4.8	Comparison of pore pressure from FEA and test results	63
4.9	Average DOC from FEA and analytical results	65
4.10	Comparison of T_v versus DOC relationships for all cases	66
4.11	Comparing DOC_u and DOC_s of a load increment in IL consolidation test	68
4.12	Comparison of average DOC with elapsed time for N-1	69
4.13	Comparison of average DOC with elapsed time for N-2	70
4.14	Variation of the value of α_1 with the compression index, C_c	72
4.15	Variation of the value of α_1 with SR	73
4.16	Relationship between α_1 and $\Delta e/C_k$	74
4.17	Illustration of two soil layer system and equipment for model test	75
4.18	Relationship between permeability and void ratio	76
4.19	Photo of model test for two-soil layer system	77

4.20	Excess pore water pressure measured at the bottom of the soil layer	78
4.21	Measured settlement for each layers	78
4.22	The model and mesh used in simulation of model tests	79
4.23	Comparison of settlement from test and FEA	80
4.24	Comparison of pore pressure from test and FEA	81
4.25	Comparison of DOC from FEA and analytical results	82
4.26	Comparison of degree of consolidation	88
4.27	Variation of β_1 with $\Delta e_1/C_k$ for $m_{v1}:m_{v2}=0.67$	89
4.28	Variation of β_1 with $\Delta e/C_k$ for $m_{v1}:m_{v2}=1.0$	90
4.29	Variation of β_1 with $\Delta e/C_k$ for $m_{v1}:m_{v2}=1.5$	90
4.30	Relationship between α and time factor	92
4.31	Average DOC from FEA and analytical results	92
4.32	Comparison of average degree of consolidation	94
4.33	Comparison of average DOC for case of Watabe et al. (2007)	96
4.34	Comparison of average DOC for case of Davis and Raymond (1965)	97
4.35	Comparison of average DOC for case of Lehka (2003)	98
4.36	Comparison of DOC from different methods for case 1	100
4.37	Comparison of DOC from different methods for case 2	101
5.1	Relationship between $(k_h/k_s)_{e0}$ and $\Delta e/C_k$ (Fig. 3.22 bis)	105
5.2	Relationship between α_1 and $\Delta e/C_k$ (Fig. 4.16 bis)	105

LIST OF NOTATIONS

a	Width of a PVD
b	Thickness of a PVD
c	Coefficient of consolidation
c'	Effective cohesion
c_h	Coefficient of radial consolidation
c_v	Coefficient of vertical consolidation
c_{v1}	Coefficient of vertical consolidation in soil layer-1
c_{v2}	Coefficient of vertical consolidation in soil layer-2
C_c	Compression index
C_k	Rate of permeability changing with void ratio
C_s	Swell index
c_{vev}	Evaluated coefficient of vertical consolidation
c_{vin}	Input coefficient of vertical consolidation
D_e	Equivalent diameter of a unit cell
d_m	Equivalent diameter of a mandrel
d_s	Equivalent diameter of a smear zone
d_w	Equivalent diameter of a drain
e	Void ratio
e_0	Initial void ratio
G_s	Specific gravity
h_0	Initial thickness of model ground for 1D consolidation
H	Thickness of model ground for PVD consolidation
H_1	Coefficient of vertical consolidation in soil layer-1
H_2	Coefficient of vertical consolidation in soil layer-2
k	Permeability
k_0	Initial permeability corresponding to e_0
k_{200}	Permeability at a radial distance of 200 mm in a PVD unit cell
k_h	Permeability in the horizontal direction

k_{h0}	Initial permeability in the horizontal direction
k_r	Permeability at a radial distance of r mm in a PVD unit cell
k_s	Permeability in the smear zone
k_v	Permeability in the vertical direction
k_{v0}	Initial permeability in the vertical direction
k_{v1}	Permeability in soil layer-1
k_{v2}	Permeability in soil layer-2
K_0	Coefficient of at-rest earth pressure
K_0^{NC}	Coefficient of at-rest earth pressure for normal consolidated soil
l	Length of a drain
m_v	Coefficient of volumetric compressibility
m_{v1}	Coefficient of volumetric compressibility in soil layer-1
m_{v2}	Coefficient of volumetric compressibility in soil layer-2
M	The slope of critical state line
p'	Consolidation stress
p'_f	Final consolidation stress
p'_0	Initial consolidation stress
q	Deviator stress
q_w	Discharge drainage capacity of a PVD
r	Radial distance in a PVD unit cell
r_e	Radius of a PVD unit cell
r_w	Radius of a drain
S	Drain spacing
t	Elapsed time
t_i	i th sampling time
T_h	Time factor of radial consolidation
T_v	Time factor of vertical consolidation
T_{v50}	Time factor at degree of consolidation is 50%
z	depth
γ_w	Unit weight of water
Δe	Change of void ratio induced by consolidation

Δe_1	Change of void ratio induced by consolidation in soil layer-1
Δp	Incremental loading
Δt	Incremental time
$\Delta \varepsilon_v$	Incremental volumetric strain
μ	Parameters including the effect of drain spacing, smear and well resistance
σ	Total stress
σ'	Effective stress
σ'_{v0}	Initial vertical effective stress
ϕ'	Friction angle

CHAPTER ONE

INTRODUCTION

1.1 Background

All structures and geotechnical projects constructed on soft clayey deposit will face a consolidation problem. How to evaluate the rate of consolidation of soft ground is an extremely important issue during both designing and operation periods.

Terzaghi (1923) proposed one-dimensional consolidation theory, and Barron (1948) and Hansbo (1981) proposed solutions for radial consolidation induced by vertical drains. Their solutions are used widely all over the world for their simplicity. In both Terzaghi's and Hansbo's theories, it is assumed that the coefficient of consolidation, c (c_v in vertical direction and c_h in the horizontal direction) of soil is a constant. While for many soft clay deposits, c_v and/or c_h vary during the consolidation process. To consider this phenomenon, some researchers (e.g. Mesri and Rokhsar, 1974, etc.) analyzed the consolidation problems incorporating the variation in compressibility and permeability (k) with void ratio (e).

For any consolidation problem, the consolidation is not uniform. Near the drainage boundary, the rate of consolidation is faster than the zone far away, and the phenomenon is designated as non-uniform consolidation. Then the void ratio (e) and therefore the value of k in the zone near the drainage boundary will decrease rapidly which will hinder the rate of pore water flowing out through the drainage boundary. Because of the effect of non-uniform consolidation, the average rate of consolidation of soil domain will be reduced significantly.

The existing solutions mentioned above are not able to consider the effect of non-uniform consolidation on the average degree of consolidation (DOC). Therefore, there is a need to develop a method to evaluate the average rate of consolidation considering the effect of non-uniform consolidation.

1.2 Objectives and scopes of the research

This study focuses on investigating the effect of non-uniform consolidation on the rate of consolidation using both laboratory tests and numerical analyses. The main objective of this research is to develop a method to consider the effect of non-uniform consolidation on the average degree of consolidation (DOC). The objective has been achieved by the following steps:

(1) The effect of non-uniform consolidation

Laboratory tests were conducted and analyzed using existing theories. By comparing the results of tests and analysis, the effect of non-uniform consolidation on the rate of consolidation can be investigated.

(2) Factors influencing non-uniform consolidation

The factors influencing non-uniform consolidation, such as (a) initial void ratio (e_0), (b) compression index (C_c), (c) loading conditions and (d) the rate of variation of permeability with void ratio, (C_k) were investigated experimentally and analytically.

(3) Method for considering non-uniform consolidation

Based on the results of experimental and numerical investigation, methods for considering the effect of non-uniform consolidation into consolidation theories of prefabricated vertical drain (PVD) induced consolidation and one-dimensional (1D) consolidation have been proposed.

1.3 Organization of dissertation

This dissertation consists of five chapters. The flow chart of the research is shown in Fig. 1.1. Chapter One introduces the background, the objective and scopes of this study. Chapter Two reviews literatures about the theories of the PVD induced consolidation and 1D consolidation, and also some research results about the non-uniform consolidation up to date. Chapters Three and Four investigate the effect of non-uniform consolidation on the rate of consolidation through laboratory tests and numerical analyses, and based on the results, explicit methods have been proposed to consider the effect of non-uniform consolidation into consolidation theories for PVD induced consolidation and 1D consolidation, respectively. Chapter Five concludes this study and gives some recommendations for the future works.

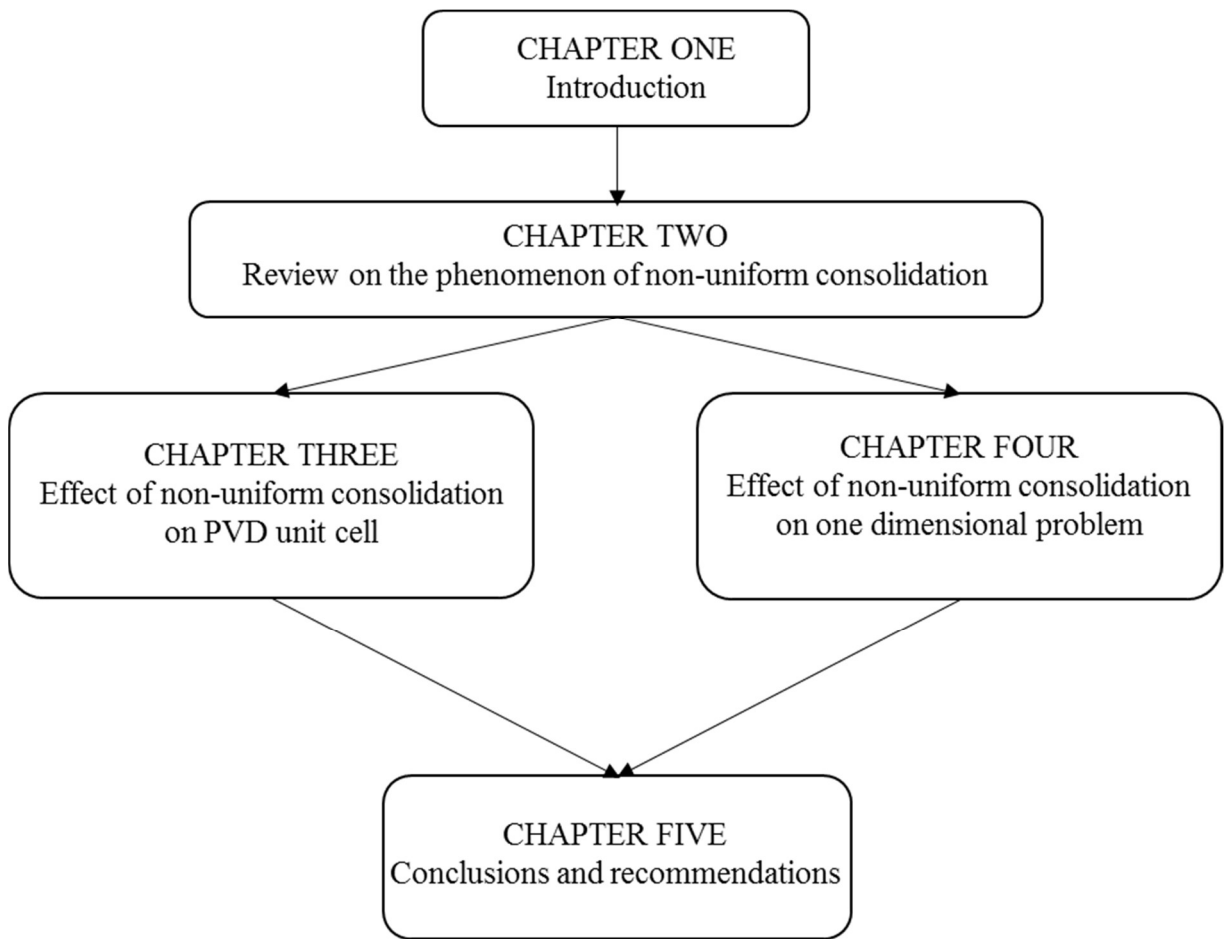


Figure 1.1 Flowchart of this research

CHAPTER TWO

REVIW ON PHENOMENON OF NON-UNIFORM CONSOLIDATION

2.1 Introduction

If an area with surcharge or structures loading is relatively large comparing with the thickness of the clayey deposit, the main consolidation effect will be due to vertical drainage of the deposit, and it is approximated as an one dimensional (1D) consolidation problem. In 1930s, the prefabricated vertical drains (PVDs) were introduced into the field practice (Hansbo, 1977). The drains allow the water to flow through the soil horizontally into the drain and drained out through the drain. For PVD induced consolidation, both vertical and radial drainage can influence its consolidation (Carrillo, 1942), while it is dominated by radial consolidation.

The mostly used theory for PVD induced consolidation is Hansbo's (1981) solution and for 1D consolidation is Terzaghi's (1923) solution. In both Hansbo's and Terzaghi's solutions, for a given geometrical condition, the rate of consolidation is mainly determined by a constant value of coefficient of consolidation (c) (in horizontal direction, c_h and in vertical direction, c_v).

During the consolidation of a soil domain, it is obvious that the coefficient of volume compressibility (m_v) and the coefficient of permeability (k) are not constant, and both of them decrease with the increase of effective stress (Schiffman, 1958; Davis and Raymond, 1965). It is well known that the coefficient of consolidation, c (c_h or c_v) is a function of permeability, k (k_h in horizontal direction and k_v in vertical direction) and coefficient of volumetric compressibility, m_v . The value of k and m_v may reduce during consolidation process, but the resulting value of c may be close to a constant, and it is argued that the Hansbo's or Terzaghi's solutions can still be used. However, it is only true if a domain is uniform. For most cases, even for an initial uniform domain, it will become non-uniform with the process of the consolidation.

Mesri and Rokhsar (1974), Basak and Madhav (1978), Lekha et al. (1998), etc., proposed some consolidation theories considering a linear variation of compressibility and permeability with void ratio (e) as well as coefficient of consolidation (c). However, in their theories the soil domain was treated as an uniform one throughout the consolidation process.

The consolidation near the drainage boundary will be much faster than the zone far away from the drainage boundary. As a result, the soil in the zone near the drainage boundary will have a higher degree of consolidation (DOC) and lower value of e and therefore k than the zone far away. Then for a non-uniform soil domain, the rate of consolidation is not uniquely controlled by c_h or c_v , but by k and m_v independently (Pyrah, 1996; Zhu and Yin, 1999; Chai et al., 2004; Lei et al., 2015). Some researchers noticed the influence of the non-uniform spatial distribution of soil properties on the average rate of consolidation (Gibson *et al.*, 1967; Xie and Leo, 2004). While up to date, there is no methods to consider the effect of non-uniform consolidation into consideration theories.

2.2 Theories for PVD induced consolidation

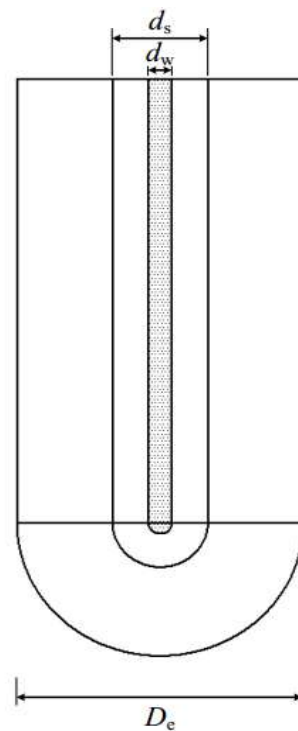
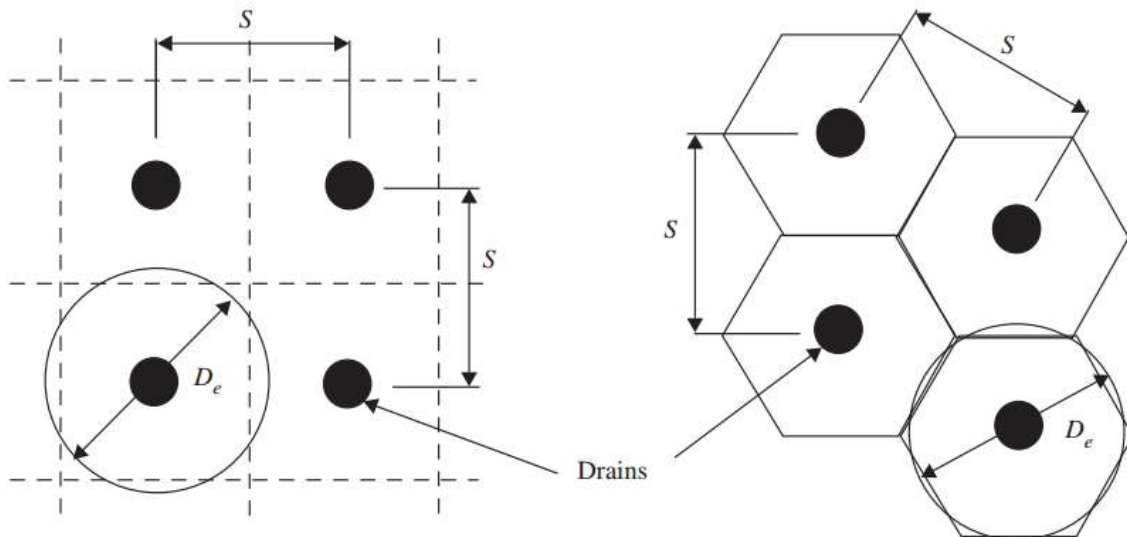


Figure 2.1 Unit cell of a PVD (after Xu 2015)

Preloading with installation of PVDs has become one of the most efficient and cost-effective soft clayey ground improvement technique and it is used worldwide (e.g. Chai et al., 2010; Pothiraksanon et al., 2010; Ghandeharioon et al., 2011; Karunaratne, 2011; Mesri and Khan, 2012; Deng et al., 2013; Oliveira, 2013; Chai et al., 2014; Parsa-Pajouh et al., 2014; Kim et al., 2014; Karim and Lo, 2015; Lu et al., 2015). Initially, PVDs were introduced into the practice in 1930s (Hansbo, 1977). The first theoretical solution for vertical drain consolidation for the unit cell (Fig. 2.1) condition (i.e., a single PVD surrounded by a soil cylinder) was proposed by Barron (1948). Further studies on the PVD unit cell behavior were made by several researches (Yoshikuni, 1979; Hansbo, 1981). It can be said that the basic theory for the design of the vertical drain improvement has been established (Chai and Miura 1999).

2.2.1 Parameters related to PVD induced consolidation

(a) Equivalent diameter of a unit cell, D_e



(a) Square pattern

(b) Triangular pattern

Figure 2.2 Drain patterns of PVD installation

The PVDs are normally installed into the soft deposits in square and triangular patterns (Barron, 1948; Hansbo, 1981) (Fig. 2.2). The equivalent diameter of a unit cell, D_e

represents the zone influenced by a PVD. The value of D_e for PVD installed in square pattern and triangular pattern can be calculated by Eq. (2.1) and (2.2) under equal area assumption, respectively.

$$D_e = 1.13S \tag{2.1}$$

$$D_e = 1.05S \tag{2.2}$$

where S is the drain spacing.

(b) Equivalent diameter of a drain, d_w

Instead of a circular cross-section which is assumed in the consolidation theory, the commercial PVDs are usually band-shaped (seen in Fig. 2.3). There is a need to convert the rectangular cross-section into an equivalent circular one.

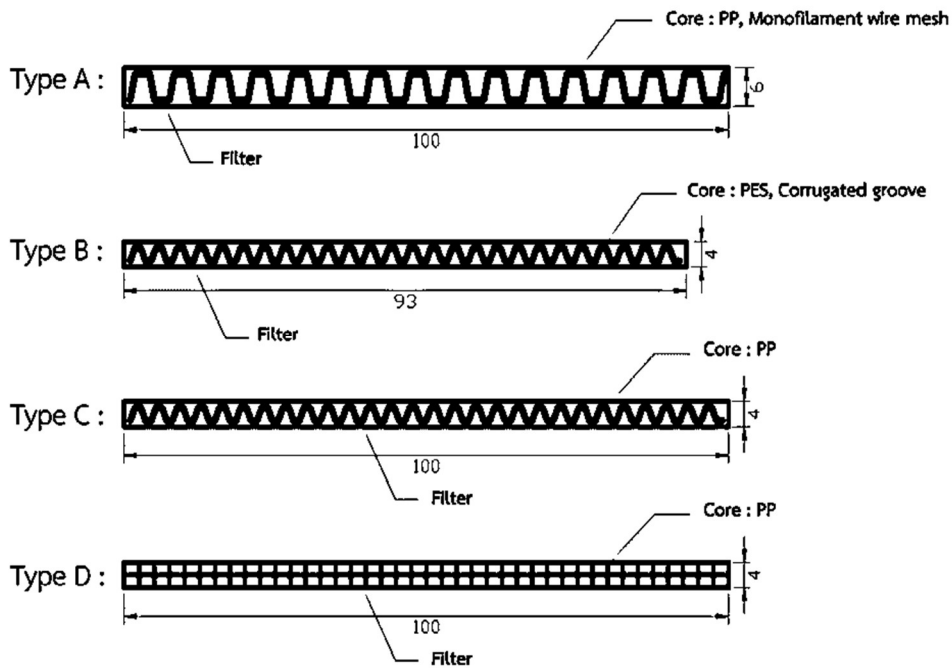


Figure 2.3 Typical commercial band shaped PVDs (after Myint Win Bo et al.)

Normally there are two methods for the conversion: (1) equal drainage perimeter (Hansbo 1979) and (2) equal drainage sectional area (Fellenius and Castonguay, 1985). The former assumes that the perimeter of the drain keeps the same before and after conversion. And the latter assumes the cross sectional area is the same. The value of d_w is

calculated by Eq. (2.3) for equal drainage perimeter method and Eq. (2.4) for the equal drainage sectional area method.

$$d_w = \frac{2(a+b)}{\pi} \quad (2.3)$$

$$d_w = \sqrt{\frac{4ab}{\pi}} \quad (2.4)$$

where a and b are the width and thickness of a band shaped drain. It was argued that the amount of water flowing into a PVD is mainly controlled by the contacting area between the PVD and the surrounding soil and therefore the equal drainage perimeter method is generally accepted.

Rixner et al. (1986) based on the results of finite element analysis, indicated that there is a “corner effect” for a rectangular shaped PVD, and the effective perimeter is less than $2 \times (a+b)$. Considering the “corner effect”, the following equation has been suggested for calculation of d_w :

$$d_w = \frac{a+b}{2} \quad (2.5)$$

(c) Smear zone

When installing a PVD, firstly a long metal mandrel together with a PVD inside is driven into the soft ground to a designed depth. Then the mandrel will be pulled out and leaves the PVD in the soft ground. During the insertion and withdrawing of the mandrel, the soil around the mandrel will be totally remolded, and the soil properties are also changed in this disturbed zone. This disturbed zone is called smear zone (Holtz and Holm, 1973; Akagi, 1977). There are two parameters for describing a smear zone, namely equivalent smear zone diameter, d_s and the permeability, k_s of the smear zone.

It was suggested by Hansbo (1981), the radius of the smear zone is 1.5 times the equivalent radius of the mandrel. Sharma and Xiao (2000) conducted laboratory experiments and reported that value of d_s/d_m was about 4, where d_m is the equivalent diameter of the mandrel. Most researches through numerous laboratory tests and finite element analyses (Barron, 1948; Bergado et al., 1991; Chai and Miura, 1999; Hird et al., 2000; Basu et al., 2007) shown that the value of $d_s = (1.5 \sim 3) d_m$. Indraratna and Redana (1998) concluded that the radius of the smear zone is 4 to 5 times the equivalent radius of drain, d_w .

A sediment soil is formed by gradually depositing thin horizontal soil layers. During this process, thin sand layers/seams can form in the deposit. At the micro level, planet clay particles tend to align in horizontal direction under the force of gravity, i.e., stress-induced microstructural anisotropy. As a result, most natural deposits exhibit anisotropic engineering properties. As for permeability, the value in the horizontal direction (k_h) is typically higher than that in the vertical direction (k_v).

Hansbo (1987) proposed that, due to the smear effect, the horizontal permeability in a smear zone (k_s) would reduce to a value identical to that in the vertical direction of a natural deposit. Thus, the value of $k_h/k_s = k_h/k_v$. The value of k_h/k_v are normally determined from laboratory test and can vary from 1 to 15 (Jamiokowski et al., 1983).

There were many other researches about determinations of the ratio of k_h/k_s . Based on laboratory tests, Bergado et al. (1991) reported that the value of k_h/k_s is about 2. Through experiments, Madhav et al. (1993) and Indraratna and Redana (1998) suggested that the value of $k_h/k_s = 1.6\sim 5$.

(d) Discharge capacity of a PVD, q_w

The well resistance of PVDs is caused by the finite discharge capacity (q_w) of PVDs. There are many factors influence the discharge capacity of a PVD (Holtz et al., 1991; Chai and Miura, 1999; Indraratna et al., 2005). Generally, for a given field condition, the influencing factors can be classified into: (1) geometry properties (including drainage length, effective cross-sectional area of the drainage channels), (2) filter behavior (clogging effect by fine soil particles entering the filter), and (3) possible air bubble trapped in the drainage channel.

Holtz et al. (1991) reported that the discharge capacity of a PVD could vary from 100-800 m^3 /year, and if under significant confining compression, values of q_w may reduce to 25-100 m^3 /year. Chai and Miura (1999) conducted long-term discharge capacity tests of PVD confined in clay, and they found that q_w reduced from an initial value of more than 200 m^3 /year to less than 50 m^3 /year with elapsed time about 100 days. Indraratna and Redana (2000) reported that long term q_w of a PVD can be reduced to 40-60 m^3 /year.

It was suggested if the discharge capacity of a PVD, q_w is larger than 100 m^3 /year and the drainage length is shorter than 15 m, the discharge capacity will not affect the rate of PVD induced consolidation significantly (Holtz et al., 1988, Indraratna et al., 2005).

2.2.2 Average degree of consolidation

The governing equation for horizontal radial consolidation is as:

$$\frac{\partial u}{\partial t} = c_h \left(\frac{1}{r} \frac{\partial u}{\partial r} + \frac{\partial^2 u}{\partial r^2} \right) \quad (2.6)$$

Where u is excess pore water pressure, c_h is the coefficient of consolidation in horizontal direction which is a constant during consolidation, t is the consolidation time and r is the radial distance from the center of the drain. The solution for average degree of consolidation (U_h) of PVD induced consolidation considering the smear effect and well resistance proposed by Hansbo (1981) is as follow:

$$U_h = 1 - \exp\left(-\frac{8T_h}{\mu}\right) \quad (2.7)$$

where T_h is the time factor and μ is a parameter including the effect of drain spacing, smear and well resistance. T_h can be calculated by Eq. (2.8):

$$T_h = \frac{c_h t}{D_e^2} \quad (2.8)$$

The value of μ can be obtained by Eq. (2.9):

$$\mu = \ln\left(\frac{D_e}{d_w}\right) - 0.75 + \left(\frac{k_h}{k_s} - 1\right) \ln\left(\frac{d_s}{d_w}\right) + \frac{2\pi l^2 k_h}{3q_w} \quad (2.9)$$

where l is the drainage length of a PVD.

2.3 One dimensional consolidation

In 1923, Terzaghi proposed the theory for one dimensional (1D) consolidation, and the theory played an important role in soil mechanics since then. This theory basically assumed the soil is a homogeneous elastic porous medium and fully saturated, the fluid is incompressible. The flow of fluid follows Darcy's law and the flow only occurs in the vertical direction as well as the deformation.

For a given soil element, the difference of the net rate of water flow out or into the soil elements should be equal to the rate of change of volume of the soil. The basic differential equation is:

$$\frac{\partial u}{\partial t} = c_v \frac{\partial^2 u}{\partial z^2} \quad (2.10)$$

where u is excess pore water pressure, z is depth, and c_v is the coefficient of consolidation. In Terzaghi's theory, the value of c_v remains constant during the consolidation.

For constant instantaneously applied load during consolidation, the solution for Eq. (2.10) is:

$$u = \sum_{m=0}^{m=\infty} \frac{2u_0}{M} \sin\left(\frac{Mz}{H}\right) \exp(-M^2 T_v) \quad (m \text{ is an integer}) \quad (2.11)$$

where u_0 is the initial excess pore water pressure, $M = \frac{\pi}{2}(2m+1)$, H = drainage length and T_v is the time factor and can be calculated by Eq. (2.12).

$$T_v = \frac{c_v t}{H^2} \quad (2.12)$$

Finally, the average degree of consolidation (DOC), U_v of the 1D consolidation from Terzaghi's solution is:

$$U_v = 1 - \sum_{m=0}^{m=\infty} \frac{2}{M^2} \exp(-M^2 T_v) \quad (2.13)$$

2.4 Consolidation theory for two-soil layer system

In the fields, generally the soil deposits are not uniform, but stratified. During a consolidation process, if the domain becomes non-uniform, its behavior will be analogue to a two-soil layer system. Therefore, the consolidation theory for two-soil layer system is reviewed here.

2.4.1 Effect of order of soil layer

Pyrah (1996) showed that for a two soil layer system under one-way drainage condition, even the values of c_v of the two soil layers are the same, but if the values of k_v and m_v are different, the rate of consolidation will be significantly influenced by the order of soil layers. Consider two cases of a two-layer system as shown in Fig. 2.4, soil A has lower value of k_v and m_v , and the value of k_v and m_v for soil B are 10 times of that of soil

A. While the coefficient of consolidation is same with each other. Based on the order of the soil layer, the two cases are designated as A/B and B/A case, respectively.

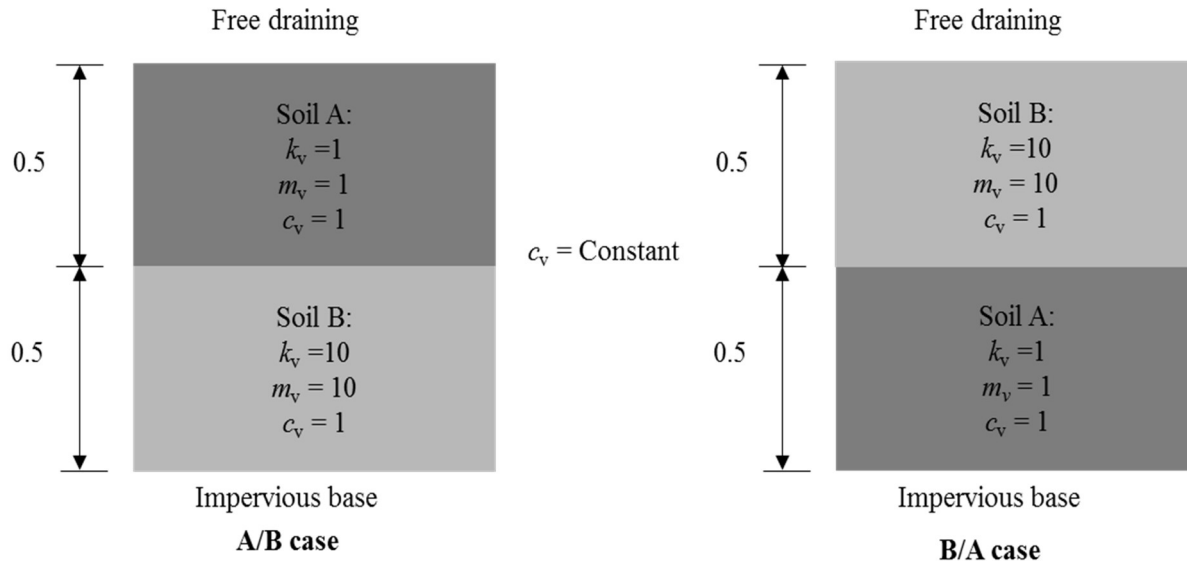


Figure 2.4 Assumed cases for two-layer system

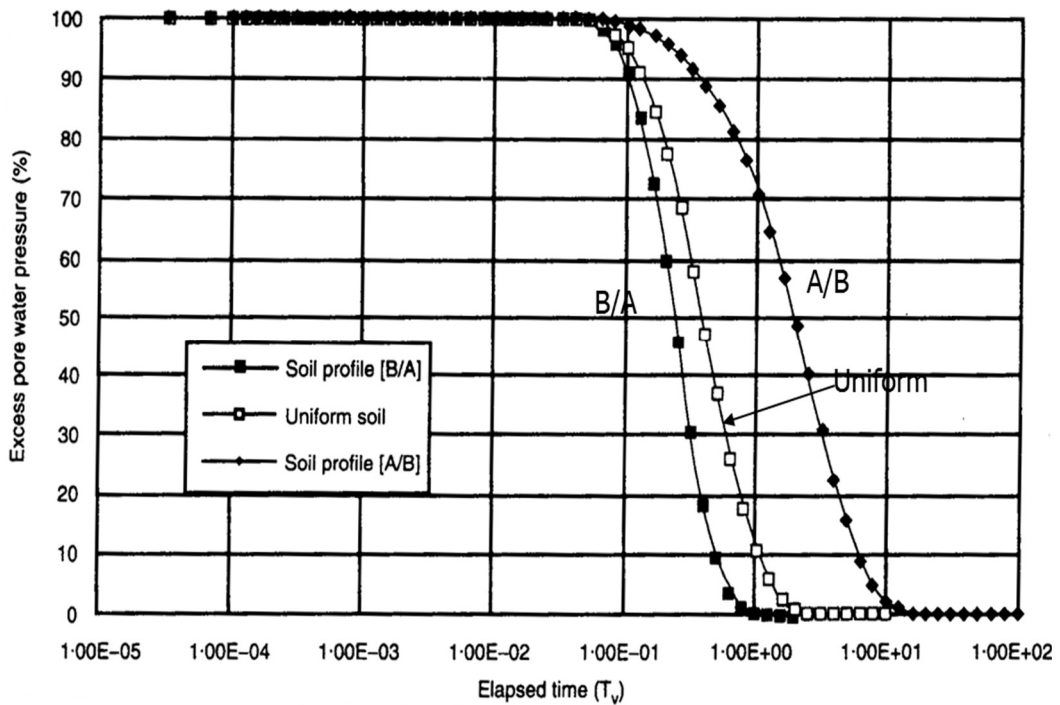


Figure 2.5 Excess pore water pressure at impervious boundary (after Pyrah, 1996)

The two cases were simulated by Pyrah (1996) using finite element analysis (FEA) together with a uniform soil domain which has a same value of c_v . The excess pore water pressure at the bottom of the soil are plotted in Fig. 2.5. The orders of the soil layers have a clear effect on the rate of consolidation. For the case A/B, the layer with lower values of k_v and m_v located at the drainage boundary, the rate of the consolidation of the system will be quite lower than the reverse order.

2.4.2 Average degree of consolidation

Several researches reported the analytical solutions of consolidation of a two-layer system (Zhu and Yin 1999; Xie et al. 2002). The soil profile for a two-layer system is shown in Fig. 2.6.

The governing equation for the consolidation of a two-soil layer system is:

$$\frac{\partial u}{\partial t} = \begin{cases} c_{v1} \frac{\partial^2 u}{\partial z^2} + \frac{\partial \sigma}{\partial t} & 0 \leq z \leq H_1 \\ c_{v2} \frac{\partial^2 u}{\partial z^2} + \frac{\partial \sigma}{\partial t} & H_1 \leq z \leq H \end{cases} \quad (2.14)$$

where σ is the vertical total stress.

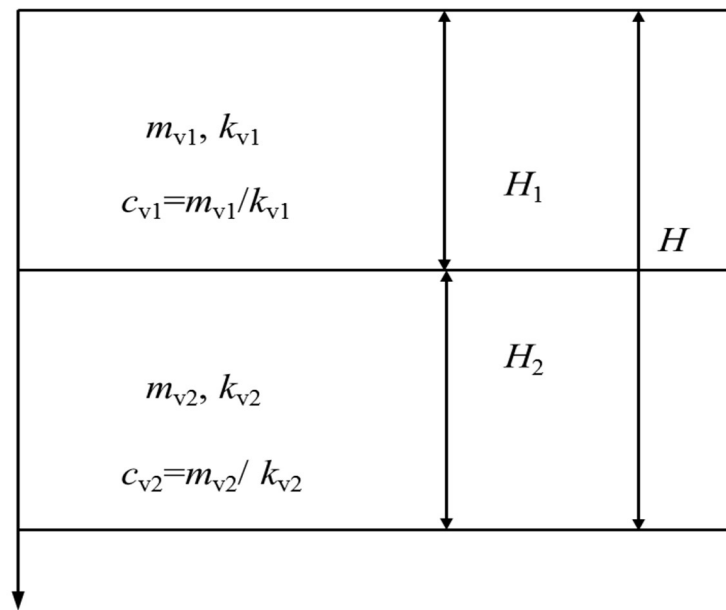


Figure 2.6 Soil profile for a two-layer system

The average degree of consolidation for a two-layer system subjected to an instantaneously applied constant load was given by the following equation (Zhu and Yin 1999):

$$U_v = 1 - \sum_{n=0}^{n=\infty} \frac{c_n}{\lambda_n^2} \exp(-\lambda_n^2 T_v) \quad (n=1, 2, 3\cdots) \quad (2.15)$$

where c_n is a function of m_{v1} , m_{v2} , H_1 , H_2 , α , β and λ_n , in which:

$$\alpha = \frac{H_1 \sqrt{c_{v2}}}{H_1 \sqrt{c_{v2}} + H_2 \sqrt{c_{v1}}} \quad (2.16)$$

$$\beta = \frac{H_2 \sqrt{c_{v1}}}{H_1 \sqrt{c_{v2}} + H_2 \sqrt{c_{v1}}} \quad (2.17)$$

and λ_n is the n th positive root of the Eq. (2.18) and Eq. (2.19) for two-way and one-way drainage, respectively:

$$\sin \lambda + p \sin(q \lambda) = 0 \quad (2.18)$$

$$\cos \lambda - p \cos(q \lambda) = 0 \quad (2.19)$$

where p is:

$$p = \frac{\sqrt{k_{v2} m_{v2}} - \sqrt{k_{v1} m_{v2}}}{\sqrt{k_{v2} m_{v2}} + \sqrt{k_{v1} m_{v2}}} \quad (2.20)$$

and q is:

$$q = \frac{H_1 \sqrt{c_{v2}} - H_2 \sqrt{c_{v1}}}{H_1 \sqrt{c_{v2}} + H_2 \sqrt{c_{v1}}} \quad (2.21)$$

c_n finally can be expressed as:

$$c_n = \frac{2 [H_1 m_{v1} \beta \sin(\lambda_n \beta) + H_2 m_{v2} \alpha \sin(\lambda_n \alpha)]^2}{\alpha^2 \beta^2 (H_1 m_{v1} + H_2 m_{v2}) [H_1 m_{v1} \sin^2(\lambda_n \beta) + H_2 m_{v2} \sin^2(\lambda_n \alpha)]} \quad (2.22)$$

for two-way drainage, and

$$c_n = \frac{2 [H_1 m_{v1} \cos(\lambda_n \beta)]^2}{\alpha^2 (H_1 m_{v1} + H_2 m_{v2}) [H_1 m_{v1} \cos^2(\lambda_n \beta) + H_2 m_{v2} \sin^2(\lambda_n \alpha)]} \quad (2.23)$$

for one-way drainage. And T_v is as:

$$T_v = \frac{c_{v1} c_{v2} t}{H_1 \sqrt{c_{v2}} + H_2 \sqrt{c_{v1}}} \quad (2.24)$$

2.5 Variation of coefficient of consolidation during consolidation process

The value of c (c_h or c_v) is a function of k and m_v :

$$c = \frac{k}{m_v \gamma_w} \quad (2.25)$$

where γ_w is the unit weight of water. For radial consolidation induced by PVD, k is taken as k_h and for vertical consolidation, k is taken as k_v .

2.5.1 Permeability changing with void ratio

Many researchers made great efforts in measuring the permeability of soils using different methods (e.g., Carrier and Bechman, 1984; Dolinar, 2009; Leroueil et al., 1990; Nagaraj et al., 1993; Samarasinghe et al., 1982; Tavenas et al., 1983a; b; Taylor, 1948; Zeng et al., 2011). Taylor (1948) proposed a linear relationship between the void ratio, e , and the logarithm of permeability, $\log(k)$:

$$k = k_0 10^{\frac{e-e_0}{C_k}} \quad (2.26)$$

where k_0 and e_0 are the initial permeability and void ratio, respectively; C_k is a constant representing the rate of change of permeability with e . After large amount of tests on the undisturbed soil samples with natural water content, Tavenas (1983a, b) gave the range of the value of $C_k = (0.4 \sim 0.6)e_0$. Taylor's equation is the most widely used approximation to describe the variation of k with e .

It was suggested by numerous researchers (e.g. Berilgen et al., 2006; Raymond, 1966; Siddique and Safiullah, 1995; Zeng et al., 2011) that Taylor's (1948) equation is also suitable to remolded clay. It was further pointed out by Zeng et al. (2011) that the relationship between k and e for remolded clay and undisturbed clay are almost identical.

The Seepage Induced Consolidation tests initially proposed by Imai (1979) and reported by many other researchers (e.g., Abu-Hejleh et al., 1996; Berilgen et al., 2006; Fox et al., 1997; Huerta et al., 1988) to study the permeability of extra soft slurry under very small loadings. The results shown that the Taylor's (1948) equation can be applied to very soft clayey deposits with very high water content.

2.5.2 Variation of coefficient of volume compressibility with stress

Except for permeability, coefficient of volume compressibility is another important factor on determination of coefficient of consolidation (c) from Eq. (2.25). The definition of m_v is:

$$m_v = \frac{\Delta \varepsilon_v}{\Delta p} \quad (2.27)$$

where $\Delta \varepsilon_v$ and Δp are incremental volumetric strain and corresponding incremental loading, respectively. The value of m_v from incremental load (IL) oedometer test in fact is an average value corresponding to a loading increment.

It is well known the stress-strain behavior of clayey soil is more likely following a linear e - $\log(p')$ relationship. In normally consolidation range, m_v can be calculated as:

$$m_v = \frac{C_c}{2.3(1+e)\sigma'} \quad (2.28)$$

where C_c is compression index and σ' is the effective consolidation stress. For over-consolidated soil, C_c should be replaced by swelling index (C_r) in Eq. (2.28). During consolidation process, although both the values of e and σ' changes, the value of m_v reduces with increases of σ' , and as a result, the coefficient of volume compressibility (m_v) will decrease in the consolidation process.

2.6 Non-uniform consolidation

2.6.1 Characteristics of PVD induced non-uniform consolidation

After the onset of PVD consolidation on an initially uniform soil domain, in the zone near the PVD, the soil will be consolidated faster and resulted in smaller void ratio, and therefore lower permeability (k). While the zone near the periphery of a PVD unit cell may need longer time to be consolidated. As a result, the values of k and m_v in the zone near the PVD will be lower than that at the periphery locations.

This non-uniformity of soil domain induced by PVD consolidation was reported by several researchers (Hird and Moseley, 2000; Sharma and Xiao, 2000; Indraratna et al., 2015; Chai and Rondonuwu, 2015). For a filed project, even a few days after the installation of PVDs and before the surcharge load application, due to local consolidation

from the dissipation of excess pore water pressure induced by the PVD installation, the soil in the zone near PVD had a lower water content (smaller e) than the soil in the zone far-away from PVD (Indraratna et al., 2015). Some researchers attributed this phenomenon of low permeability near drainage boundary to smear effect in consolidation analysis. While the definition of ‘smear’ is ‘to spread a soft substance over a surface in a rough or careless way’. Based on this definition, the effect of local consolidation induced permeability reduction can not be classified as an effect of mechanical smear.

2.6.2 Characteristics of one-dimensional non-uniform consolidation

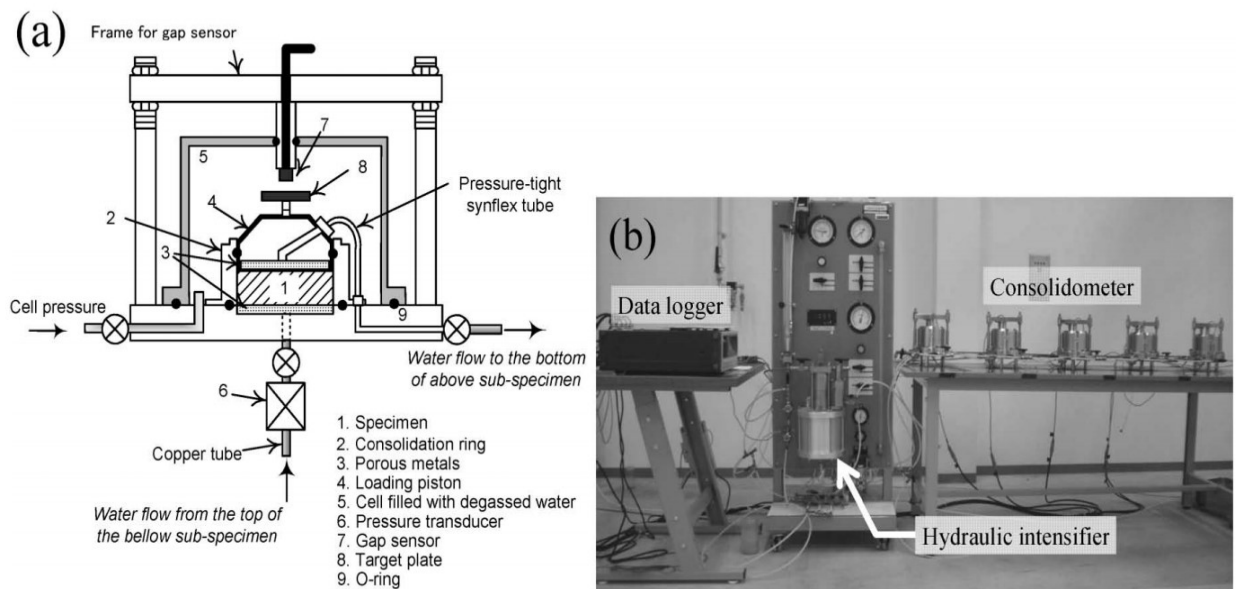


Figure 2.7 Schematic layout of the test system (a) illustration of consolidometer and (b) photograph of consolidometers in a series (by Watabe et al. 2008)

The phenomenon of 1D non-uniform consolidation was reported by some researches (e.g. Imai and Tang, 1992; Tanaka, 2005; Watabe et al., 2008). They conducted a series of “inter-connect” one-dimensional consolidation tests and the “total” specimen of the consolidation tests consisted of several subspecimens with 15 or 25 mm in height and 60 mm in diameter. Each subspecimen with the same soil properties was set into a consolidometer, and inter-connected in a series by copper tube to allow the water flowing freely between each other. The water finally and only can be drained out though the top

surface of the first subspecimen. The equal pressure can be applied on each subspecimen and the settlement of each subspecimen was recorded. Through this way, consolidation test on a soil sample with a larger thickness was simulated, and the excess pore water pressure and the compression of each subspecimen were monitored. The schematic layout of the test system can be seen in Fig. 2.7.

Imai and Tang (1992) conducted this kind of tests on reconstituted samples of Yokohama Bay mud with high initial water content. The void ratio variations with elapsed time for each subspecimen was drawn and shown in Fig. 2.8. Near the drainage boundary (subspecimen 1), the void ratio reduced most rapidly and converged with others at the final stage. Watabe et al. (2008) obtained similar results by plotting the vertical strain variation with elapsed time.

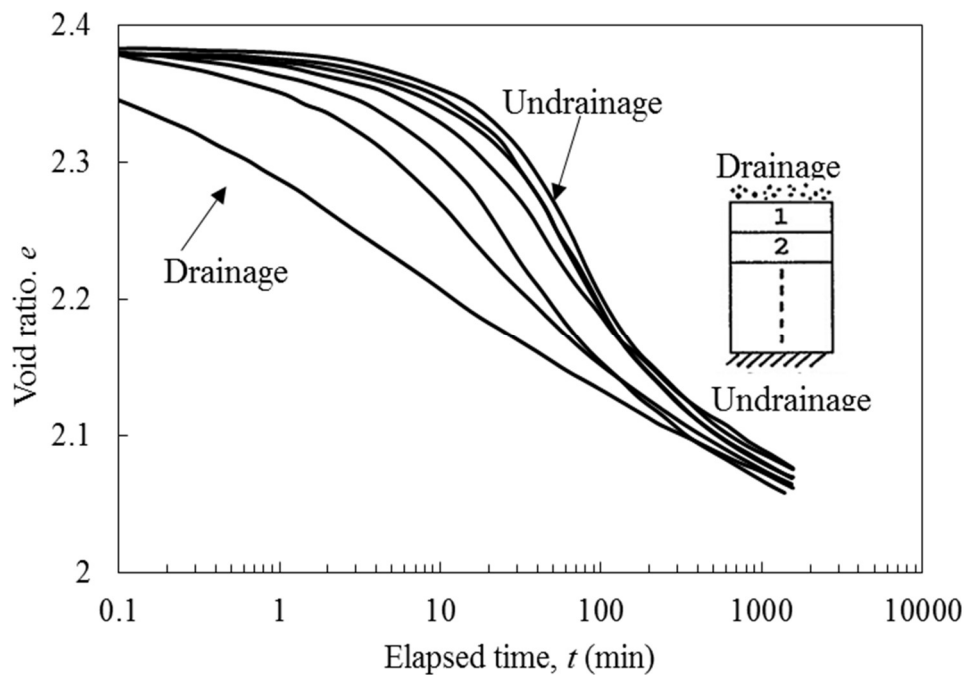


Figure 2.8 Void ratio variation with elapsed time for each subspecimen (After Imai and Tang 1992)

2.7 Researches needed

There are three typical consolidation models according to different assumptions about the changing permeability (k) and compressibility (m_v) during consolidation process.

These three models are illustrated in Fig. 2.9 and 2.10 for radial consolidation and 1D consolidation, respectively.

For radial consolidation:

(a) Linear model: the coefficient of consolidation (c_h) keeps constant during consolidation process as well as the ratio of k_h/k_s . Under this condition, the Hansbo's (1981) solution is valid.

(b) Non-linear model: the coefficient of consolidation (c_h) is changing with consolidation as a result of variation permeability (k) and coefficient of volume compressibility (m_v) alone reduction of void ratio. The ratio of k_h/k_s is constant. But this model still assumes that the PVD unit cell is a uniform one. Numerous researches (Zhuang et al., 2005; Geng et al., 2012; Lu et al., 2015) were conducted adopting this model.

(c) Non-uniform model: both the coefficient of consolidation (c_h) and the ratio of k_h/k_s is changing with time (t) and location (r). Up to date, there is no theories for this kind of model.

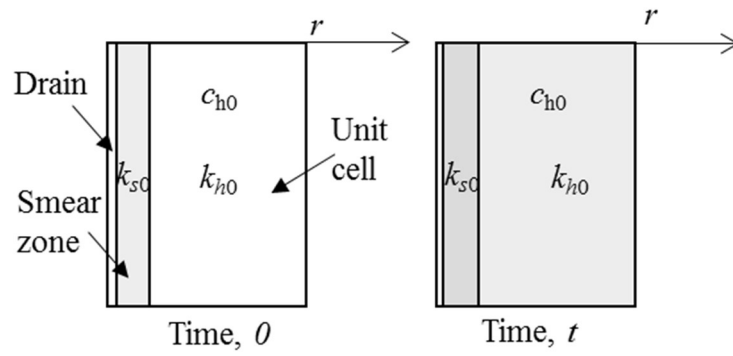
For one-dimensional consolidation:

(a) Linear model: the coefficient of consolidation (c_v) keeps constant during consolidation process. Terzaghi's (1923) solution adopts this assumption.

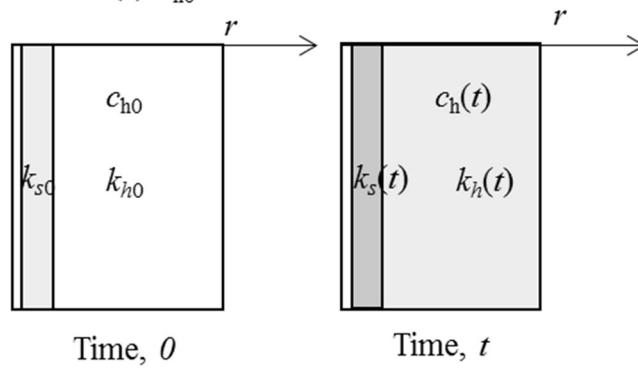
(b) Non-linear model: the k and m_v changes with void ratio, but the soil domain is regarded as a uniform one. Many researchers (Schiffman, 1958; Davis and Raymond, 1965) studied this kind of model and proposed some solutions.

(c) Non-uniform model: the k and m_v changes with time (t) and depth (z). No existing solutions considered this model until now.

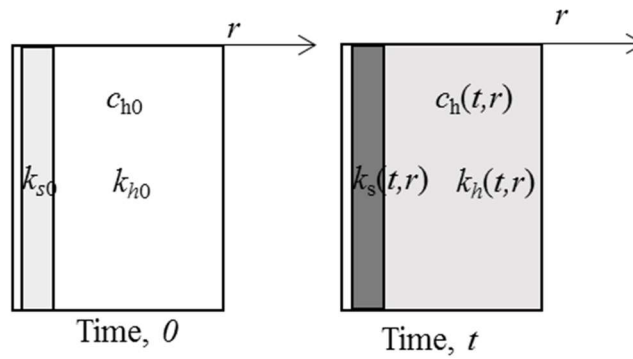
With above discussion, it is clear that models (c) in Figs. 2.9 and 2.10 are more realistic, and certainly there is a need to develop consolidation theory for these models.



(a) c_{h0} is constant with time

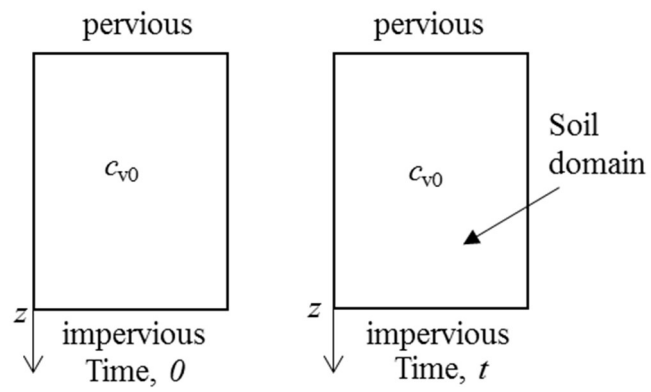


(b) $c_h(t)$ varies with time

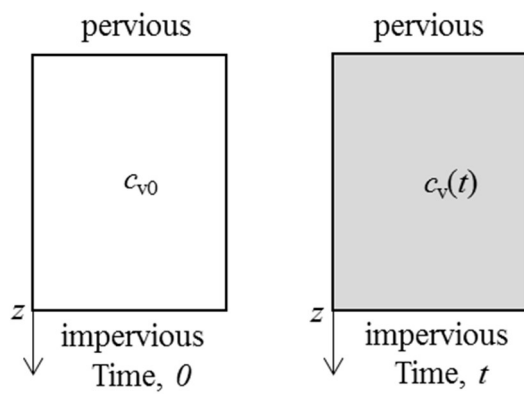


(c) $c_h(t,r)$ varies with time and radial distance

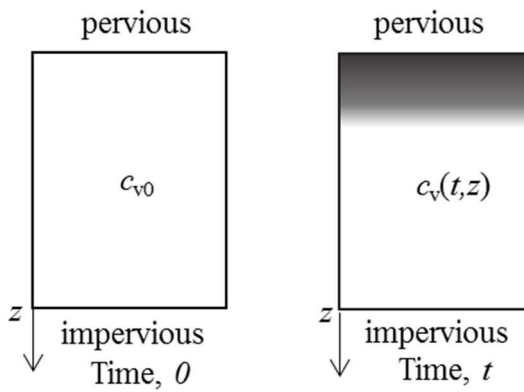
Figure 2.9 Illustration of typical models for PVD induced consolidation



(a) c_{v0} is constant with time



(b) $c_v(t)$ varies with time



(c) $c_v(t,z)$ varies with time and depth

Figure 2.10 Illustration of typical models for 1D consolidation

CHAPTER THREE

EFFECT OF NON-UNIFORM CONSOLIDATION ON PVD UNIT CELL

3.1 Introduction

The prefabricated vertical drains (PVDs) are widely used as an effective technique of soft ground improvement. The classic consolidation theories were proposed by Barron (1949) and Hansbo (1981), and then developed by many others researchers (Zhuang et al., 2005; Geng et al., 2012; Lu et al., 2015) to consider the variation of coefficient of consolidation with time. While the PVD induced consolidation is not uniform, and the phenomenon of non-form consolidation were reported recently (Hird and Moseley, 2000; Sharma and Xiao, 2000; Indraratna et al., 2015; Chai and Rondonuwu, 2015). Up to date, there is no method considering the effect of non-uniform consolidation into the consolidation theory. This chapter investigated the effect of non-uniform consolidation on the rate of consolidation by larger scale laboratory tests and finite element analysis (FEA). A method considering the effect of non-uniform consolidation was proposed finally to predict the average degree of consolidation (DOC).

3.2 Laboratory model tests

3.2.1 Test devices

The tests device mainly consists of a consolidation chamber, loading system and monitoring equipments. The test device is illustrated in Fig. 3.1.

(1) Consolidation chamber

The consolidation chamber is a polyvinyl chloride (PVC) cylinder which is 0.9 m in height and 0.45 m in inner diameter.

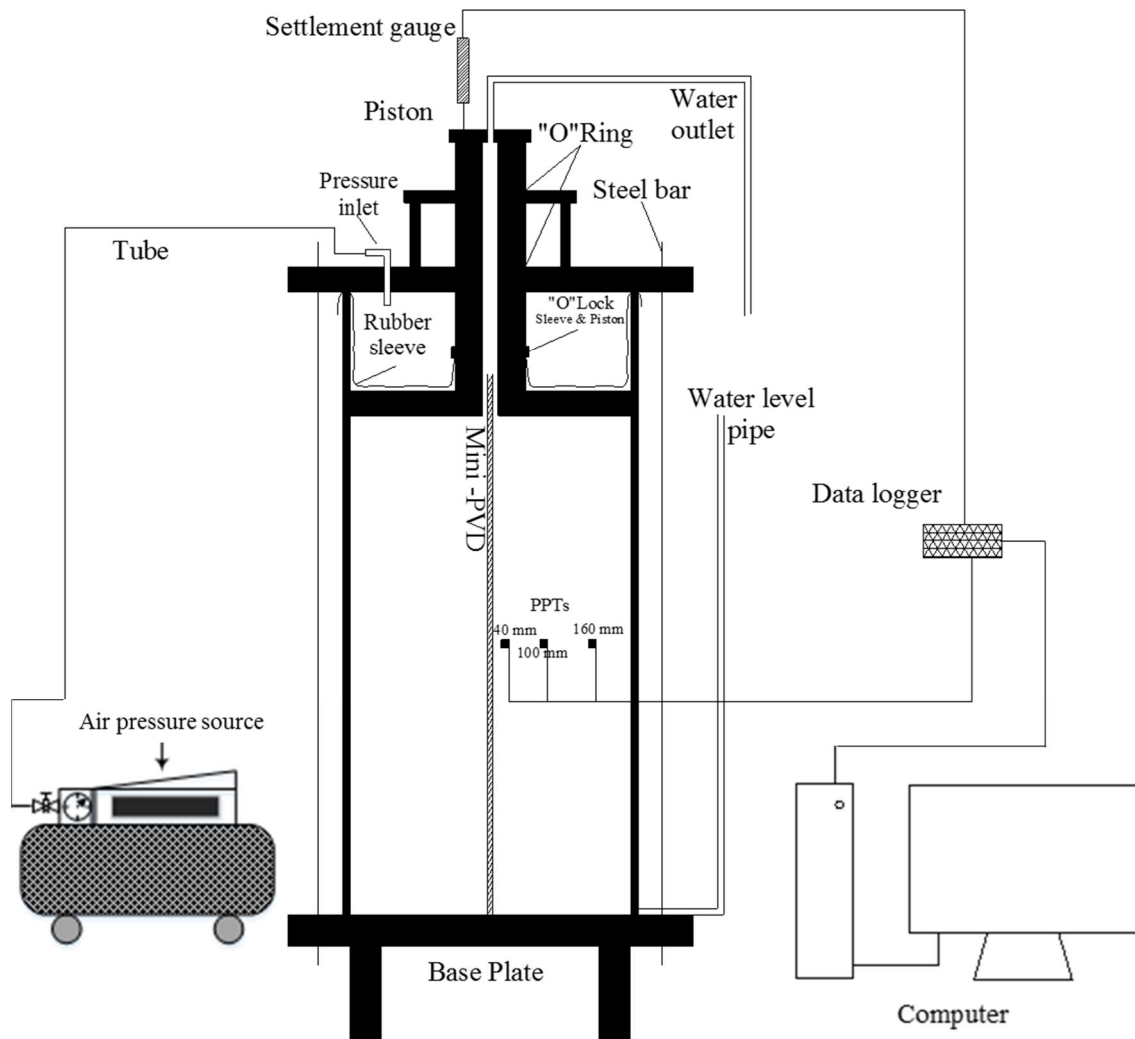


Figure 3.1 Devices for model tests

(2) Loading system

The loading system primarily consists of a loading piston, a rubber sleeve and an air pressure source. The loading piston has a stiff flat plate with a thickness of 40 mm and a hollow shaft. The hollow shaft is 100 mm and 30 mm in outer and inner diameter, respectively. The shaft provides a drainage path and the mini-PVD placement can go into it (to avoid bending the mini-PVD due to settlement of the model ground). A rubber sleeve with a thickness of 1 mm was installed above the piston. An “O” locker was used to fix the rubber sleeve to the shaft of the piston. The rubber sleeve can prevent the leakage of the air pressure. Initially the rubber sleeve was folded in vertical direction to enable it to follow the vertical displacement of the piston during consolidation. After placing the cap on the chamber, the pressure was applied to rubber sleeve from the air pressure source.

(3) Monitoring equipment

In the tests, the surface settlement and pore pressures in the middle height of the model ground were monitored. The pore pressure transducer (PPT) used in model tests is 2.0 cm in diameter and 2.5 cm in length provided by Kyowa Electronic Instruments Co., Ltd. The picture of the transducer is shown in Fig.3.2. The settlement and pore pressures were recorded by the computer through a data logger.



Figure 3.2 Pore pressure transducer used in model test

3.2.2 Materials used in test

(1) Soils used

Two tests were conducted using two types of remoulded soils. The two types of soils were remoulded Ariake clay (Case 1) and Ariake clay/sand mixture (Case 2), respectively. The clay/sand mixture was made of remolded Ariake clay and sands (pass 0.2 mm sieve) with 1:1 ratio by dry weight.

The compression index (C_c), swell index (C_s), coefficient of consolidation (c_v) and volumetric coefficient of compressibility (m_v) of the soils were obtained from the results

of conventional incremental loading (IL) oedometer tests. The properties of the soils used in the tests are shown in Table 3.1. The remoulded soils were firstly mixed thoroughly with the water content of 1.0~1.2 times of the corresponding liquid limits. The initial water content were 130% and 73% for Ariake clay and the clay/sand mixture, respectively. The initial void ratio (e_0) was evaluated by assuming the value of specific gravity (G_s) is 2.65 and the degree of saturation is 100%.

Table 3.1 Properties of remoulded soil in PVD unit cell test

Soil	Clay	Mixture
Properties	Values	
Specific gravity, G_s	2.65	
Liquid limit, w_l : %	112	61
Plastic limit, w_p : %	51	24
Compression Index, C_c	0.740	0.328
Swell Index, C_s	0.082	0.030
Initial void ratio, e_0	3.45	1.93
C_k	1.145	0.714

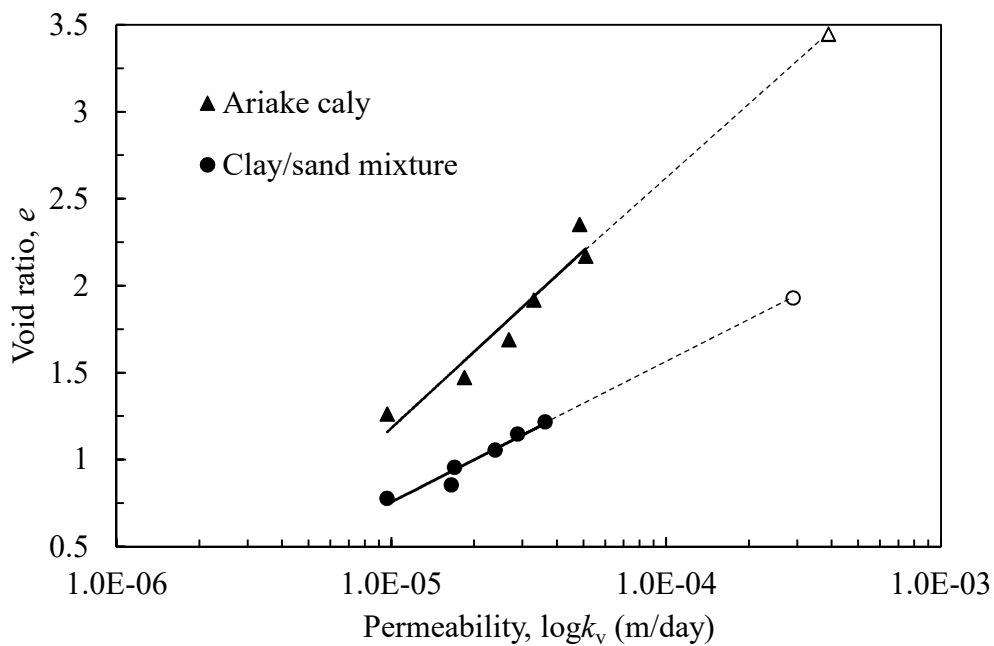


Figure 3.3 Relationships between void ratio and permeability of soils tested

The variation of permeability with void ratio (e) can be calculated by Eq. (2.25) and the variation with the void ratio in semi-logarithm are plotted in Fig. 3.3 for the both soils. It can be seen that the relationship between permeability and void ratio (solid line) can be expressed by the Taylor (1948) equation very well, and the value of C_k is 1.415 ($0.41e_0$) and 0.714 ($0.37e_0$) for Ariake clay and clay/sand mixture, respectively.

(2) Mini-PVD

The mini prefabricated vertical drain (mini-PVD) used in the model tests had a cross-section of 20.0 mm \times 5.0 mm which is $\frac{1}{4}$ of a commercial PVD. The picture of the mini-PVD is shown in Fig. 3.4.

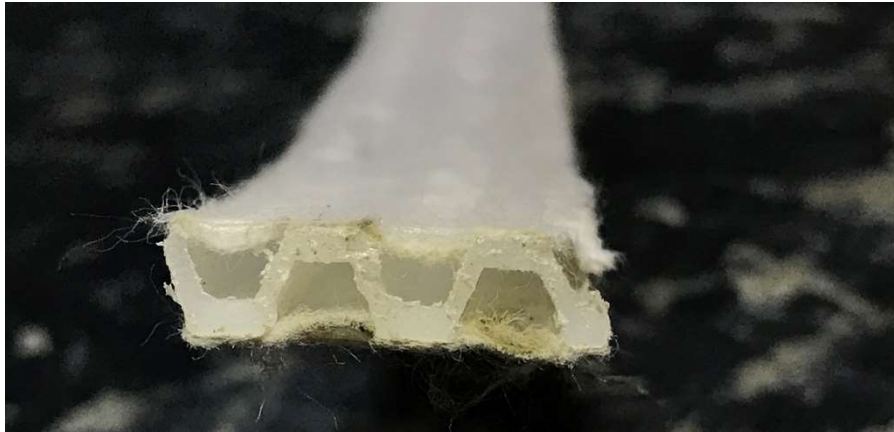


Figure 3.4 Picture of mini-PVD used in model tests

3.2.3 Test procedures

Total three model tests were conducted using remolded soil. The first two tests (Case 1 and Case 2) were used to study the effect of non-uniform consolidation on the rate of consolidation and an additional tests was used to investigate the reduction of void ratio near PVD induced by installation of PVD.

The procedures for conducting the model tests of Case 1 and Case 2 are as follows:

(a) Apply silicon grease: Silicon grease was smeared onto the inner wall of the chamber to reduce the friction between the model ground and the wall.

(b) Install mini-PVD: The mini-PVD was set in the centre of the chamber and kept standstill thereafter.

(c) Place the model ground: The soil slurry was put into the chamber carefully layer by layer up to the middle height of the model ground. Then three pore water transducers (PPTs) were set at 40, 100, 160 mm far from the center of the model ground along the radial direction. The slurry was continuously put into the chamber after installation of PPTs until the desired final height was reached.

(d) Set-up loading system: The piston and rubber sleeve were installed above the model ground. Before applying the loading, eight steel bars were used to connect the cap and the base plate of the chamber tightly. A settlement gauge was installed above the piston to measure the vertical displacement of the model ground. The photograph of the model test is shown in Fig. 3.5.



Figure 3.5 Photo of test device

(e) Pre-consolidation. The pre-consolidation test began after applying 100 kPa air pressure on the piston. The test was stopped periodically and soil samples were taken to measure the water contents. At each pause, five soil samples of approximately 10 g each were obtained with a small spoon at radial distances of approximately 30, 45, 100, 150, and 200 mm from the centre of the model. To avoid the disturbance of the soil immediately adjacent to the mini-PVD, the nearest sample was taken at a radial distance of about 30 mm. The sampling locations were altered on each sampling time (t_1 to t_6) as shown in Fig. 3.6. After soil sampling, the sampled points in the unit cell were refilled with soil slurry again and the loading system was reset to continue the consolidation test. After the consolidation, the soil sample at any radial distance (e.g. 10 mm from the centre of mini-PVD) can be obtained to measure their water contents.

Conceptually, this removing and refilling process could affect the unit cell behaviour due to refilled soil possessing different water content when comparing with the initial consolidated model ground. However, the affected area in each instance was less than 1% and the amount of refilled soil was very small, and thus it is considered that this effect can be ignored.

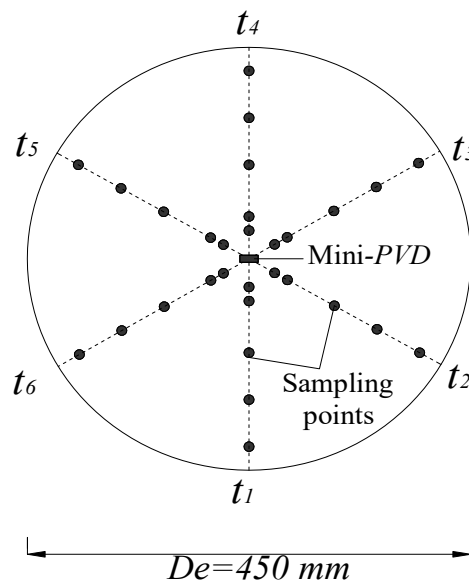


Figure 3.6 Illustration of sampling points

While the monitored settlement curves will be fragmentary due to unloading-reloading process. To obtain a continuous consolidation settlement curve to compare with the analytical results, the effect of unloading-reloading was excluded by checking both monitored settlements and excess pore pressures. The height of the top surface of the model ground was recorded prior to unloading. After reloading, the monitored settlements were connected to the pre-unloading curves when the height of the top surface of the model ground reached the pre-unloading level. After unloading, the model ground was in an over-consolidated state, and it took several hours for the settlement to reach the pre-unloading level.

The test procedure of Case 3 is similar to that of Case 1 and Case 2 generally. While the soil slurry was placed into the chamber and preloaded under 20 kPa under two-way drainage condition. Then the mini-PVD was installed into the model ground after the end of primary consolidation. Finally, the water contents of different radial distance at two different depth were measured.

3.3 Test results and analysis

3.3.1 Settlement-time curves

The settlement-time curves for Case 1 and Case 2 are shown in Fig. 3.7 and 3.8, respectively. It can be seen that with an elapsed time about 45 days, the primary consolidation was finished. The settlement-time curve from test will be used to compare with the results from finite element analysis (FEA) in the latter section.

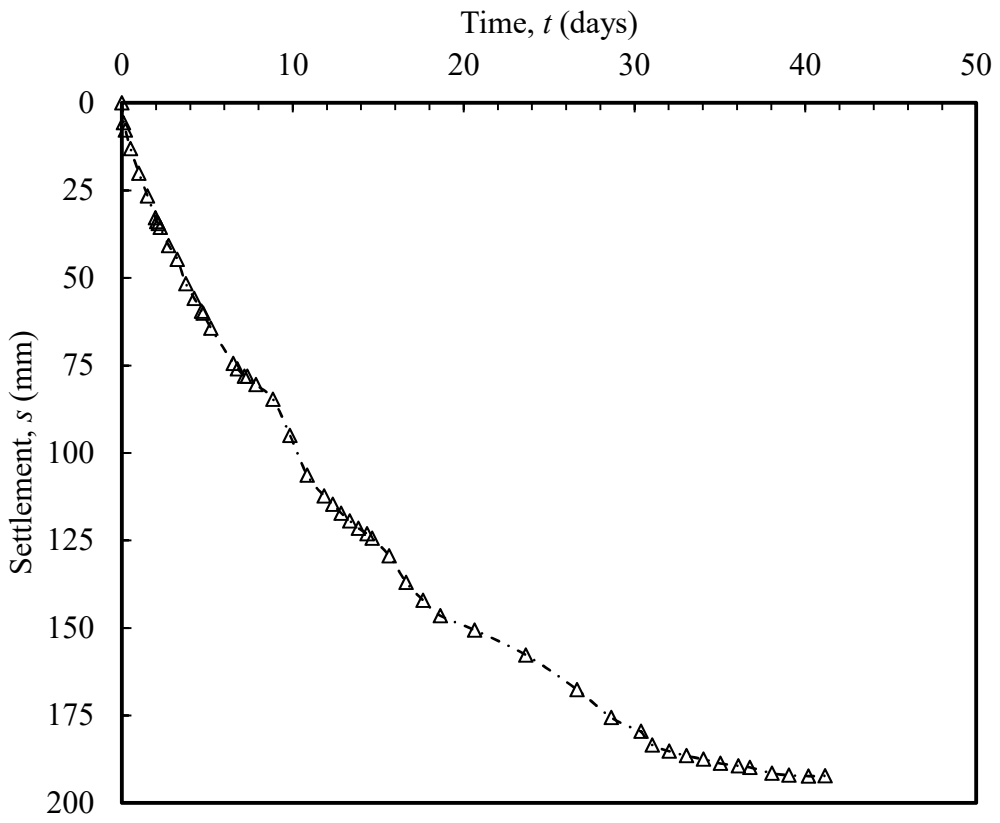


Figure 3.7 Settlement-time curve for Case 1

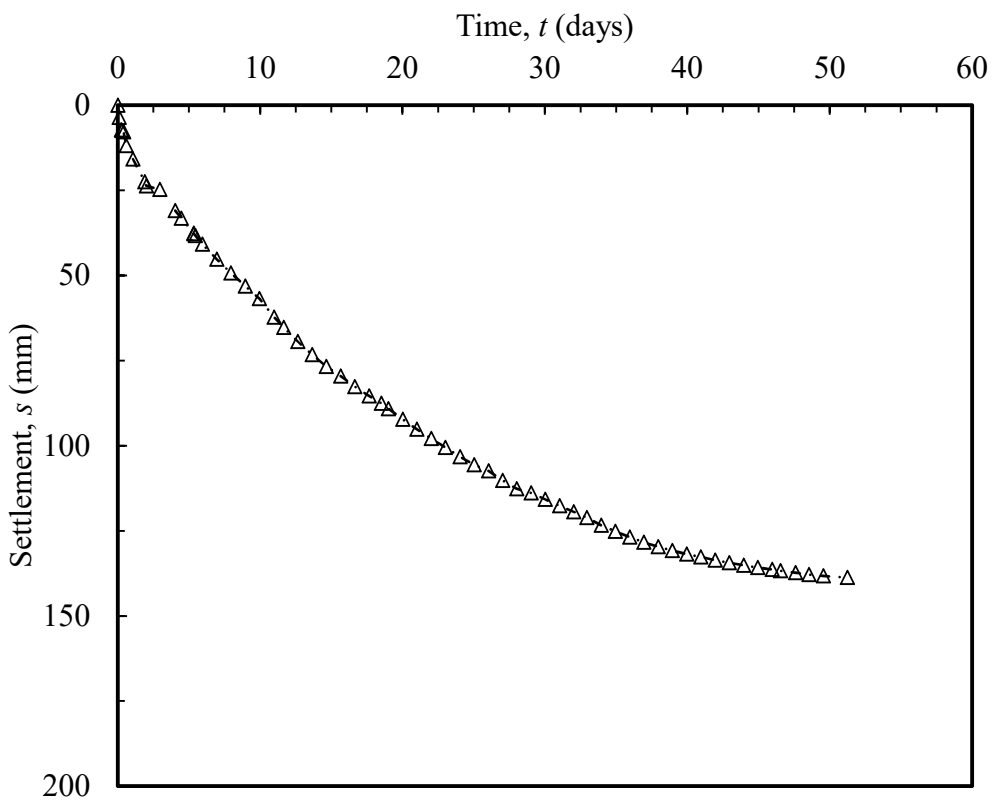


Figure 3.8 Settlement-time curve for Case 2

3.3.2 Excess pore water pressure

The measured pore water pressure with time for both cases are shown in Fig. 3.9 and 3.10, respectively. As discussed in Chapter Two, the consolidation is not uniform. The pore water pressure at the points about 40 mm from the center of the model decreased much faster than points at 100 and 160 mm from the center, and the differences is the maximum at the early stage of consolidation. The pore water pressure at different distances converged at the final stage of the consolidation. Although effort was made to obtain continuous curve by checking the height of the model ground before unloading and after reloading, there were some jump-points on the curves. The pore water pressure was used to calculated the average degree of consolidation (DOC) comparing with the results from FEA in the latter section.

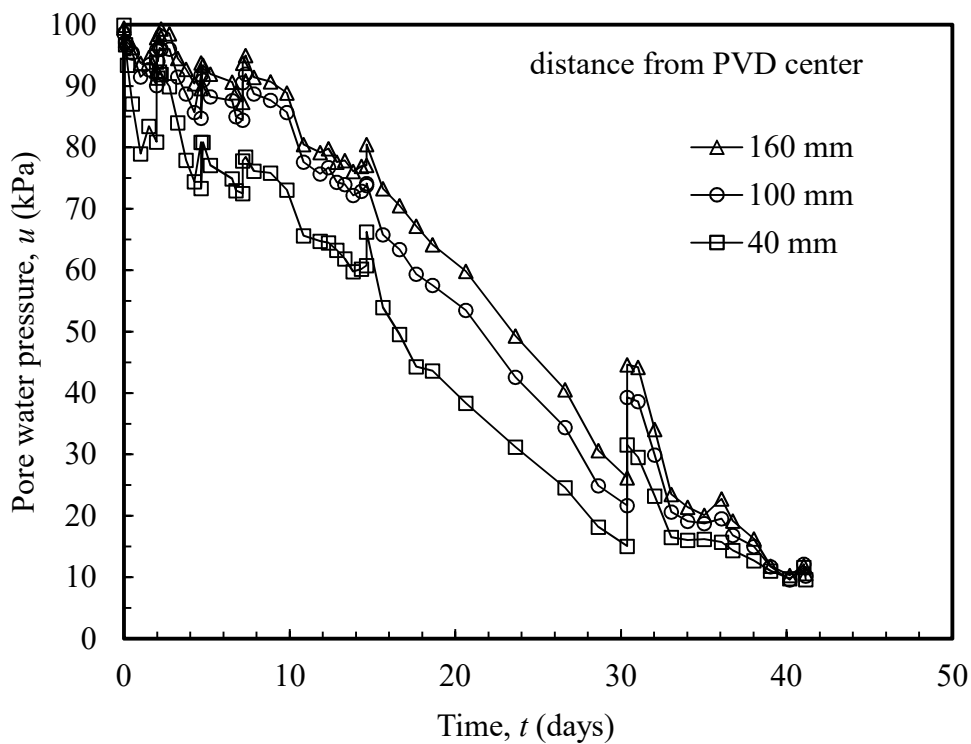


Figure 3.9 Measured pore water pressure variation for Case 1

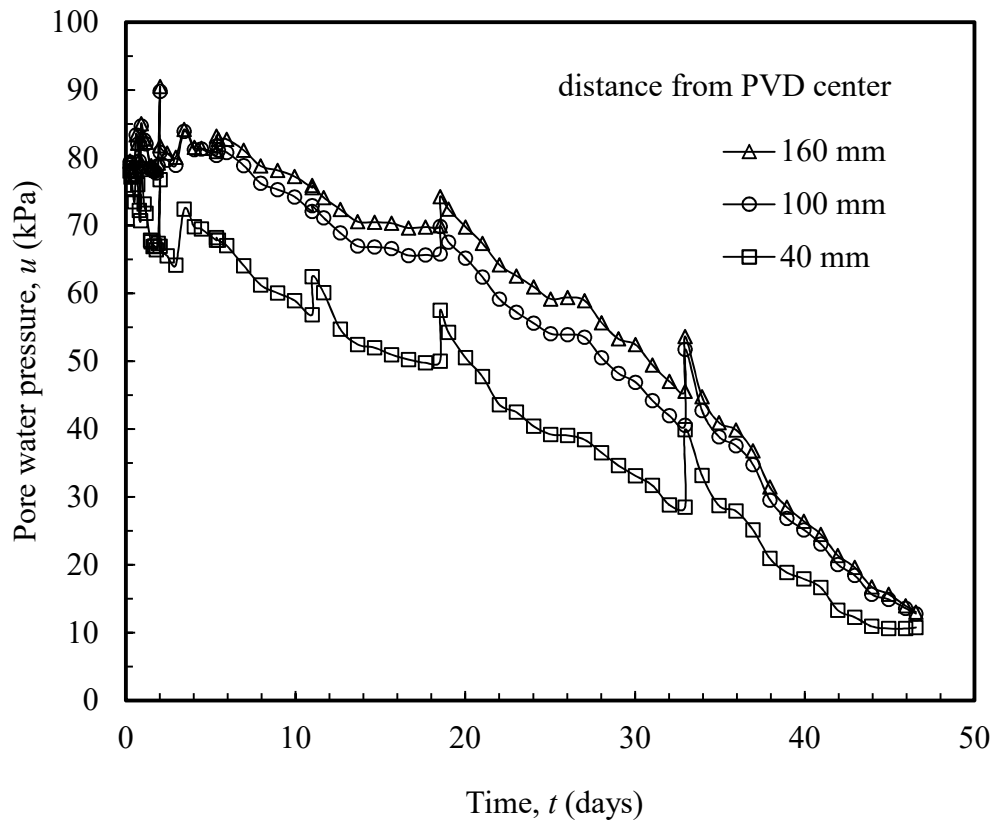


Figure 3.10 Measured pore water pressure variation for Case 2

3.3.3 Variation of water content and permeability ratio

In Fig. 3.11 and 3.12, the water content variations with radial distance are plotted for both cases respectively. During the test, the water contents at 10 mm from the center of the model were extrapolated referring to the finally measured water contents and their tendency and indicated as dashed lines. In general, the water content reduced sharply at a zone near the PVD during the early stages of consolidation (elapsed times of 2, 5 and 8 days), which indicated a faster rate of consolidation at the inner zone. Similar results were reported by Rujikiamjorn et al. (2013).

Based the results of permeability variations with void ratio in Fig. 3.2, the initial value of permeability (k_{v0}) corresponding to initial water content can be extrapolated for both cases (dash line). Another factor needed to be considered is the stress-induced anisotropy during consolidation process. Due to this factor, the horizontal permeability (k_h) would be larger than the vertical permeability (k_v) during consolidation. Chai et al. (2015) reported that the value of $k_h/k_v \approx 1.5$ for remoulded Ariake clay for consolidation stress up to 1,000 kPa. While for clay/sand mixture, the stress-induced anisotropy will be less significant

than pure clay because of a lower clay content. Considering the consolidation stress of about 100 kPa adopted in the model test, the value of $k_h/k_v = 1.3$ for Ariake clay and 1.1 for clay/sand mixture were adopted in this study. The initial value of horizontal permeability (k_{h0}) for Case 1 and Case 2 are 5.0×10^{-4} m/day and 3.3×10^{-4} m/day, respectively.

For a given water content, the void ratio can be calculated, and then the permeability corresponding to any void ratio can be evaluated by Taylor's (1948) equation. Defined k at $r = 200$ mm (farthest measuring point) as k_{200} , and at r radial distance as k_r , the calculated k_{200}/k_r ratios (PR) are depicted in Fig. 3.13 and 3.14 for both cases.. At $r = 10$ mm, the largest estimated values of PR are 18 for Case 1 and 15 for Case 2. In addition, PR reduced rapidly with increase of radial distance. Even at the end of the test, k_{200}/k_r ranged from 2 to 3 in the zone close to the mini-PVD. Ideally, at the final stage of consolidation, the unit cell will be uniform again and the value of PR should be around 1. While due to the local horizontal movement of the soil domain, the consolidation induced non-uniformity remained at the end of primary consolidation.

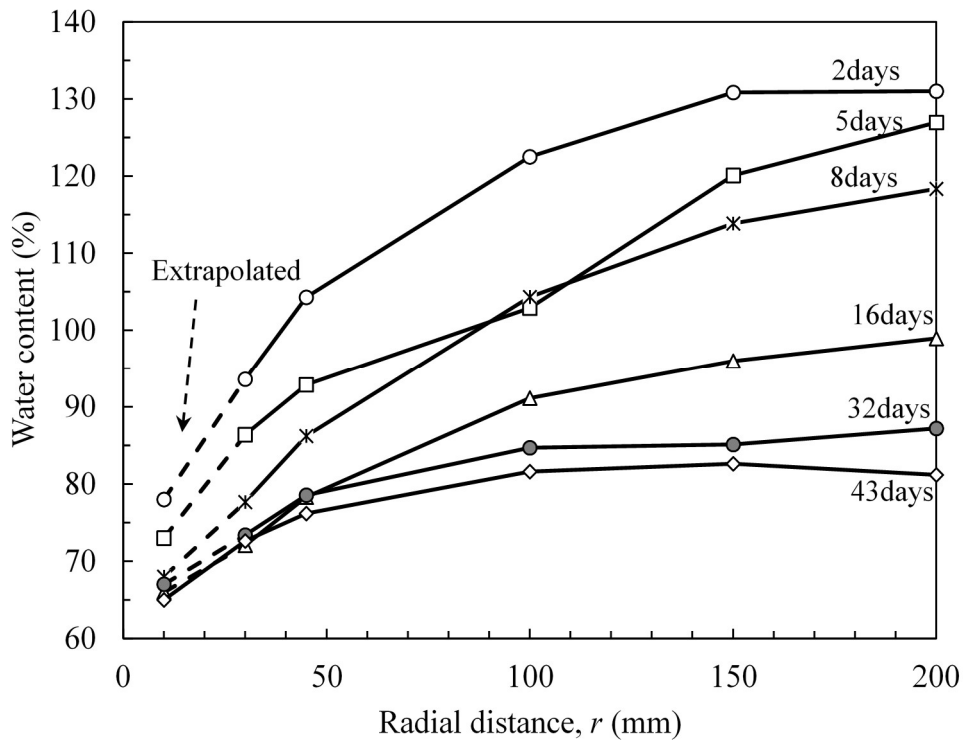


Figure 3.11 Variations of water content with radial distance for Case 1

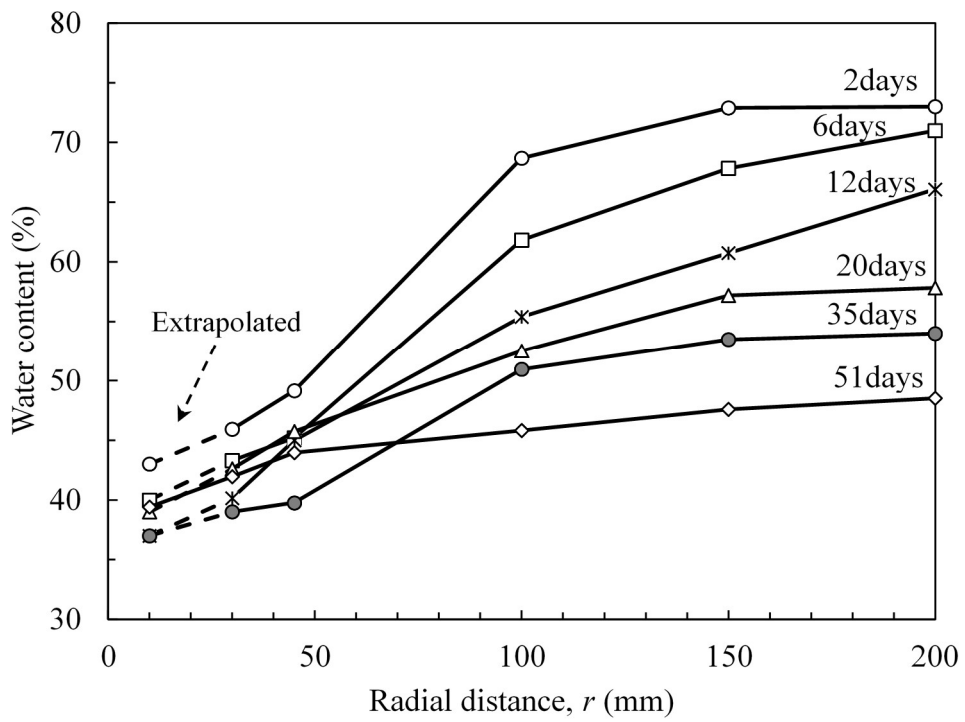


Figure 3.12 Variations of water content with radial distance for Case 2

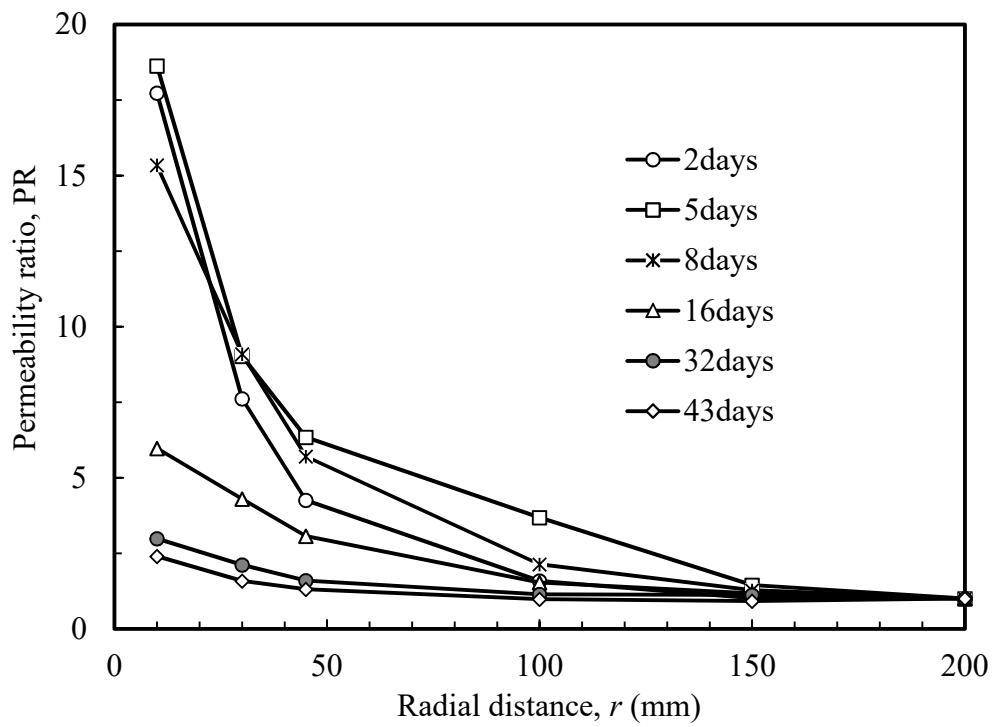


Figure 3.13 Variations of permeability ratio with radial distance for Case 1

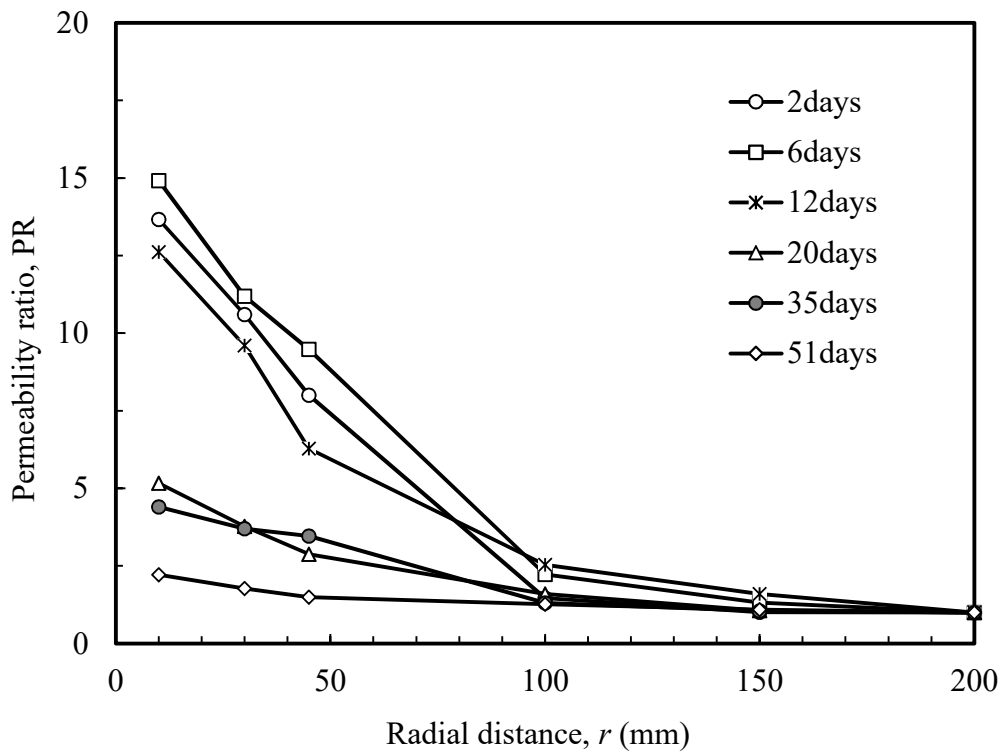


Figure 3.14 Variations of permeability ratio with radial distance for Case 2

3.3.4 Reduction of water content induced by installation of PVD

Figure 3.15 shows the variation of water content with radial distance after the test of Case 3. Before installation of mini-PVD, i.e. after the end of primary consolidation of preloading, the soil domain should be uniform horizontal radially. While it can be seen clearly that the soil domain became non-uniform finally after the test. Even without incremental surcharge loading, the water content near the mini-PVD reduced to 95% and near the periphery of the wall of chamber is approximately 110%. Similar phenomenon was observed by Indraratna et al. (2015) in the field. This reduction of water content near the PVD was due to the dissipation of excess pore water pressure induced by installation of mini-PVD. As a result, the void ratio and the permeability of the soil in the zone near the mini-PVD will reduce concurrently. The soil with low permeability near the PVD definitely will influence the rate of consolidation. This reduction of permeability near the PVD should not be included into mechanical ‘smear effect’.

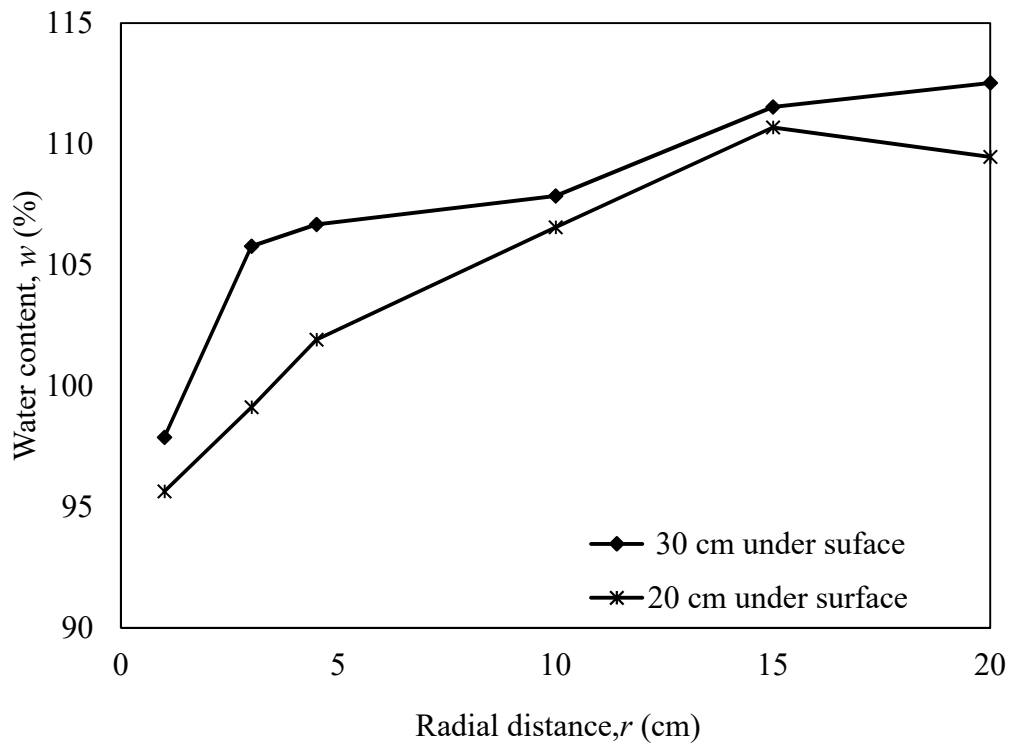


Figure 3.15 Reduction of water content induced by installation of PVD

3.3.5 Summary and comments

The test results shown that the PVD induced consolidation is not uniform. The variation of excess pore water pressure indicated that the soil in the zone near mini-PVD consolidated much faster and the effective stress increased more rapidly compared with the soil in the zone far away from the mini-PVD. The estimated value of permeability (k) ratio (PR) (ratio of k at $r=200$ mm to k at the r distance) at the periphery of the mini-PVD is the maximum at the early stage of consolidation.

3.4 Numerical investigation

3.4.1 Simulating model test

3.4.1.1 Model used

The model tests were simulated by finite element analysis (FEA). The model used in FEA were shown in Fig. 3.16. The radius of unit cell, $r_e = 225$ mm and the drain, $r_w = 6.3$ mm calculated by Eq. (2.3). And $H = 0.8$ m and 0.75 m for Case 1 and Case 2, respectively.

The FEA was conducted using Plaxis 2D V.8.2 and the Soft Soil Model (SSM) was adopted (PLAXIS 2D-Version, 2012) to present the mechanical properties of soil. The SSM incorporated into Plaxis was essentially in the framework of the Modified Cam Clay (MCC) model (Rosco and Burland, 1968). However, there were some differences with the MCC model:

(1) The SSM included cohesion (c') as a strength parameter, but the MCC model assumed $c' = 0$.

(2) In the SSM, the slope of the critical state line, M , in the p' - q (p' is the mean effective stress and q is the deviator stress) plot is primarily a function of the coefficient of at-rest earth pressure under a normally consolidated state (K_0^{NC}), $K_0^{NC} = 1 - \sin\phi'$ (ϕ' is the internal friction angle of the soil) (PLAXIS 2D-Version, 2012). However, the failure was controlled by the Mohr-Coulomb criterion.

The SSM captures yielding, volumetric strain hardening and the failure behaviour of clayey soil, and the model parameters can be easily determined from the results of oedometer and triaxial tests. However, it does not consider anisotropic behaviour and secondary consolidation. Because the PVD unit cells considered in this study is close to a one-dimensional compressive state and the time period considered was relatively short (about 1.5 months), the SSM was considered suitable for the situation. The model parameters used in FEA are same as Table 3.1.

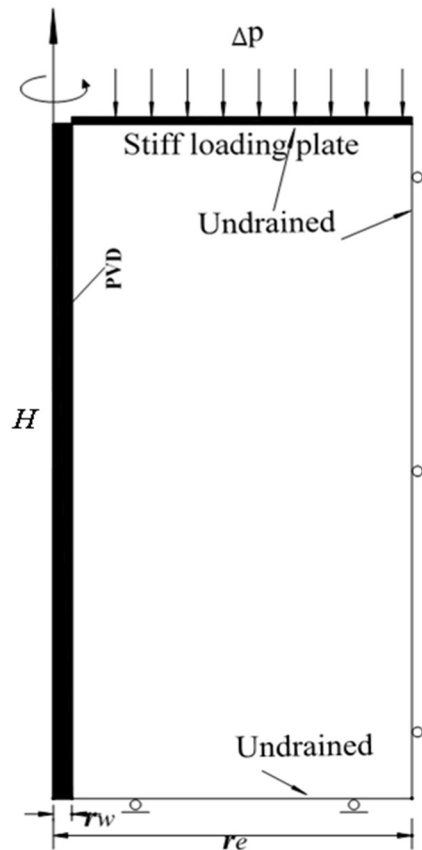


Fig. 3.16 Model used in FEA

The steps for simulating the model test of Case 1 and Case 2 are as follows:

Step 1: Preloaded under initial effective stress (σ'_{v0}). The soil model in this step is Linear-Elastic model with a high modulus and a high permeability. This step is aiming at generating a desirable initial stress condition, meanwhile with an ignorable strain. To fit the measured settlement curves, $\sigma'_{v0} = 3$ kPa for Case 1 and 2 kPa for Case 2 were back-evaluated. These stresses could be explained as electric repulsive forces between the soil particles.

Step 2: Apply consolidation pressure increment. In this step, the material is reset to be “clay”, modelled by Soft Soil Model. Resetting the deformations to zero and an increment load was applied under undrained condition.

Step 3: Consolidation simulation. During the consolidation process, changing of k with void ratio (e) is simulated using Taylor’s (1948) equation (Eq. (2.26)).

3.4.1.2 Evaluation of skin friction

Although grease was applied onto the wall of the chamber to reduce friction, the skin friction was not completely removed. Chai and Nguyen (2013) reported a skin friction angle between a greased steel plate and clay of approximately 3° . Assuming the same skin friction angle and a coefficient of at-rest earth pressure (K_0) of 0.5, approximately 9 kPa of the friction-induced vertical stress reduction could be evaluated at the middle of the model ground, corresponding to the final effective stress condition. Although the effective stress (and the friction) in the model ground increased with the degree of consolidation, an average of 4.5 kPa reduction in vertical consolidation stress was considered in the finite element analysis (FEA) for simplicity.

3.4.1.3 Simulation results

The simulated settlements are then compared with the measured results in Fig. 3.17 and 3.18. It can be observed that the FEA simulated the settlement curves very well. Using the results of excess pore water pressure in Fig. 3.9 and Fig. 3.10 and assuming that each point represented the average value of an annular area containing the point, the DOCs were also calculated as measured and show in Fig. 3.19 and 3.20 as measured ones. In calculating the DOC using the measured pore water pressures, the amount of friction-induced total vertical stress reduction was evaluated by using the effective stress state of the previous step. Although there are discrepancies, in general the FEA yielded a fair simulation of the measurements.

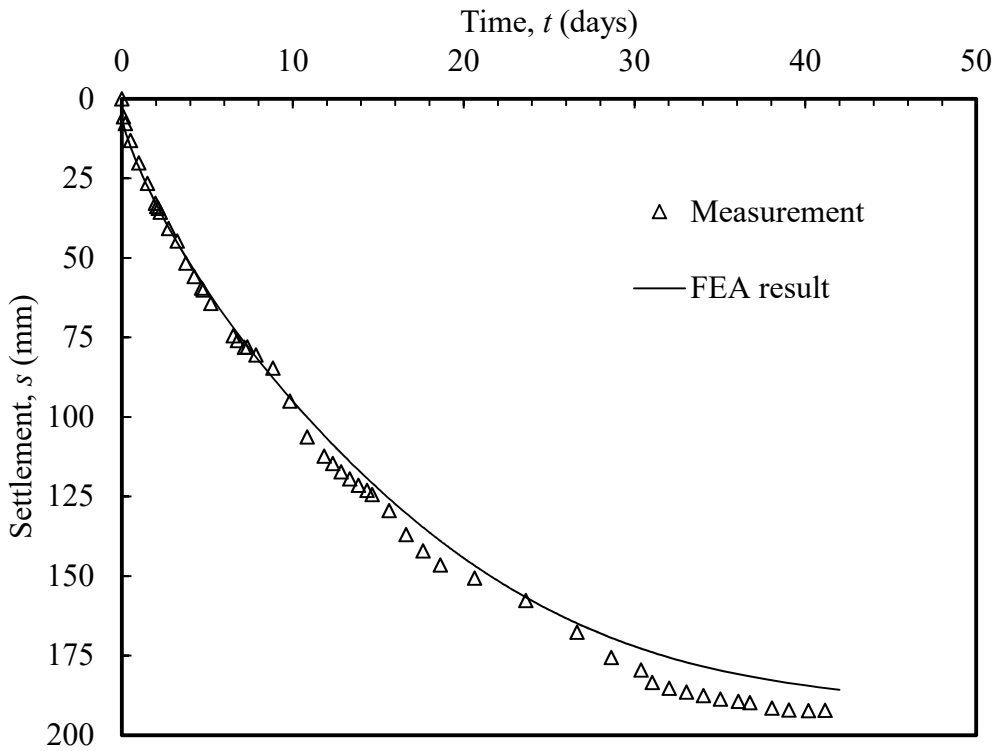


Fig. 3.17 Comparison of settlement-time curve for Case 1

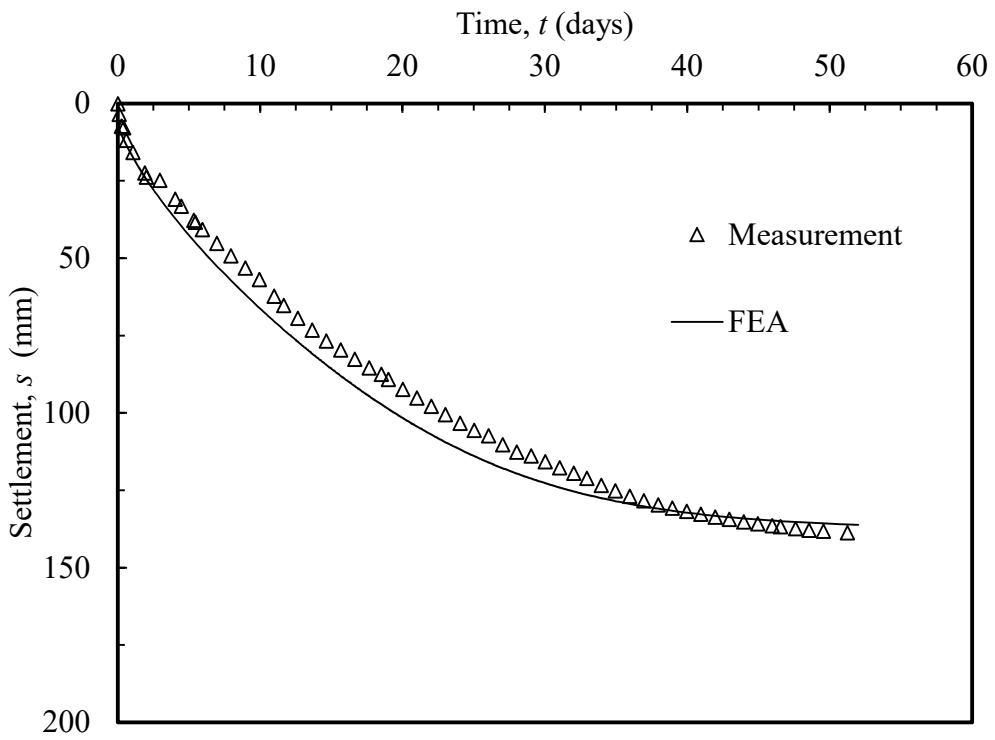


Fig. 3.18 Comparison of settlement-time curve for Case 2

3.4.1.4 Equivalent ‘smear’ effect due to non-uniform consolidation

The model tests were also analysed using Hansbo’s (1981) solution. The average value of coefficient of consolidation (c_h) has been evaluated as:

$$c_h = \frac{2.3(1+e)k_h p'}{C_c \gamma_w} \quad (3.1)$$

where γ_w is the unit weight of water, and k_h is the average permeability in radial direction corresponding to average void ratio, e . The average void ratio e was obtained at mean consolidation stress, p' which is calculated as (JSA 2000a, b):

$$p' = \sqrt{p_f \times p_0} \quad (3.2)$$

where p_0' and p_f' are the vertical effective stresses corresponding to the initial and the final stages of consolidation, respectively. From Eq. (3.1) and Eq. (3.2), average values of $c_h = 4.09 \times 10^{-3} \text{ m}^2/\text{day}$ and $c_h = 3.36 \times 10^{-3} \text{ m}^2/\text{day}$ were obtained for Case 1 and Case 2, respectively. The analysed DOCs are provided in Fig. 3.19 and 3.20. It can be observed that Hansbo’s solution, which does not consider the effect of non-uniform consolidation, significantly overestimated the average rate of consolidation for DOC less than 80%.

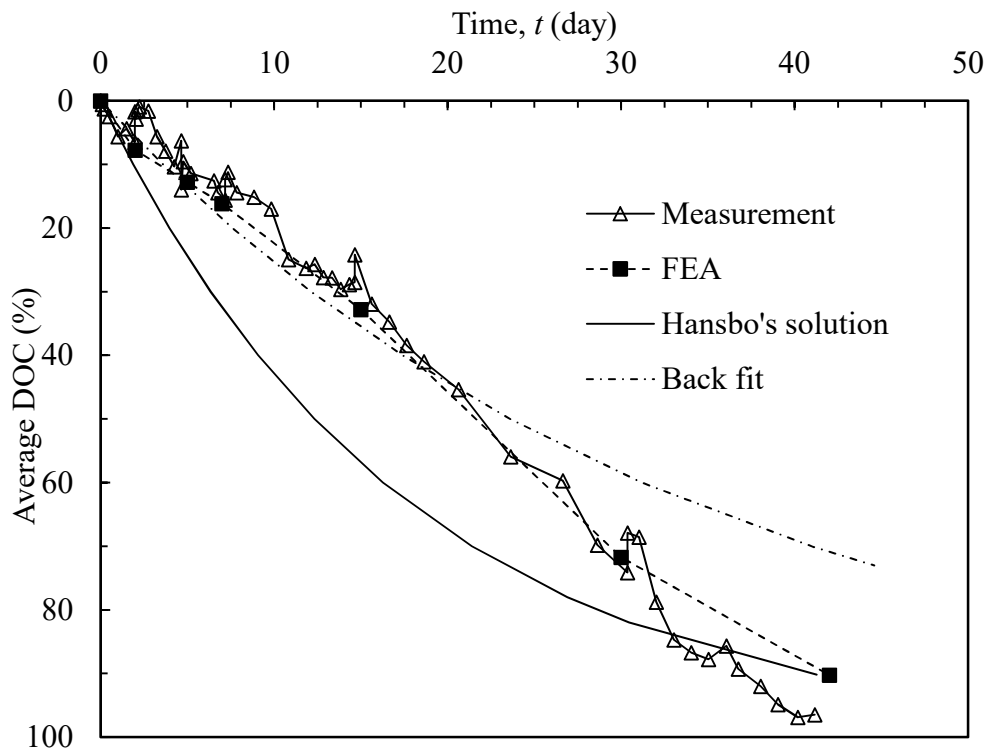


Fig. 3.19 Comparison of average degrees of consolidation for Case 1

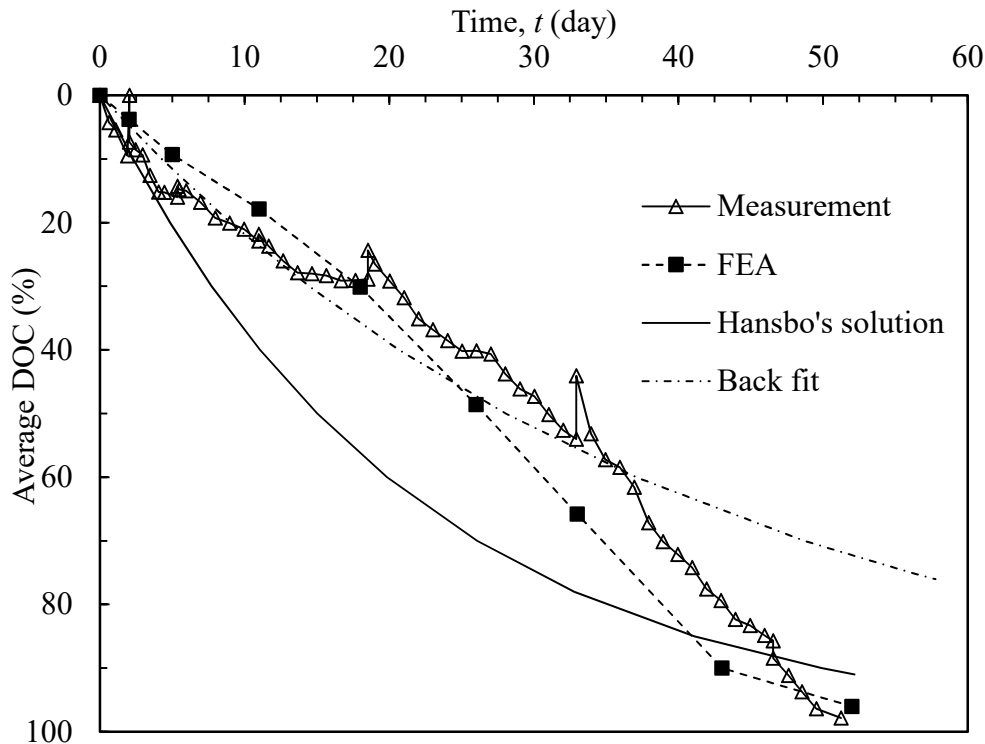


Figure. 3.20 Comparison of average degrees of consolidation for Case 2

Physically, non-uniform consolidation results in lower values of k in a zone surrounding a PVD, which is analogous to a “smear zone”. However, the effect of this ‘smear’ effect varies during the consolidation process, particularly during the early stage of consolidation. Therefore, it is not possible to precisely consider the effect of non-uniform consolidation with a constant smear effect value.

There were two parameters for the smear effect, the ratio between equivalent diameter of smear zone and the drain, d_s/d_w and the ratio between permeability in smear zone and undisturbed zone, k_h/k_s . But only one condition, the average DOC, could be used to optimize them. We therefore initially fixed d_s/d_w at this stage and back fitted k_h/k_s ratio. To back fit the numerical results with Hansbo’s solution, a “smear” zone is assumed to consider the effect of non-uniform consolidation. The following assumptions were adopted:

(1) Diameter of the smear zone, $d_s = 50$ mm ($d_s/d_w = 4$).

(2) By matching the DOC of the analytical solution (Hansbo, 1981) to the results of the FEA at DOC = 50%, we obtained an equivalent value of k_h/k_s termed $(k_h/k_s)_{e0}$. The back-fitted value of $(k_h/k_s)_{e0}$ is 2.9 and 2.8 for Case 1 and Case 2, respectively.

The back-fitted results are also shown in Fig. 3.19 and 3.20, respectively. The results of back-fitting agree with the results of tests well up to DOC of about 50%. For DOC >50%, the back fitted results under-estimated the test results.

3.4.2 Numerical experiments

3.4.2.1 Cases analysed

Because the tested cases are limited, numerical experiments were conducted to investigate the effect of soil properties and magnitude of applied load on the non-uniform consolidation of a PVD unit cell.

The cases analysed were divided into 3 series and the parameters of soil, drainage and loading conditions are listed in Table 3.2 to 3.6 for each series, respectively. The cases of the three series are classified as follows:

(1) Series 1: Unit cell geometry was fixed, and soil properties and loading conditions were varied. But by adjusting the value of C_k in Eq. (2.26), the value of c_h was maintained as a constant during the consolidation process for each case.

(2) Series 2: Unit cell geometry was fixed, and values of C_k were assumed as $C_k = 0.4 e_0$ (2a), $0.5 e_0$ (2b) and $0.6 e_0$ (2c) (Tavenas et al. 1983b). The representative value of c_h used in the theoretical analysis was evaluated by Eqs. (3.1) and (3.2).

(3) Series 3: Soil properties were fixed, but the diameters of the PVD and unit cells simulated were varied.

For each case, DOC versus elapsed time was calculated using simulated excess pore water pressures. Using the back-fitting method aforementioned fixing $d_s/d_w = 4$, the $(k_h/k_s)_{e_0}$ for each case can be obtained.

Table 3.2 Parameters used for numerical simulations for Series 1

No.	C_c	e_0	p'_0 :kPa	Δp :kPa	$k_v:10^{-4}$ m/day	d_w :mm	D_e/d_w	C_k
1	0.5	2.5	10	100	6.0	50	20	0.54
2	1.0	2.5	10	100				1.17
3	1.5	2.5	10	100				2.00
4	1.0	1.5	10	100				1.30
3 (5)	1.0	2.5	10	100				1.17
6	1.0	3.5	10	100				1.12
7	1.0	2.5	5	100				1.19
3 (8)	1.0	2.5	10	100				1.17
9	1.0	2.5	20	100				1.16
10	1.0	2.5	30	100				1.16
11	1.0	2.5	50	100				1.15
12	1.0	2.5	75	100				1.15
13	1.0	2.5	100	100				1.15
14	1.0	2.5	10	50				1.16
3 (15)	1.0	2.5	10	100				1.17
16	1.0	2.5	10	150				1.18
17	1.0	2.5	10	200				1.19

Table 3.3 Parameters used for numerical simulations for Series 2a

No.	C_c	e_0	p'_0 :kPa	Δp :kPa	$k_v:10^{-4}$ m/day	d_w :mm	D_e/d_w	$C_k: 0.4 e_0$
1	0.3	2.5	10	100	6.0	50	20	1.0
2	0.5	2.5	10	100				1.0
3	1.0	2.5	10	100				1.0
4	1.5	2.5	10	100				1.0
5	2.0	2.5	10	100				1.0
6	3.0	3.5	10	100				1.4
7	1.0	1.5	10	100				0.6
8	1.0	2.5	10	100				1.4
3 (9)	1.0	3.5	10	100				1.0
10	1.0	2.5	5	100				1.0
11	1.0	2.5	10	100				1.0
3 (12)	1.0	2.5	20	100				1.0
13	1.0	2.5	30	100				1.0
14	1.0	2.5	50	100				1.0
15	1.0	2.5	75	100				1.0
16	1.0	2.5	100	100				1.0
17	1.0	2.5	10	50				1.0
18	1.0	2.5	10	100				1.0
3 (19)	1.0	2.5	10	150				1.0
20	1.0	2.5	10	200				1.0

Table 3.4 Parameters used for numerical simulations for Series 2b

No.	C_c	e_0	p'_0 :kPa	Δp :kPa	$k_v:10^{-4}$ m/day	d_w :mm	D_o/d_w	$C_k: 0.5 e_0$
1	1.0	2.5	10	100	6.0	50	20	1.25
2	2.0	2.5	10	100				1.25
3	1.0	1.5	10	100				0.75
4	1.0	2.5	30	100				1.25
5	1.0	2.5	10	150				1.25

Table 3.5 Parameters used for numerical simulations for Series 2c

No.	C_c	e_0	p'_0 :kPa	Δp :kPa	$k_v:10^{-4}$ m/day	d_w :mm	D_o/d_w	$C_k: 0.6 e_0$
1	1.0	2.5	10	100	6.0	50	20	1.50
2	2.5	3.0	10	100				1.80
3	1.0	3.5	10	100				2.10
4	1.0	2.5	75	100				1.50
5	1.0	2.5	10	200				1.50

Table 3.6 Parameters used for numerical simulations for Series 3

No.	C_c	e_0	p'_0 :kPa	Δp :kPa	$k_v:10^{-4}$ m/day	d_w :mm	D_o/d_w	C_k
1	1.0	2.5	10	100	4.3	50	14	1.173
2						50	20	
3						50	30	
4						50	40	
5						50	50	
6						20	50	
7						100	10	

3.4.2.2 Effect of compressibility on non-uniform consolidation

The relationship of compression index, C_c and the value of the $(k_h/k_s)_{e_0}$ were shown in Fig. 3.21 based on the results of Case No. 1 to No. 5 in Series 2a. The value of the $(k_h/k_s)_{e_0}$ increased with the value of C_c which suggested that for a soil with higher compressibility will result in a larger equivalent 'smear' effect due to the non-uniform consolidation. With the same loading condition and initial void ratio, the soil in the zone near drainage boundary will be compressed more for a soft clay compared with a stiff soil. And therefore more reduction on the permeability near the drain at the early stages of consolidation.

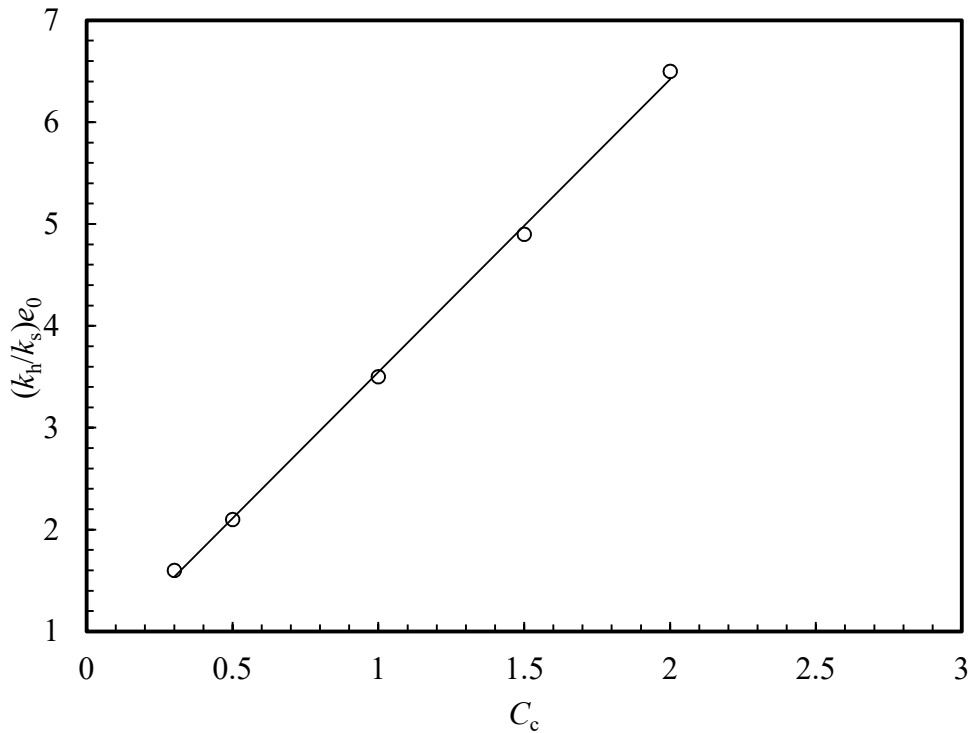


Figure 3.21 Relationship between $(k_h/k_s)_{e0}$ and C_c

3.4.2.3 Effect of stress ratio on non-uniform consolidation

For given parameters of a soil, the initial and final stress will control the amount of reduction of void ratio during consolidation. Here a term (SR) is defined as:

$$SR = \frac{p_f'}{p_0'} = \frac{(\Delta p + p_0')}{p_0'} \quad (3.3)$$

Fig. 3.22 shows the relationship between the back-fitted results of $(k_h/k_s)_{e0}$ and SR in a semi-logarithm scale based on the results of Case 11 to 21 in Series 2a. The correlation is quite linear and the value of $(k_h/k_s)_{e0}$ increases with SR. A larger value of SR will induce a large reduction of void ratio and then a larger decrease of permeability in the zone near the PVDs in the early stage of consolidation. As a result, for the cases with larger value of SR, the effect of non-uniform of consolidation is more significant.

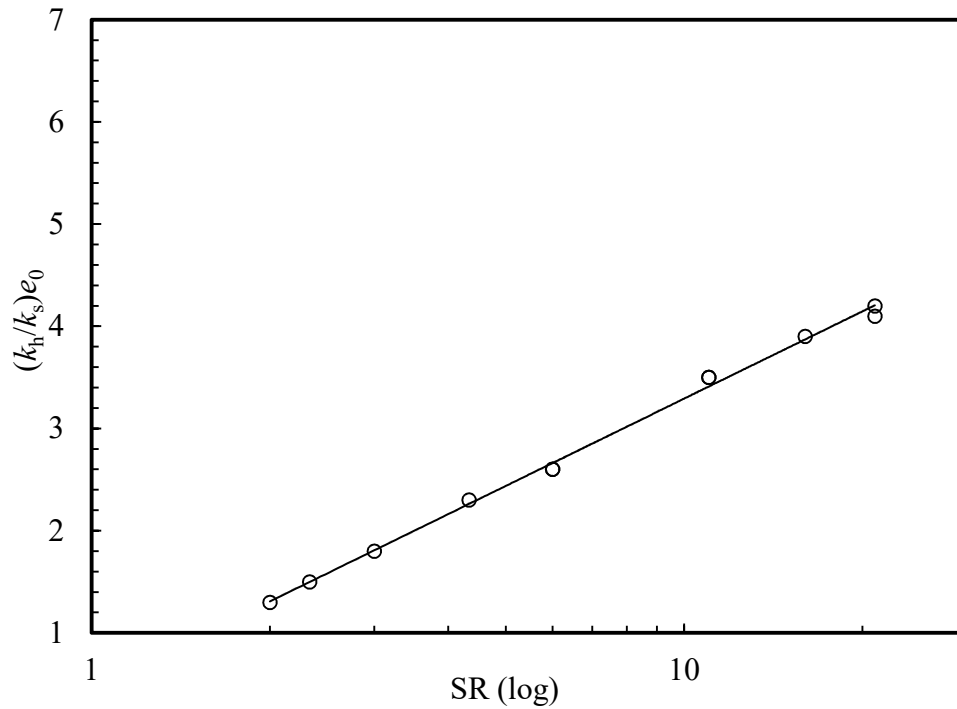


Figure 3.22 Relationship between $(k_h/k_s)_{e0}$ and SR

3.4.2.4 Equivalent ‘smear’ effect and $\Delta e/C_k$

The permeabilities in the horizontal direction before and after consolidation are termed k_{h0} and k_{hf} , respectively. The fundamental effect of non-uniform consolidation on the average DOC is caused by the permeability at a zone adjacent to a PVD reaching the value of k_{hf} shortly after the onset of consolidation while the zones away from the drain may still have a value of k_{h0} . Therefore, the value of $(k_h/k_s)_{e0}$ could be related to k_{h0}/k_{hf} . By rearranging Taylor’s (1948) equation (Eq. (2.26)), it was easy to show that $\log(k_{h0}/k_{hf}) = \Delta e/C_k$, where Δe is the consolidation-induced reduction of the void ratio that could be calculated by using the basic soil properties and loading condition. The FEA results of Series 1 and 2 are plotted in form of $\Delta e/C_k$ versus $(k_h/k_s)_{e0}$ in Fig. 3.23, and quite good correlation can be observed.

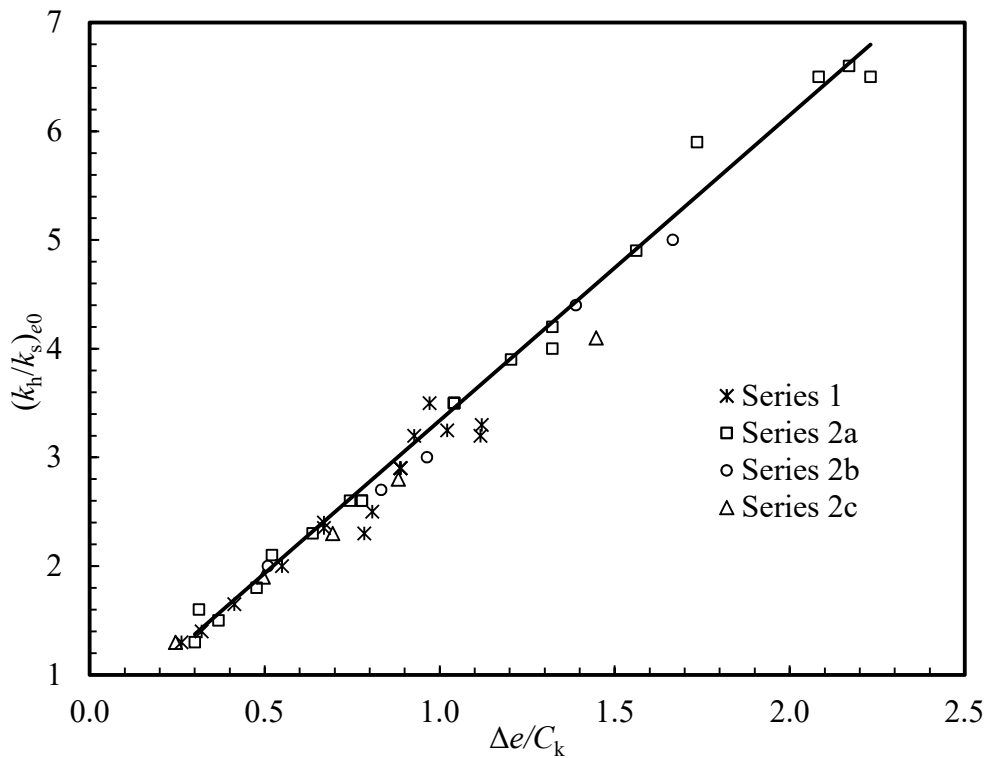


Figure 3.23 Relationship between $(k_h/k_s)_{e0}$ and $\Delta e/C_k$

3.4.2.5 Summary and comments

The equivalent ‘smear’ effect induced by non-uniform consolidation is related with basic soil properties and loading conditions and the term, $\Delta e/C_k$ can be used to represent quantitatively the effects of soil properties and loading conditions. There is a close linear correlation between $\Delta e/C_k$ and $(k_h/k_s)_{e0}$.

3.5 Equivalent ‘smear’ effect approach

The relationship presented in Fig. 3.23 was obtained under the conditions of $d_s/d_w = 4$ and $D/d_w = 20$. While the field situation are not limited to these conditions.

3.5.1 Proposed method

- (1) Effect of D/d_w ratios

The previous results of $(k_h/k_s)_{e0}$ in Series 1 and 2 applied for the conditions of the diameter of the unit cell, $D_e/d_w=20$ and $d_s/d_w = 4$. However, an actual project with PVD improvement could have different values of D_e/d_w and d_s/d_w .

In Series 3, the FEA used $d_s/d_w = 4$ but for a different D_e/d_w , and the results are shown in Fig. 3.24. Adopting the equivalent permeability ratio for any D_e/d_w but with $d_s/d_w = 4$ as $(k_h/k_s)_{e1}$, the ratio of $(k_h/k_s)_{e1}/(k_h/k_s)_{e0}$ is:

$$\frac{(k_h / k_s)_{e1}}{(k_h / k_s)_{e0}} = 0.012 \left(\frac{D_e}{d_w} \right) + 0.72 \quad (3.4)$$

(2) Effect of d_s/d_w ratios

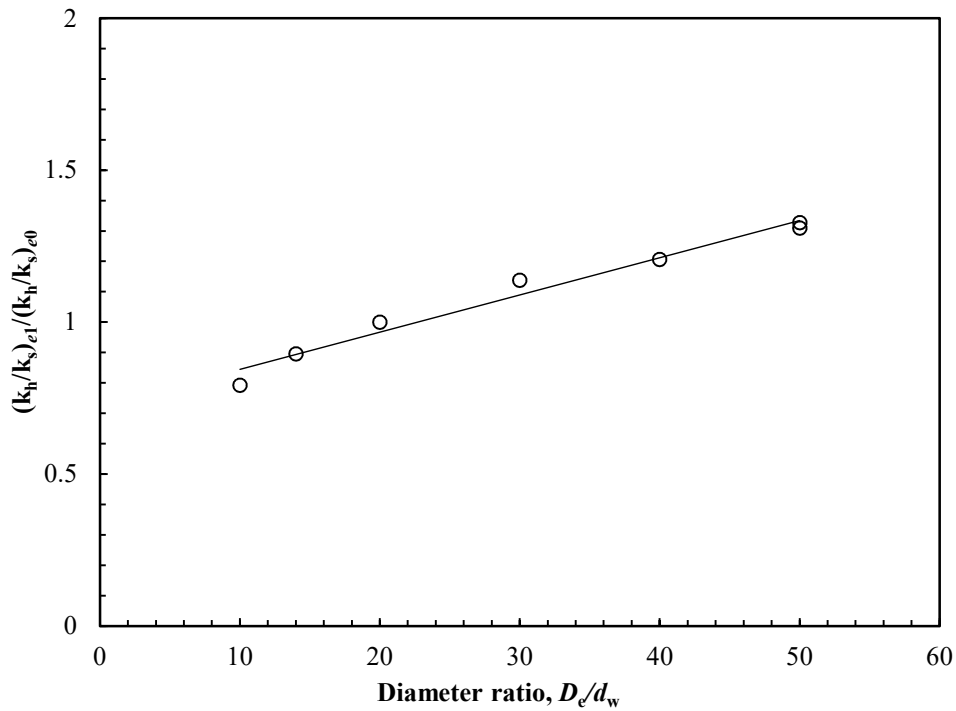


Figure 3.24 $(k_h/k_s)_{e1}/(k_h/k_s)_{e0}$ variation with D_e/d_w of unit cell

In Hansbo's (1981) solution, the smear effect (se) is expressed by the following term:

$$se = (k_h / k_s - 1) \ln(s) \quad (3.5)$$

where $s = d_s/d_w$. The DOC is affected by the value of se . Thus, for a given value of se , the values of both k_h/k_s and s can be changed. Designating value of k_h/k_s for any value of s as

$(k_h/k_s)_e$, and using $s_0 = 4$ and the corresponding value of k_h/k_s for any value of D_e/d_w as $(k_h/k_s)_{e1}$, $(k_h/k_s)_e$ can then be expressed as:

$$(k_h / k_s)_e = \left[(k_h / k_s)_{e1} - 1 \right] \frac{\ln(s_0)}{\ln(s)} + 1 \quad (3.6)$$

(3) Generalised expression for equivalent ‘smear’ effect

Substitute Eq. (3.5) into Eq. (3.6), the final expression for $(k_h/k_s)_e$ will be:

$$(k_h / k_s)_e = \left[\left(0.012 \left(\frac{D_e}{d_w} \right) + 0.72 \right) \left((k_h / k_s)_{e0} \right) - 1 \right] \frac{\ln(s_0)}{\ln(s)} + 1 \quad (3.7)$$

where $s_0 = 4$ and $(k_h/k_s)_{e0}$ from Fig. 3.23.

(4) Variation of $(k_h/k_s)_e$ with degree of consolidation

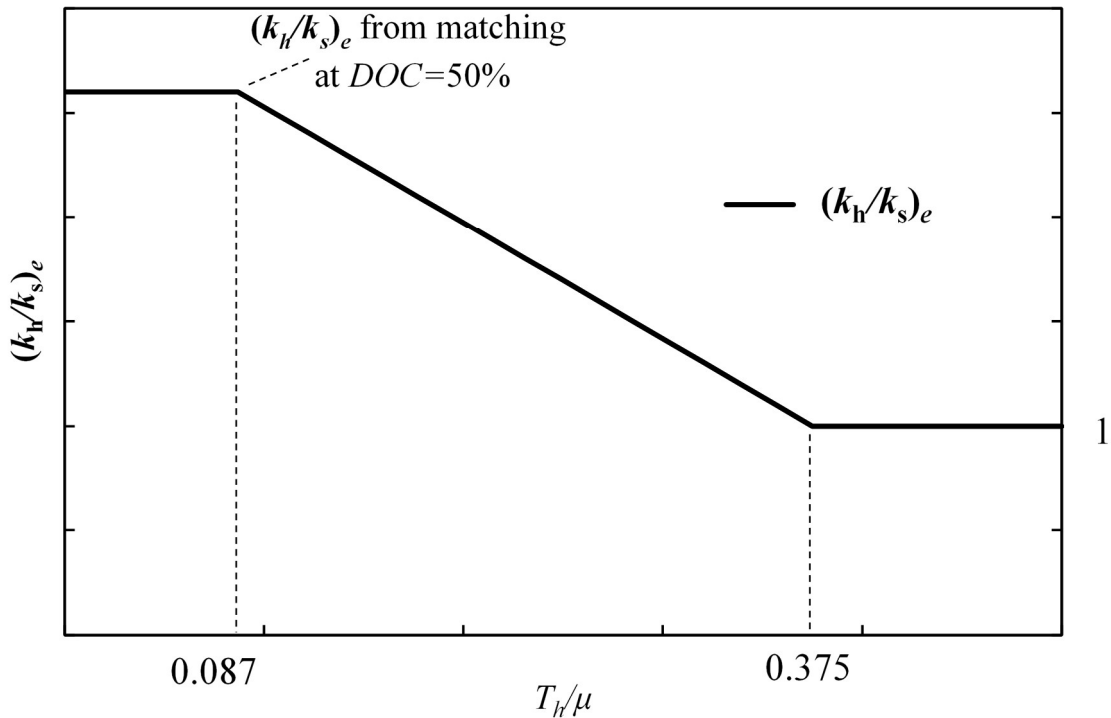


Figure 3.25 Variations of $(k_h/k_s)_e$ with T_h/μ

As shown in Figs. 3.13 and 3.14, the effect of non-uniform consolidation on the permeability ratio (PR) was significant during the early stages of consolidation. Using the

value of $(k_h/k_s)_e$ from Eq. (3.7), the calculation considerably underestimated DOC compared to the FEA results when the average DOC was greater than 50%. To improve the accuracy of the calculated DOC, it is proposed that (1) the value of $(k_h/k_s)_e$ estimated from Eq. (3.7) can only be used for $\text{DOC} \leq 50\%$; (2) when the $\text{DOC} > 95\%$, the effect of non-uniform consolidation on DOC could be ignored, i. e., $(k_h/k_s)_e = 1.0$; (3) for $50\% < \text{DOC} \leq 95\%$, $(k_h/k_s)_e$ linearly varied from the value from Eq. (3.7) to 1.0.

In Hansbo's (1981) solution, the average DOC is controlled by T_h/μ . A $\text{DOC} = 50\%$ corresponded to a $T_h/\mu = 0.087$ and a $\text{DOC} = 95\%$ corresponded to a $T_h/\mu = 0.375$. The proposed $(k_h/k_s)_e \sim T_h/\mu$ relationship is shown in Fig. 3.25. Because the value of μ is a function of $(k_h/k_s)_e$ (Eq. (2.9)), an iteration process is needed to use Fig. 3.25. Designating the current time as t_0 for a given time increment Δt , i. e., $t = t_0 + \Delta t$, the corresponding value of $(k_h/k_s)_e$ can be obtained with the following steps:

(a) Calculate T_h corresponding to time t and μ using $(k_h/k_s)_{e-t_0}$ corresponding to time t_0 , and obtain an initial value of $(T_h/\mu)_0$.

(b) Obtain $(k_h/k_s)_{e-t}$ corresponding to $(T_h/\mu)_0$.

(c) Calculate $\delta = \left| (k_h/k_s)_{e-t_0} - (k_h/k_s)_{e-t} \right|$; if $\delta \leq 0.1$, finish the iteration, and if $\delta \geq 0.1$, put $(k_h/k_s)_{e-t}$ as $(k_h/k_s)_{e-t_0}$, repeat steps (1) and (2). Normally, 1-2 iterations are sufficient.

Assuming $d_s/d_w = 4$, the values of $(k_h/k_s)_e$ from Eq. (3.7) were 2.9 and 2.8 for Case 1 and Case 2, respectively. Considering the variation of $(k_h/k_s)_e$ with DOC, the back-calculated $\text{DOC} \sim \text{time}$ curves are also included into Figs. 3.26 and 3.27 as solid lines. It can be observed that the back-calculated values by the proposed method are close to both the measured and FEA results.

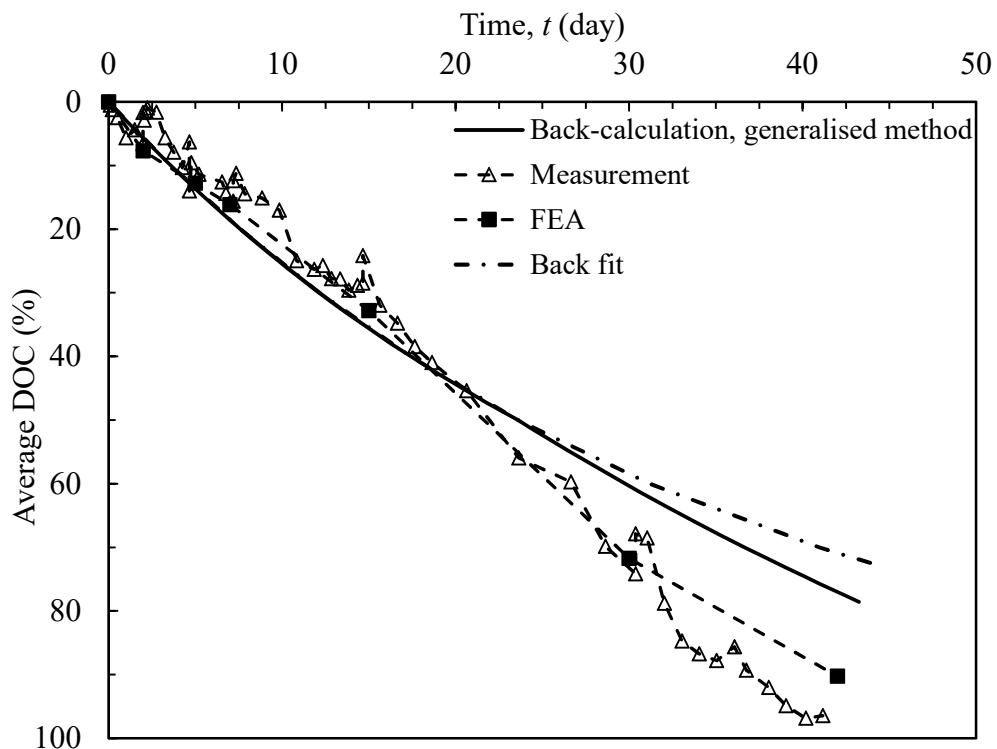


Figure 3.26 Comparison of average DOC for Case 1

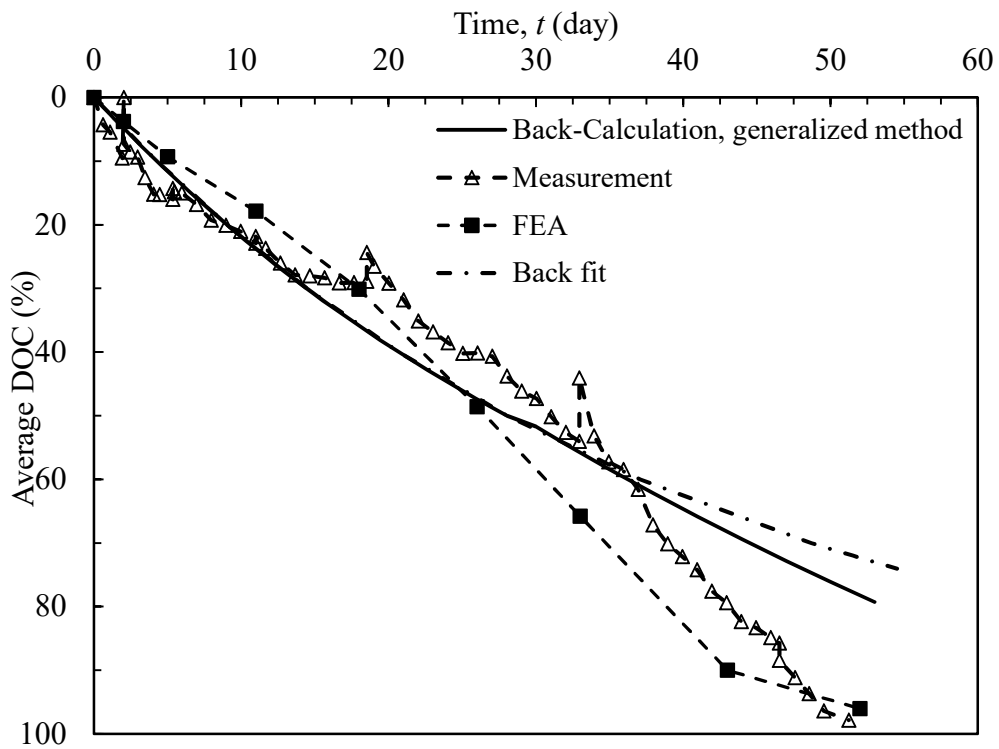


Figure 3.27 Comparison of average DOC for Case 2

(5) Procedure for evaluating equivalent “smear” effect

The following steps can be adopted to evaluate the equivalent smear effect due to non-uniform consolidation:

(a) Calculate the consolidation-induced change of void ratio (Δe) using soil parameters and loading conditions and then calculate the value of $\Delta e/C_k$.

(b) Obtain $(k_h/k_s)_{e0}$ from Fig. 3.23 corresponding to the value of $\Delta e/C_k$.

(c) If s is not 4 and/or D_e/d_w is not 20, calculate $(k_h/k_s)_e$ corresponding to s and D_e/d_w with Eq. (3.7).

(d) Consider the variation of $(k_h/k_s)_e$ with T_h/μ using Fig. 3.25.

(6) Overall smear effect

For a PVD-improved deposit during consolidation process, there is a PVD installation induced mechanical smear effect, and there also is non-uniform consolidation induced apparent “smear” effect. Let us denote the mechanical smear effect as $(k_h/k_s)_m$; the overall smear effect, k_h/k_s , can then be expressed as:

$$k_h / k_s = (k_h / k_s)_m (k_h / k_s)_e \quad (3.8)$$

3.5.2 Application of proposed method

Two field case histories reported by Chai and Miura (1999) and Shen et al. (2005) are collected and the summary of the two cases are as followings:

(1) Case of Chai and Miura (1999):

The project reported by Chai and Miura (1999) are two tests embankments constructed on natural soil and PVD-improved subsoil, respectively. Each test embankment has a total height of 3.5 m which can apply about a surcharge loading of 70 kPa. The soft deposits mainly consists highly compressible Ariake clay, and the main clay layer had a thickness of 15 mm form 6 m to 21 m in depth. The propoties of the main clay layer are listed in Table 3.7. The PVD used in one of the test embankments has a value of $d_s/d_w=6.2$ and $D_e/d_w=35.2$.

(2) Case of Shen et al. (2005):

Two tests embankments constructed on natural soil and PVD-improved subsoil in Hangzhou-Ningbo (NH) express way were reported by Shen et al. (2005). The main clay layer is very soft clay from 5 m to 15 m in depth and the soil properties are shown in Table 4.7. The PVD used has a value of $d_s/d_w=6.7$ and $D_e/d_w=29.7$.

In these two cases, the values of field k_h were back-calculated from the field-measured results of embankments on natural ground. Therefore, the authors believed that the back-calculated k_h/k_s values are reliable. It can be observed that the back-analyzed field values of k_h/k_s are quite large, about 10 and 13.5, respectively. With the method proposed in this study, the evaluated values of $(k_h/k_s)_e$ are (for $\text{DOC} \leq 50\%$) 2.3 and 1.8, respectively. Using equation (3.8), the values of $(k_h/k_s)_m$ are evaluated as 4.3 and 7.5, respectively. These results indicated that (a) even for a uniform and homogeneous clayey soil domain, non-uniform consolidation could cause an equivalent value of $(k_h/k_s)_e \approx 2$ (DOC 50%), and (b) the back-fitted values of k_h/k_s reported in the existing literature may not represent the true mechanical smear effect, but rather the lump sum of the mechanical smear effect and the effect of non-uniform consolidation.

Table 3.7 Summary of case histories analysed

Case No.	Location	Soil profile of main soil layer				Δp kPa	d_s/d_w	D_e/d_w	k_h/k_s	$(k_h/k_s)_e$ (DOC \leq 50%)
		Depth m	γ_{sat} kN/m ³	C_c	e_0					
1	Saga Airport, Japan	6-21	14.5	2.0	2.5	70	6.2	35.2	10	2.3
2	NH expressway, China	5-14	17.3	0.64	1.36	118	6.7	29.7	13.5	1.8

C_k is assumed to be 0.4 e_0 in the calculation of $(k_h/k_s)_e$.

The practical implication of Eq. (3.8) is that the smear effect can be evaluated more reliably and the DOC can be predicted more accurately. In the existing literature, most back-fitted field values of k_h/k_s are much larger than the laboratory measured values. By separating the smear effect into mechanical and non-uniform consolidation-induced components, the mechanical component can be evaluated by laboratory test results. For the two case histories considered, the back-fitted values of k_h/k_s were 10~13.5 (Table 3.7); however, for these two deposits, no published laboratory test results show k_h/k_s values as high as these values. For the case reported by Chai and Miura (1999), the value of $(k_h/k_s)_m$

will about be 4.5, which is closer to the previously published test results (Madhav et al, 1993).

3.6 Summary

The effect of non-uniform consolidation on the average degree of consolidation (DOC) of a prefabricated vertical drain (PVD) unit cell (a PVD and its improvement zone) was investigated through laboratory model tests and finite element analyses (FEA). Based on the results of the tests and the FEA, the following conclusions can be drawn:

(1) From the results of large-scale laboratory model tests, the variation of void ratio and permeability with radial distances have been studied. By analysing the test results, the effect of non-uniform consolidation on the rate of consolidation has been confirmed.

(2) For PVD-induced consolidation, a concept of an equivalent “smear” effect was used to express the effect of non-uniform consolidation on the rate of consolidation. The equivalent “smear” effect can be evaluated by basic soil properties and loading conditions.

(3) A method for considering the effect of non-uniform consolidation in consolidation analysis has been proposed and explicit solution has been established to predict the average degree of PVD induced consolidation. The practical implications of the method is discussed.

CHAPTER FOUR

EFFECT OF NON-UNIFORM CONSOLIDATION ON ONE-DIMENSIONAL PROBLEM

4.1 Introduction

Consolidation problem is a long lasting and essential issue for geotechnical engineering, and the simplest consolidation problem is one-dimensional (1D) one. Numerous researches did plenty of efforts to investigate the rate of 1D consolidation. Terzaghi (1923) proposed one-dimensional consolidation theory assuming the value of coefficient of consolidation is a constant. Mesri and Rokhsar (1974) investigated the consolidation problems considering a variation of coefficient of consolidation during consolidation process. While during consolidation process, the degree of consolidation (DOC) within a domain is not uniform. The zone near the drainage boundary always has a higher DOC than that in a zone away from the drainage boundary before average DOC reaches 100%. Therefore, even for an initially uniform domain, during consolidation process it can become non-uniform. However, for a 1D problem, there had been no solution available for considering k_v and m_v variation with location in the domain (z) and time (t) so far.

In this chapter, firstly, the effect of non-uniform consolidation on average DOC of 1D consolidation is investigated by laboratory model test, and then analyzing the laboratory model consolidation test analytically and numerically. Then a series of finite element analyses (FEAs) for one soil layer system and two-soil layer system have been conducted to quantify the effect of non-uniform consolidation and linked the effect with basic soil parameters and stress conditions. Finally a pragmatic method has been proposed to consider the effect of non-uniform consolidation into Terzaghi's 1D consolidation theory.

4.2 Experimental investigation one soil layer system

4.2.1 Test device and soil

4.2.1.1 Test for one layer system

The test device used is illustrated in Fig. 4.1. The device primarily consists of a steel consolidation chamber with 30 cm in height, 25 cm in diameter and a loading system using air pressure and a piston. Porous stones were set on the top and bottom of the soil sample to provide drainage. And the bottom drainage can be closed by switching off the valve 1 and the excess pore water pressure can be measured at the bottom.

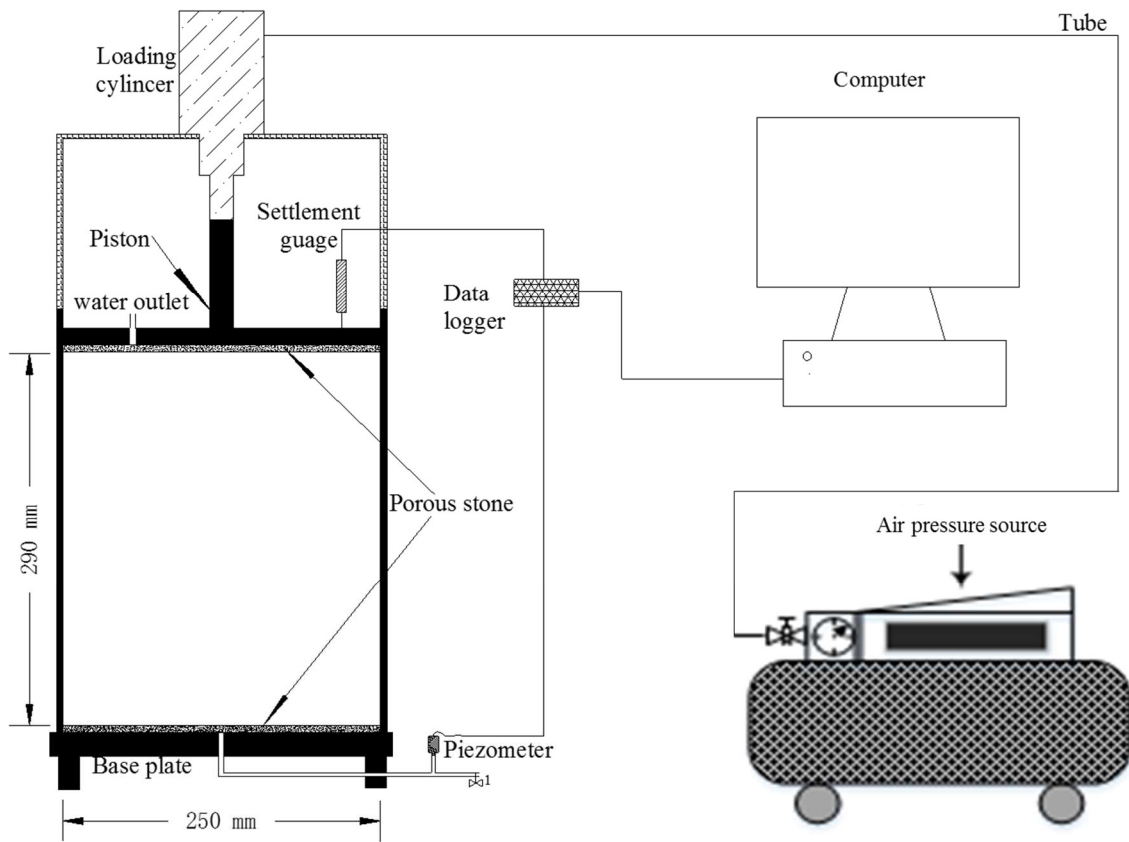


Figure 4.1 Illustration of device used in model test

The soil used in the model test is a remoulded Ariake clay. The basic properties of the clay are listed in Table. 4.1. The compression index (C_c) and swell index (C_s) were obtained from conventional incremental loading (IL) oedometer test. The relationship between void ratio (e) and permeability (k_v) from IL oedometer test are shown in Fig. 4.2. The measured variation of permeability (k_v) with e followed the Taylor (1948) equation well and the value of C_k is 1.2 was back-fitted. The point with dashed line is extrapolated to get the value of k corresponding to the initial water content. The initial water content

(w_0) of the slurry used was controlled to be 1.2 times the liquid limit and the initial void ratio was evaluated as $e_0 = G_s \cdot w_0$ by assuming the value of specific gravity, $G_s = 2.65$ and the degree of saturation is 100%.

Table 4.1 Properties of remoulded soil in model test

Properties	Values
Specific gravity, G_s	2.65
Liquid limit, w_l : (%)	117
Plastic limit, w_p : (%)	54.4
Compression Index, C_c	0.702
Swell Index, C_s	0.078
C_k	1.20
Initial void ratio, e_0	3.71
Initial height, h_0 : (mm)	290

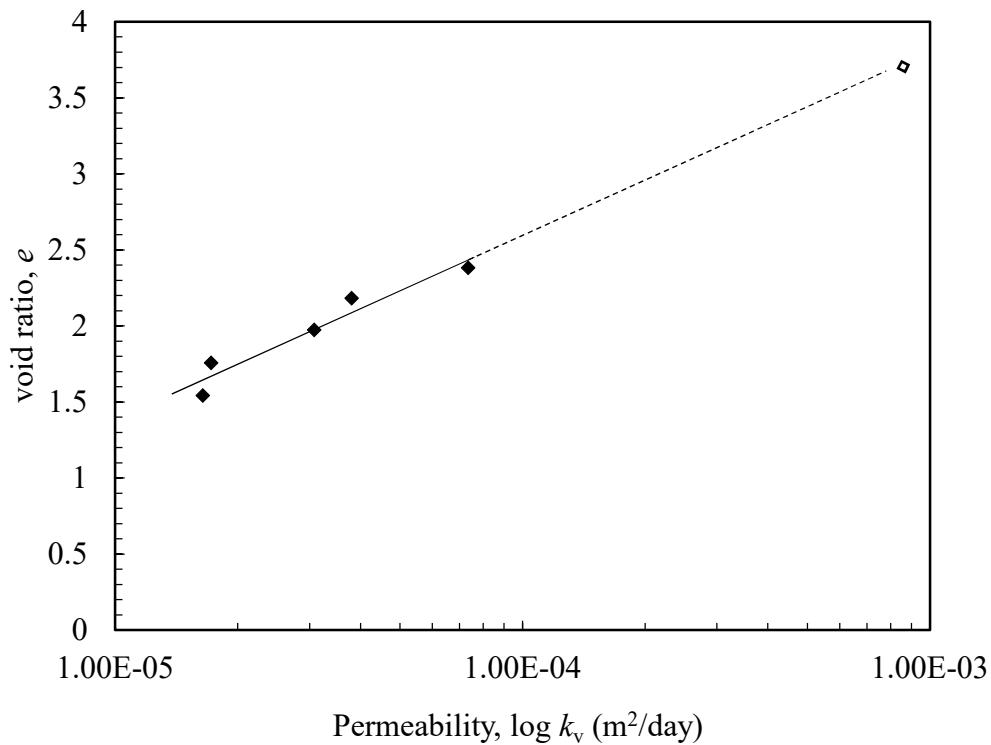


Figure 4.2 Variation of permeability with void ratio

4.2.1.2 Test for two-layer system

4.2.2 Test procedure

For one layer system:

(a) Apply silicon grease: The silicon grease was smear on the inner wall of the chamber to reduce the friction.

(b) Set-up model ground: A sheet of filter paper was put on the top of bottom porous stone. The remoulded soil slurry was put into the steel consolidation chamber layer by layer carefully to a total thickness of 290 mm. Then a sheet of filter paper was put on the top of the model ground.

(c) Set-up loading system: The loading system was installed and the settlement gauge was set on the top of the piston plate to measure the surface settlement. The photo of the model test are as Fig. 4.3



Figure 4.3 Photo of the model test

(d) Pre-consolidation test. A preloading pressure of 10 kPa was applied to preload the model ground under two-way drainage condition.

(e) Consolidation-test. After the pre-consolidation was finished (checking the settlement-log time curve), the bottom valve 1 was closed to allow the consolidation test to be under one-way drainage condition. An incremental load of 100 kPa was applied and started the consolidation test. During this process, the pore water pressure at the bottom of the model was monitored.

For two-layer system:

4.2.3 Test results

The measured settlement-time curve of model test are shown in Fig. 4.4. It can be seen that the primary consolidation finished at around 17 day and then the consolidation-test started and finished at about 47 days. The measured pore pressure at the bottom during the stage of consolidation test are shown in Fig. 4.5. The measured results of settlement and pore water pressure will be used to compare with the results from finite element analysis (FEA) in latter section.

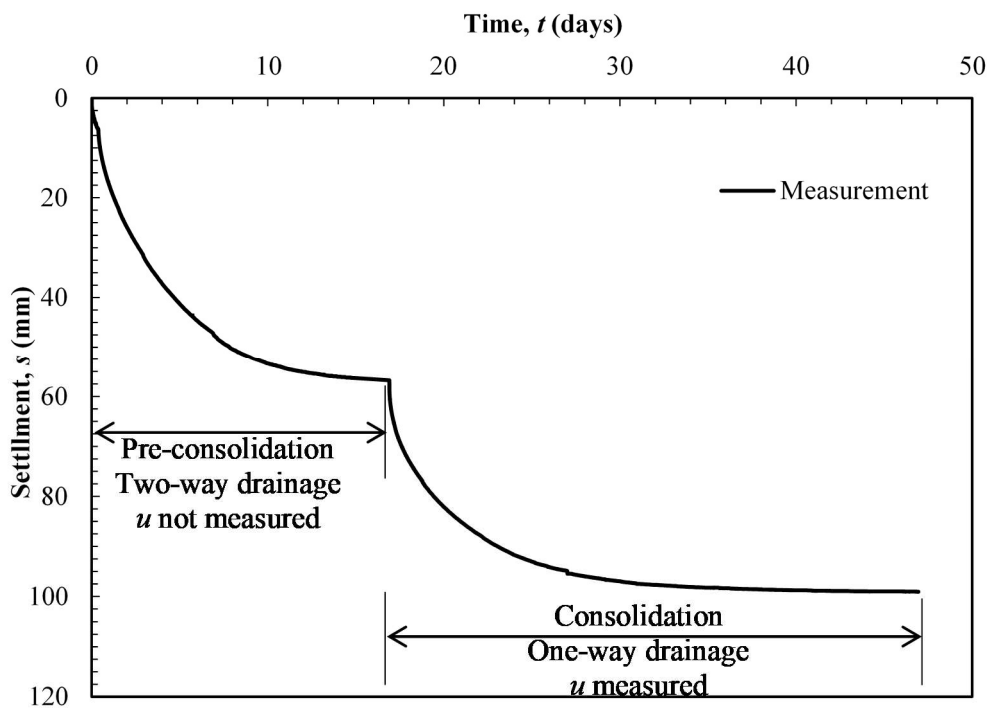


Figure 4.4 Measured settlement-time curve of model test

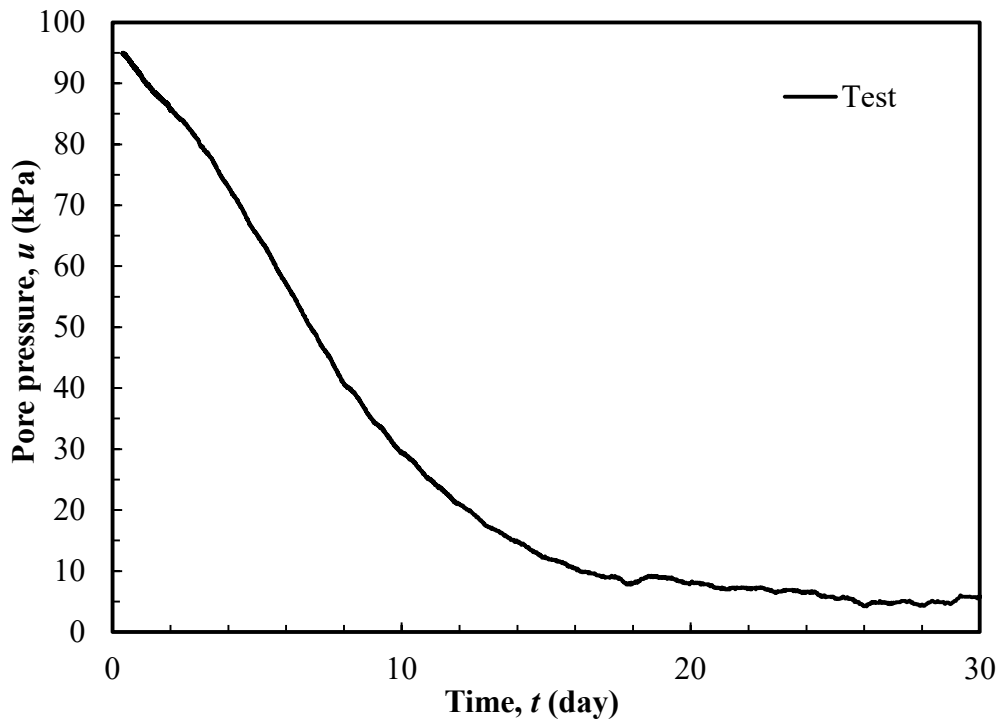


Figure 4.5 Measured pore water pressure at bottom for consolidation test

4.3 Numerical investigation one soil layer system

4.3.1 Simulating model test

4.3.1.1 Model used

The model test was simulated by FEA. The model and the mesh used in FEA are shown in Fig. 4.6. The soil was represented by 15-node triangular elements with excess pore water pressure degree of freedom at all nodes. The soft soil model (SSM) (Plaxis, 2012) was adopted to represent the mechanical behavior of the soil. Except the soil parameters listed in Table 4.1, the internal friction angle of soil, $\phi' = 30^\circ$, and coefficient of at-rest earth pressure under normally consolidated state, $K_0^{NC} = 0.5$ were adopted. The drainage and boundary conditions are also shown in Fig. 4.6. The permeability variation with void ratio was considered using Taylor' (1948) equation (Eq. (2.26)). The initial permeability corresponding to $e_0 = 3.71$ was extrapolated from Fig. 4.2 (dash line) and $k_{v0} = 7.2 \times 10^{-4}$ m/day.

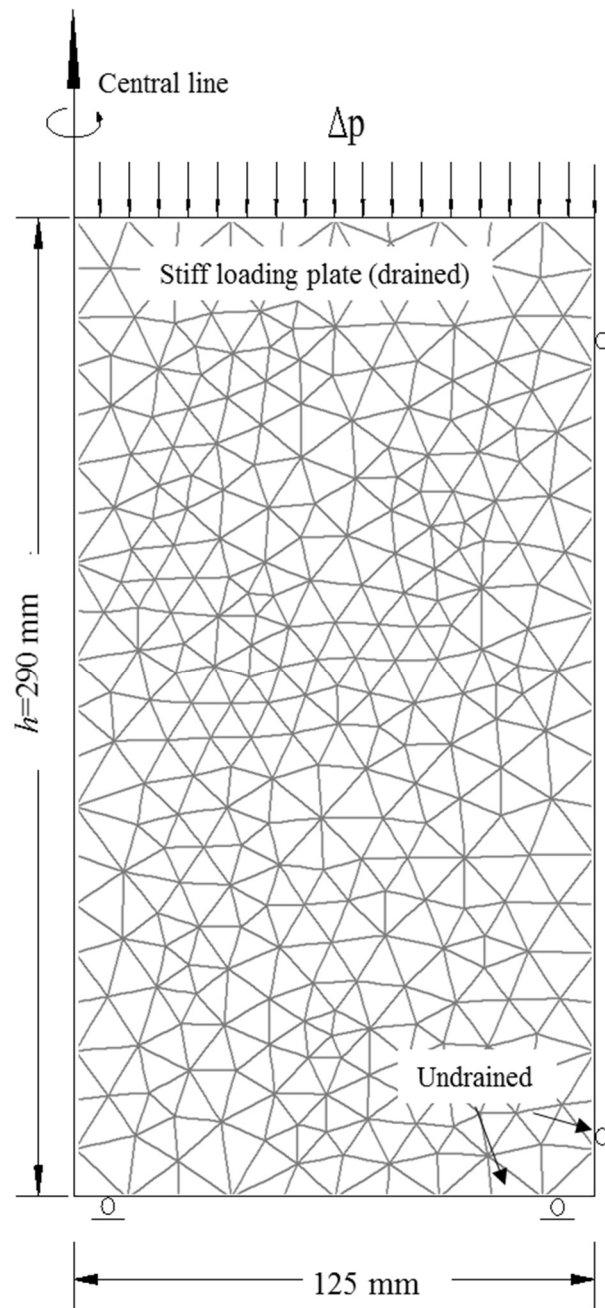


Figure 4.6 Model used in FEA

4.3.1.2 Simulation results

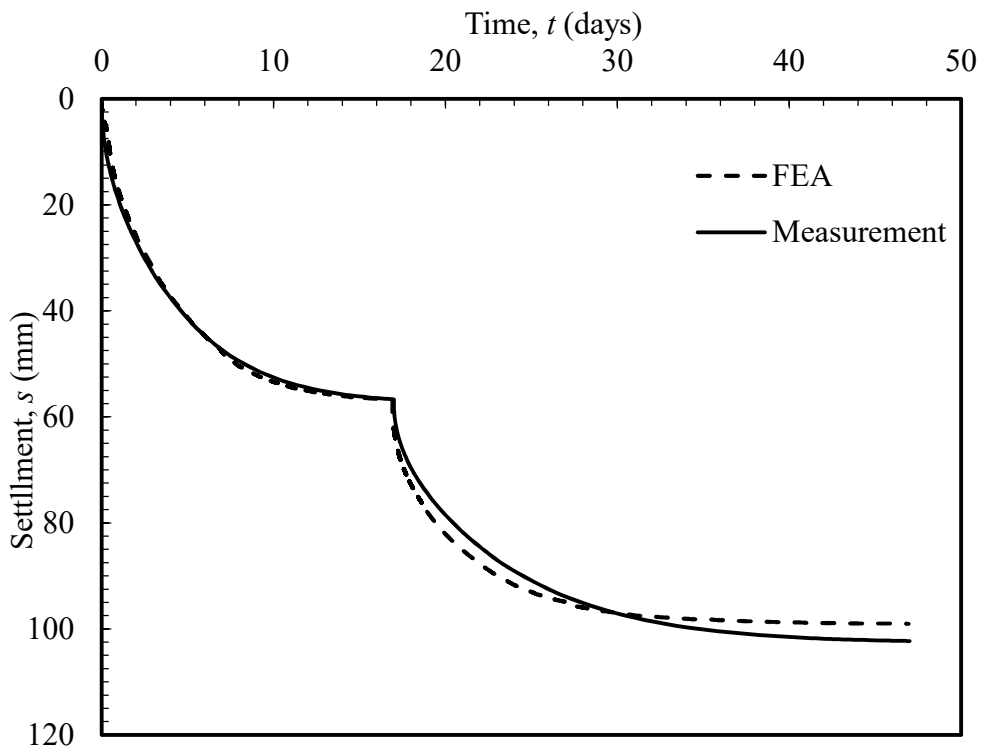


Figure 4.7 Comparison of settlement from FEA and model test

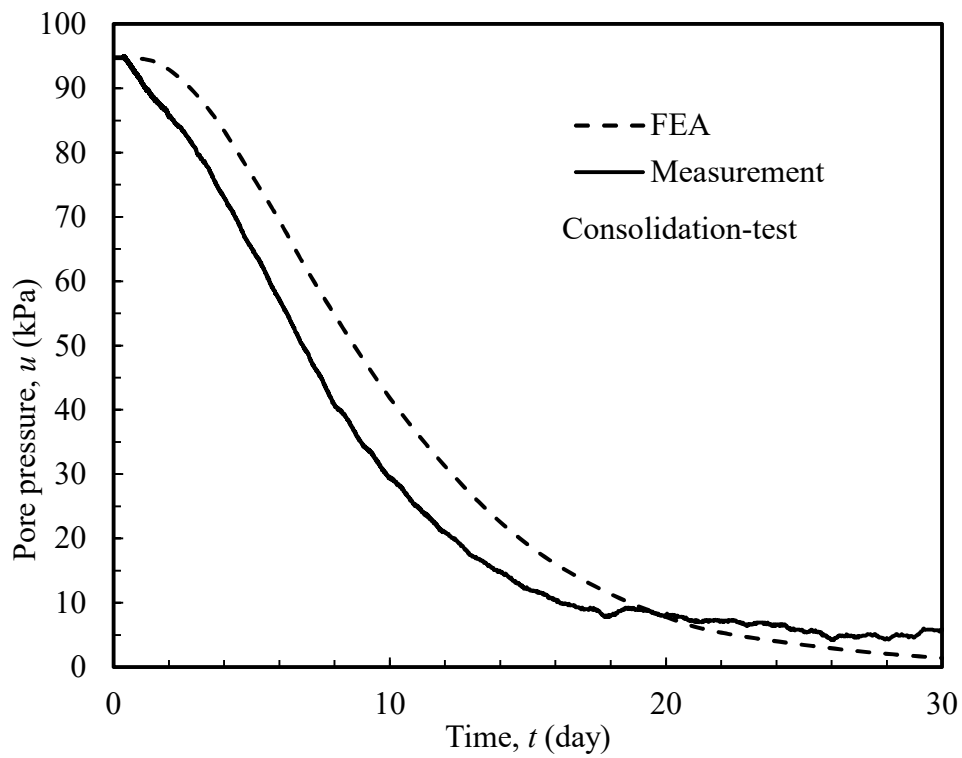


Figure 4.8 Comparison of pore pressure from FEA and test results

The measured and simulated settlement-time curve of the model test are shown in Fig. 4.7. It can be seen that the FEA simulated the measured result of the model test well for both pre-consolidation and consolidation test. For simulating the pre-consolidation process, an initial vertical effective stress of 0.25 kPa was assumed in the model ground.

The measured and simulated excess pore water pressures at the bottom of the model ground for consolidation-test are compared in Fig. 4.8. For the period of elapsed time less than about 18 days, the simulated pore water pressures are higher than the measurements and the reason is not clear yet. Nevertheless, it is considered that FEA fairly simulated the test results.

4.3.1.3 Analysis of average degree of consolidation

The simulated excess pore water pressures of consolidation test was used to calculate the average degrees of consolidation (DOC). The results of average DOC from FEA are plotted in Fig. 4.9. The average DOCs of consolidation test were also analyzed by Terzaghi's one dimensional consolidation theory. In the theoretical analysis, the representative coefficient of consolidation, c_v for consolidation test is needed. In order to calculate the value of c_v , the initial permeability (k_{v0}) and initial void ratio (e_0) corresponding to the beginning of the consolidation-test (end of primary pre-consolidation) have to be evaluated. The pre-consolidation induced a settlement of 56 mm, and after that the thickness of the model ground, $h_0 = 234$ mm and the void ratio, $e_0 = 2.83$. The value of k_0 corresponding to $e_0 = 2.83$ can be obtained by Taylor's (1948) equation (Eq. (2.26)) and $k_{v0} = 1.6 \times 10^{-4}$ m/day. The value of c_v for consolidation-test can be calculated as:

$$c_v = \frac{2.3(1+e)k_v p'}{C_c \gamma_w} \quad (4.1)$$

where k_v is the average permeability corresponding to average void ratio (e) of consolidation-test. The average void ratio e was obtained at mean consolidation stress, p' which is calculated as (JSA 2000a, 2000b):

$$p' = \sqrt{p'_f \times p'_0} \quad (4.2)$$

where p'_0 and p'_f are the initial and final consolidation stresses of the consolidation-test, respectively. In this model test, $p'_0 = 10$ kPa and $p'_f = 110$ kPa. With a constant value of c_v

the average DOCs were calculated and shown in Fig. 4.9. Terzaghi's theory over-predicted the rate of consolidation and the maximum difference between the analytical and FEA results is about 20%.

In order to back fit the average DOC of FEA by analytical solution, a reduction of the value of c_v is needed. Assuming $c_{v1} = \alpha_1 c_v$ ($\alpha \leq 1.0$) and use c_{v1} in the theoretical analysis. To match the time for average DOC = 50% by both the FEA and the theoretical analysis, a α_1 value of 0.6 was back-estimated. This back-fitted result is designated as Back-fitted-1 and also plotted in Fig. 4.9. It can be seen that up to 50% DOC, the Back-fitted-1 agrees with the results from FEA well. However, when DOC is larger than 50%, Back-fitted-1 under-estimated the DOC compared to that from FEA significantly.

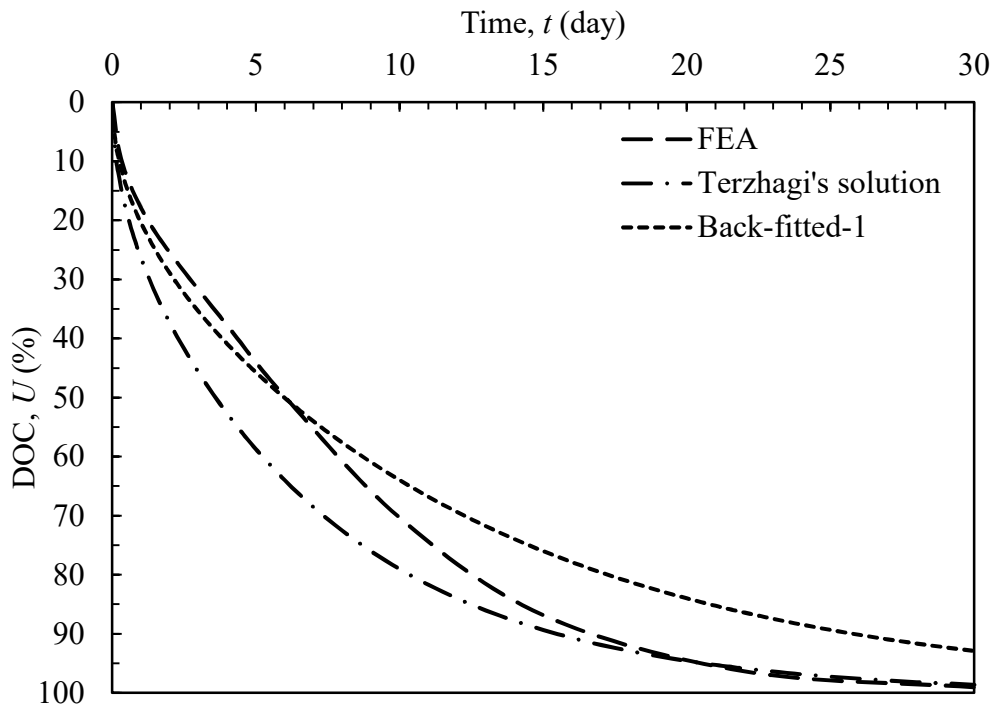


Figure 4.9 Average DOC from FEA and analytical results

4.3.2 Influence of drainage length

Five one-dimensional consolidations with different drainage length under one-way drainage condition were simulated numerically using the model shown in Fig. 4.6. The main soil properties are listed in Table 4.2.

Table 4.2 Parameters used for numerical simulations

No.	C_c	e_0	p'_0 :kPa	Δp :kPa	k_v : 10^{-4} m/day	h_0	C_k : $0.47 e_0$
1	1	2.5	10	100	6	1	1.17
2						2	
3						3	
4						4	
5						5	

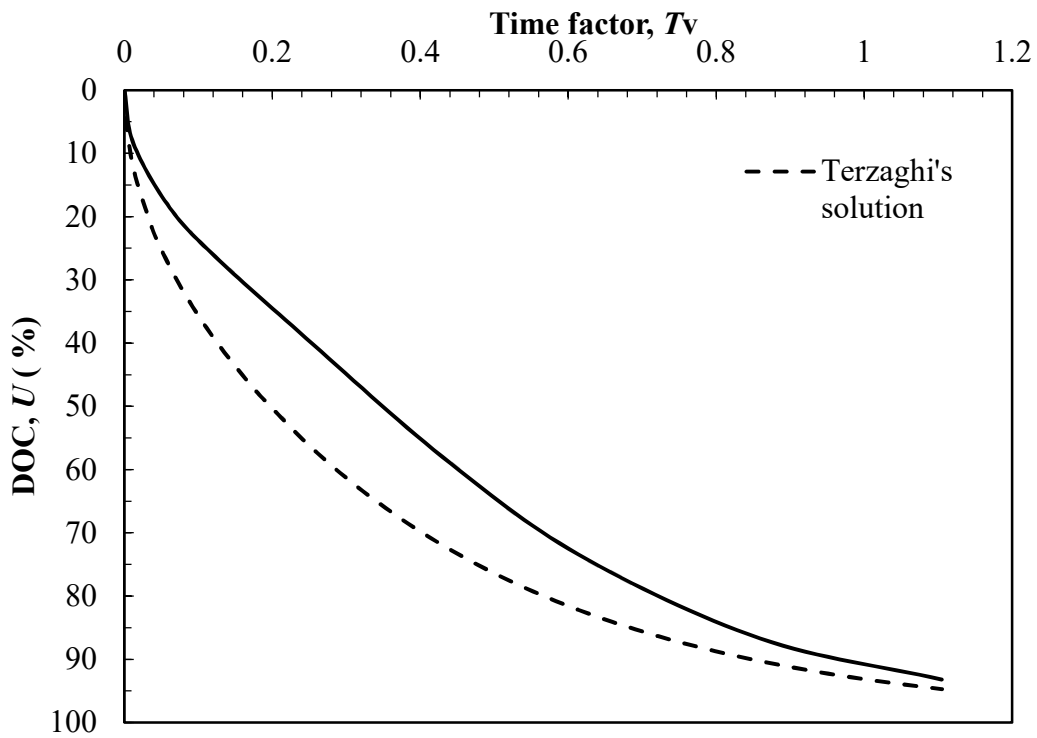


Figure 4.10 Comparison of T_v versus DOC relationships for all cases

For each case, the average DOC was calculated from the simulated excess pore water pressures as well as by Terzaghi's 1D consolidation theory. In the theoretical analysis, the representative values of the coefficient of consolidation were evaluated by Eqs (4.1) and (4.2). The value of C_k was determined to result in a constant value of coefficient of consolidation. For all the cases, the results are shown in Fig. 4.10. Compared with the results from Terzaghi's consolidation theory, the effect of non-uniform consolidation reduced the rate of consolidation significantly. Further it can be seen that the degree of the effect of non-uniform consolidation on the average DOC is not a function of drainage

length. This indicates that even for a soil sample of oedometer test (with a drainage length of about 10 mm), the average DOC will be influenced by the non-uniform consolidation. Then there is a practical question that does the interpreted value of c_v from the results of an oedometer test represent the true value of the soil sample?

4.3.3 Numerical simulation of incremental load oedometer test

The coefficient of consolidation (c_v) can be determined from the settlement-time curve of incremental load (IL) oedometer test by either root-time (\sqrt{t}) method (Taylor, 1948) or log-time ($\log(t)$) method (Casagrand and Fadum, 1940). These two methods can result in more or less the similar value of c_v (e.g. Stickland et al. 2005)

It is well known that there are two definitions about DOC. One is defined by excess pore water pressure (u) (DOC_u), and another is by settlement (DOC_s). For a soil, when it behaves elastically, these two definitions give the same value of DOC. While when a soil behaves elasto-plastically, the two definitions will result in different values of DOC, and normally, DOC_s > DOC_u. Adopting a linear e -log (p') relationship, for a standard IL consolidation test, the consolidation load increment is the same as the already applied effective consolidation stress. With this loading condition, for each load increment, the theoretical difference between DOC_s and DOC_u is shown in Fig. 4.11. It can be seen that the maximum difference is about 9% occurred at DOC_u \approx 40%.

In IL consolidation test, pore water pressure is not measured, the value of c_v is determined from measured settlement – time curve, i.e. using DOC_s. Since DOC_s > DOC_u, c_v evaluated from DOC_s will be higher than that from DOC_u if u would be measured. While in all consolidation theories, the DOC is defined using u (i.e. DOC_u).

The non-uniform consolidation will have an influence on the measured settlement curve. As a tendency, it will reduce the settlement rate at the earlier stage of the consolidation. It is possible that the measured DOC_s is closer to an idea DOC_u (not affected by the non-uniform consolidation). Even though the effect of the non-uniform consolidation is neither considered implicitly nor explicitly in the process of evaluating the value of c_v . Further the effect of non-uniform consolidation is a function of compressibility, rate of changing permeability (k_v) with e of a soil and the state of initial effective stress and the magnitude of load increment.

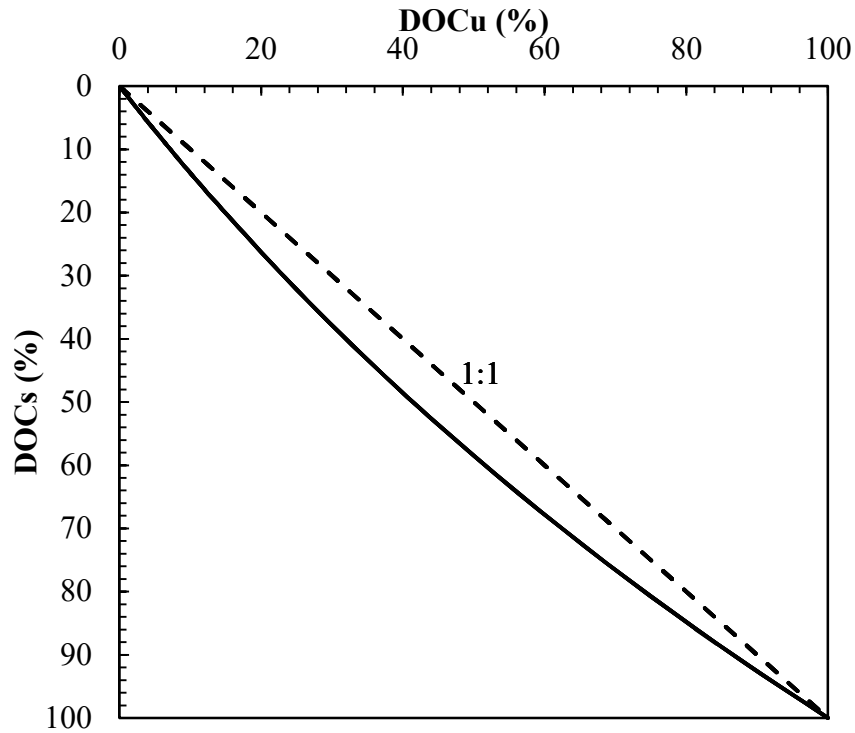


Figure 4.11 Comparing DOCu and DOCs of a load increment in IL consolidation test

Two numerical IL oedometer tests were performed and analyzed. Again, the soil was modeled by SSM and a very fine mesh with an element (15 nodal triangular element) side length of about 1.5 mm was adopted. The boundary conditions were the same as indicated in Fig. 4.6, but the geometry modeled was 10 mm high with a radius of 30 mm. The permeability variation with void ratio was considered in the FEA. The assumed conditions for these two numerical IL tests are listed in Table 4.3. The purposes of the analysis are: (1) comparing the c_v value evaluated using root-time method with the inputted value for the FEA; (2) investigating the effect of non-uniform consolidation on evaluated value of c_v , and (3) comparing the numerically simulated average DOC with that calculated by Terzaghi's consolidation theory using both the inputted and evaluated values of c_v . The evaluated value of c_v by root-time method using the simulated settlement-time curves are listed in Table 4.3 also. The "Inputted" values of c_v were evaluated using Eqs (4.1) and (4.2). The relative errors (RE) were calculated as:

$$RE = \frac{c_{vin} - c_{vev}}{c_{vin}} \quad (4.3)$$

where c_{vin} and c_{vev} are inputted and evaluated values of c_v respectively.

Generally, the evaluated values of c_v are smaller than the inputted values. From Eq. (2.26), it can be seen that the relative change of permeability is a function of $\Delta e/C_k$. For N-1, the value of $\Delta e/C_k$ is about 0.24 and for N-2 it is about 0.06. N-1 has a larger reduction of permeability and a larger effect of non-uniform consolidation on the average DOC. Therefore, the relative error depends on the compressibility of the soil.

Table 4.3 The assumed conditions and results of two numerical IL oedometer tests

Case	C_c	e_0	p'_0 (kPa)	Δp (kPa)	C_k	c_v ($10^{-2}m^2/day$)		RE (%)
						Inputted c_{vin}	Evaluated c_{vev}	
N-1	2.0	2.5	20	20	$0.5e_0$	0.359	0.303	15.6
N-2	0.3	1.5	20	20	$0.5e_0$	2.781	2.671	3.8

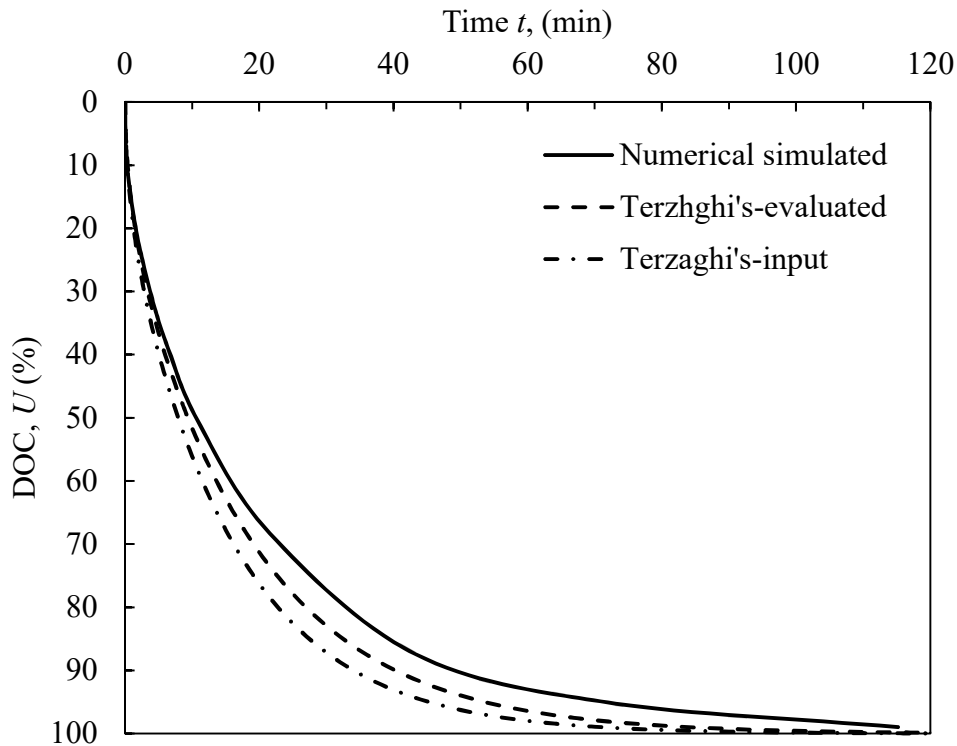


Figure 4.12 Comparison of average DOC with elapsed time for N-1

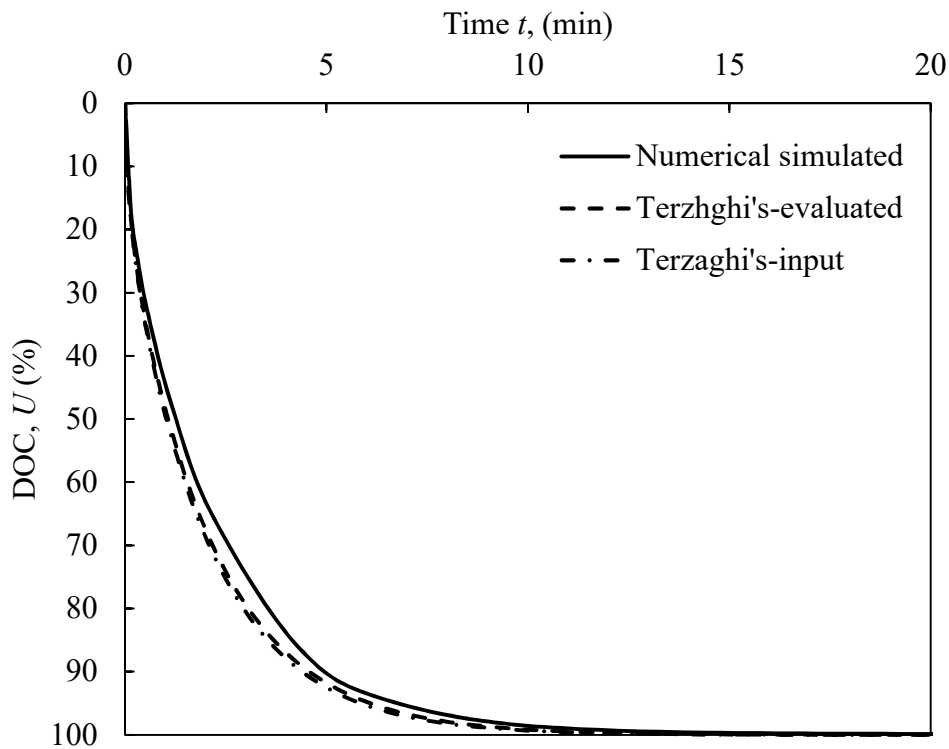


Figure 4.13 Comparison of average DOC with elapsed time for N-2

Another point is that even with the correctly evaluated value of c_v , Terzaghi's theory will over-predict the average DOC. Figs. 4.12 and 4.13 show the comparison of the average DOCs from FEA simulation and Terzaghi's theory using the inputted and the evaluated values of c_v . Using the inputted value of c_v over-estimated the average DOC to a larger extent, especially for case N-1. With the evaluated values of c_v which are smaller than the inputted values, Terzaghi's theory still over-predicted the average DOCs.

4.3.4 Numerical experiments

4.3.4.1 Cases analysed

Totally 29 cases divided into two series (Table 4.4, 4.5) were investigated numerically. Definitions for the two series are as follows:

- (1) Series 1. The model geometry was fixed and the value of C_k was assumed to be $0.4e_0$.

Series 1a: The value of compression index, C_c was varied.

Series 1b. The stress conditions (initial stress, p'_0 and incremental load, Δp) were varied.

(2) Series 2. The value of initial void ratio, e_0 and C_k were varied. While, the model geometry, compressibility of the assumed soil and stress conditions were fixed.

Table 4.4 Parameters used for numerical simulations for Series 1

No.	C_c	e_0	p'_0 :kPa	Δp :kPa	k_v : 10^{-4} m/day	h_0	C_k : $0.4 e_0$
1a	1	0.3	10	100	6.0	2	1.0
	2	0.5	10	100			
	3	1.0	10	100			
	4	1.5	10	100			
	5	2.0	10	100			
1b	1	1.0	5	100			
	2	1.0	20	100			
	3	1.0	30	100			
	4	1.0	50	100			
	5	1.0	75	100			
	6	1.0	100	100			
	7	1.0	10	50			
	8	1.0	10	100			
	9	1.0	10	150			
	10	1.0	10	200			

Table 4.5 Parameters used for numerical simulations for Series 2

No.	C_c	e_0	p'_0 :kPa	Δp :kPa	k_v : 10^{-4} m/day	h_0	C_k : $(0.4-0.6) e_0$
1	1	1.5	10	100	6.0	2	1.29
2		2.5					1.17
3		3.5					1.12
4		1.5					0.60
5		2					0.80
6		2.5					1.00
7		3					1.20
8		3.5					1.40
9		1.5					0.75
10		2.5					1.25
11		3.5					1.75
12		1.5					0.90
13		2.5					1.50
14		3.5					2.1

The numerical results were analyzed focused on the average DOCs. Firstly the DOC from the numerical results was calculated using the simulated excess pore water pressures

in the domain. Then each case was analyzed using Terzaghi's 1D consolidation theory with a reduced value of coefficient of consolidation, $\alpha_1 \times c_v$ (α_1 is a reduction factor). In the analysis, α_1 was varied to yield a result at DOC = 50%, the time is the same as that from the numerical result. And the corresponding value of α_1 is designated as the value for considering the effect of non-uniform consolidation.

4.3.4.2 Effect of compressibility on non-uniform consolidation

Figure 4.14 shows the variation of the value of α_1 with the compression index, C_c from the results of the Series 1a. The value of α_1 decreased with the increase of the value of C_c . This indicates that more compressible a soil is, more significant the effect of non-uniform consolidation on the average DOC will be, as already discussed in the previous section. A softer clay will have a larger reduction of void ratio and therefore the permeability under the same initial stress condition and incremental consolidation pressure. For a softer soil, during the consolidation process, the difference of the permeability of the soil in the zones near and away from the drainage boundary will be larger.

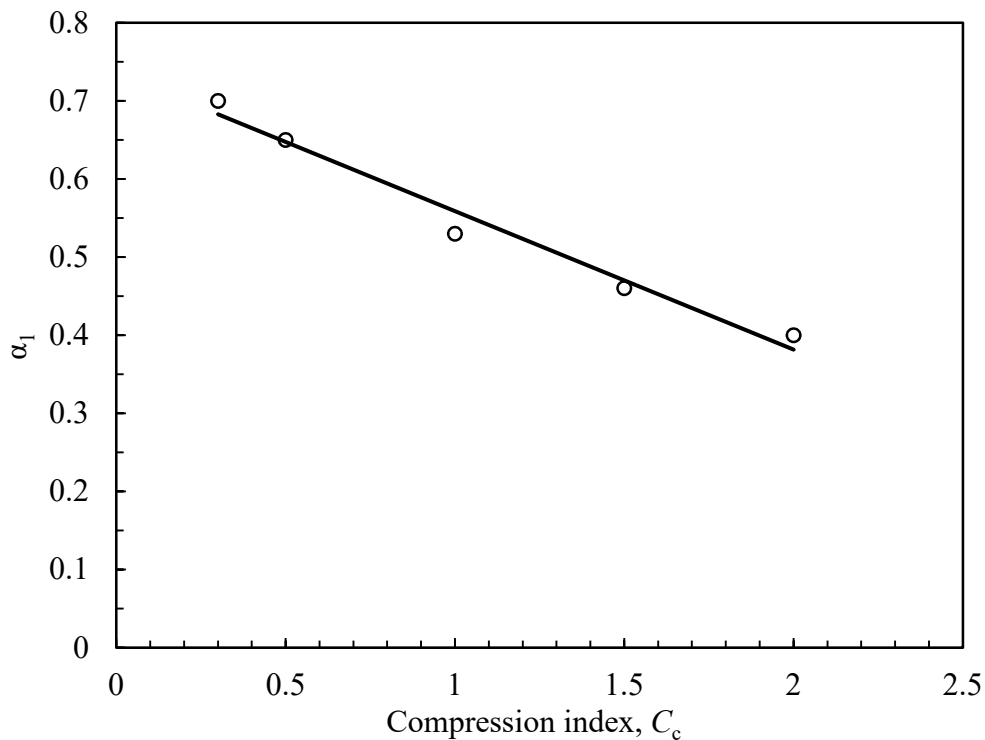


Figure 4.14 Variation of the value of α_1 with the compression index, C_c

4.3.4.3 Effect of stress ratio on non-uniform consolidation

The parameter of stress ratio (SR) is used here to investigate the effect of the initial stress condition and the magnitude of applied incremental consolidation pressure (Δp) and SR is:

$$SR = \log\left(\frac{\Delta p + p_0'}{p_0'}\right) \quad (4.4)(3.3bis)$$

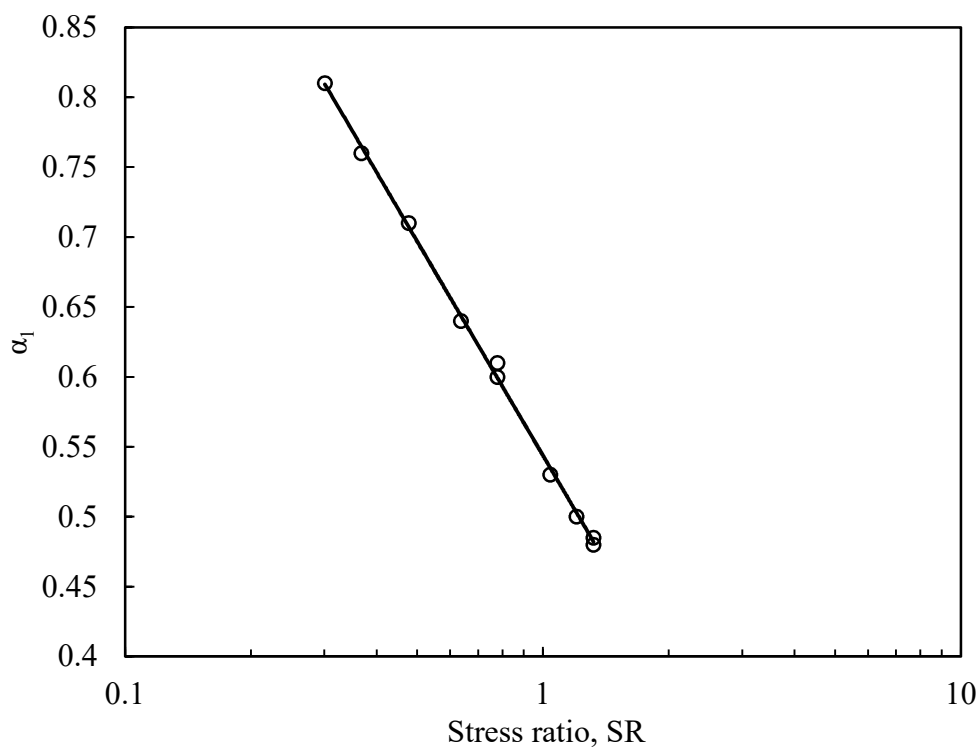


Figure 4.15 Variation of the value of α_1 with SR

Figure 4.15 shows the variation of the value of α_1 with SR from the results of Series 1b. The value of α_1 almost linearly decreased with the increase of SR . For given soil properties, a larger value of SR means a larger reduction of void ratio and permeability. Therefore, a larger incremental stress induces a more significant effect of non-uniform consolidation.

4.3.4.4 Reduction for coefficient of consolidation and $\Delta e/C_k$

Since $\Delta e = C_c \cdot SR$, it is considered that both the effect of C_c and SR can be expressed using Δe . Let's designate the permeability before and after consolidation as k_{v0} and k_{vf} , respectively. The fundamental reason behind the effect of the non-uniform consolidation on the average DOC is caused by the permeability at the zone adjacent to drainage boundary reaching the value of k_{vf} shortly after the commencing of the consolidation, while in other zones the value of permeability may still be k_{v0} . Therefore, the value of α_1 can be related to k_{v0}/k_{vf} . By rearranging Taylor (1948) equation, it can be found that $\log(k_{v0}/k_{vf}) = \Delta e/C_k$. Here Δe is the consolidation-induced reduction of the void ratio which can be calculated using C_c and SR.

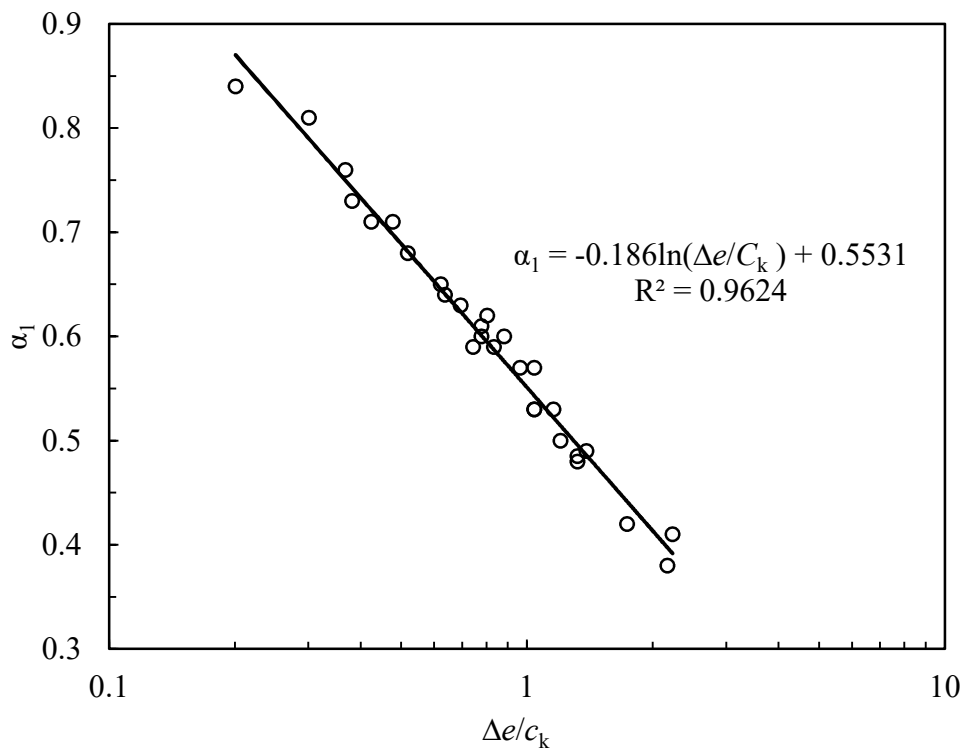


Figure 4.16 Relationship between α_1 and $\Delta e/C_k$

All numerical results are plotted in Fig. 4.16 in the form of $\Delta e/C_k$ versus α_1 in a semi-logarithm form. A very good linear relationship can be obtained, which can be used to predict the value of α_1 with known value of $\Delta e/C_k$.

4.4 Experimental investigation on two-soil layer system

4.4.1 Test device and soil

The equipment used is Maruto multiple oedometer apparatus (Tokyo, Japan) (Chai et al. 2005) consists of five consolidometers which can be used individually or connected internally to form layered system. In this research, two consolidometers were interconnected and used to conduct model tests on two-soil layer system. The soil sample used is 60 mm in diameter and 20 mm in height. The two-soil layer system and equipment for the model test are illustrated as Fig. 4.17. The air pressure is applied onto the water in the chamber and then the water will press the piston to provide vertical load for the soil samples. The bottom of soil layer-1 and top of soil layer-2 is connected through a tube and the pore water can only be drained out from the top surface of layer-1. The settlement and pore water pressure at bottom of each layer can be measured during test.

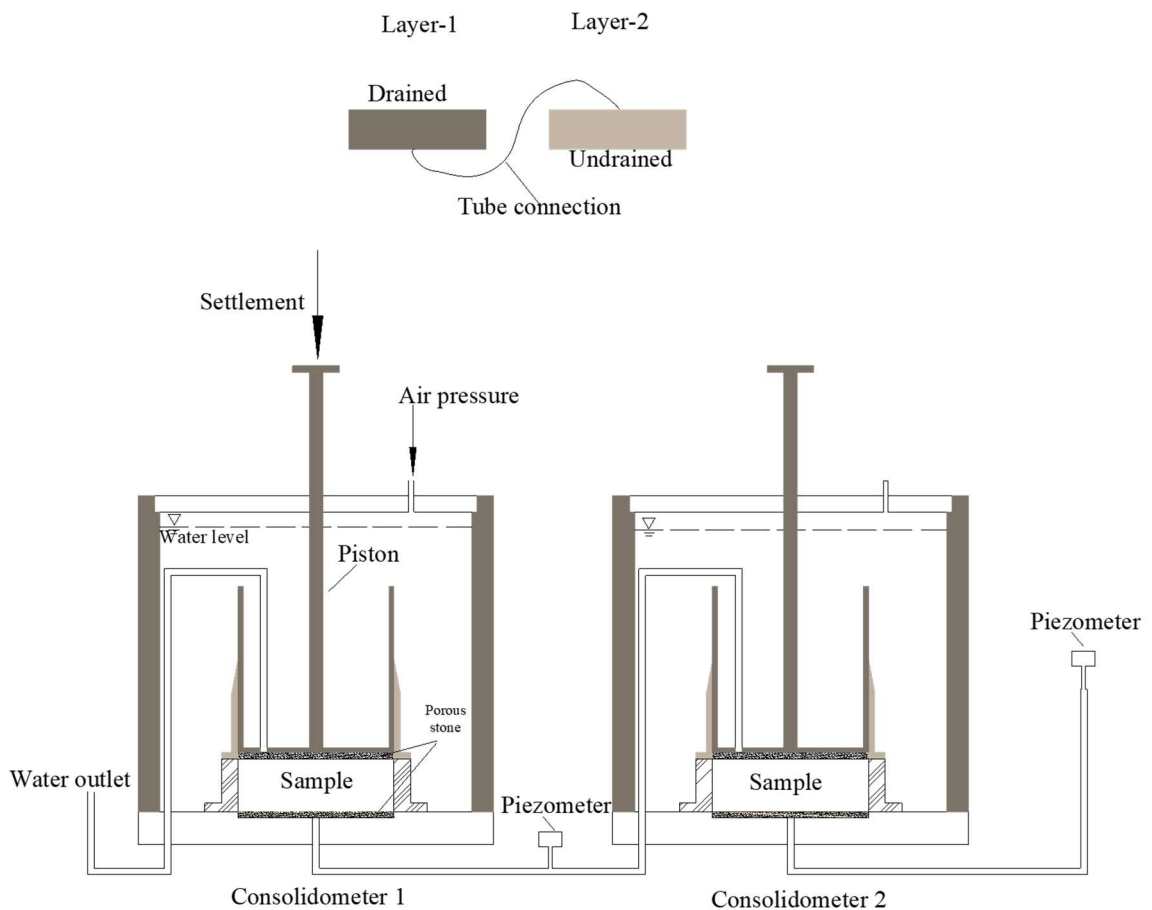


Figure 4.17 Illustration of two soil layer system and equipment for model test

The soils used in the model tests are remolded Ariake clay and Ariake clay/sand mixture. The mixture consists of 50% Ariake clay and 50% sand (passing 2 mm sieve) by dry weight. The compression index (C_c) for clay and clay/sand mixture from oedometer tests are 0.69 and 0.30, respectively. The permeability behaviors of clay used is shown in Fig. 4.18. The relationship between the permeability (k_v) and void ratio (e) is following the Taylor's (1948) equation very well.

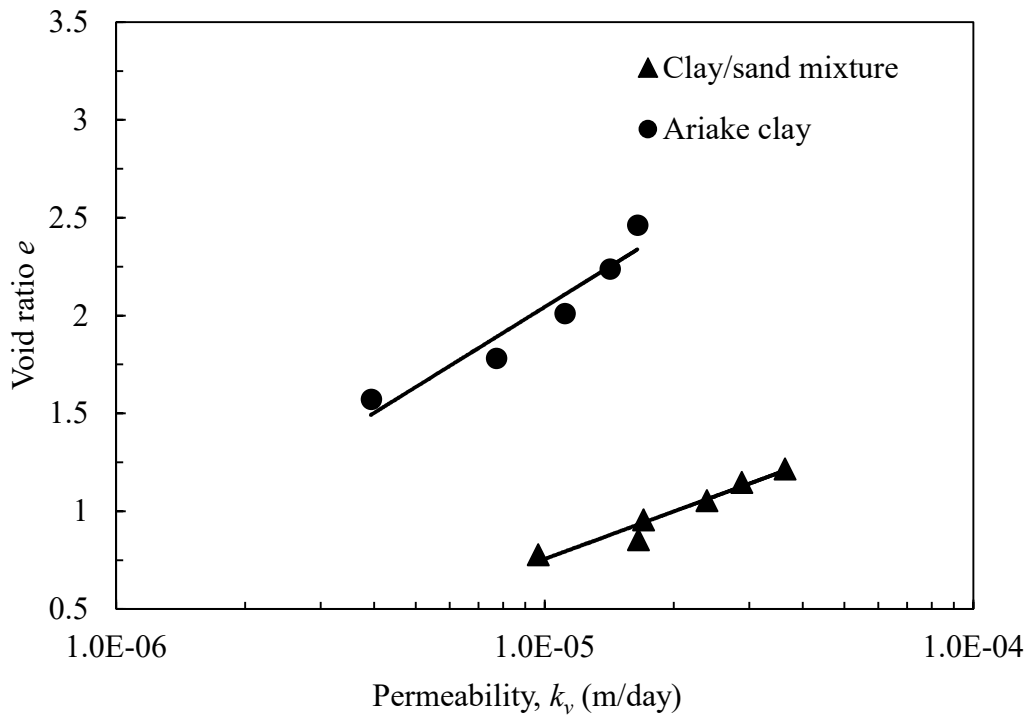


Figure 4.18 Relationship between permeability and void ratio

4.4.2 Test procedure

The test procedures for the model tests of two soil-layer system are as followings:

- (a) Sample preparation: The remolded soil in slurry state was first preloaded to 20 kPa and then cut into samples with a typical height of 20 mm.
- (b) Initial stress recovery: The samples then were moved into the consolidometer cells and started consolidation under 20 kPa and two-way drainage condition. By this step, the soil samples will regain the initial stress of 20 kPa.
- (c) Consolidation test: After the dissipation of the excess pore water pressure, the soil samples are inter-connected and only the top surface of layer-1 is set to be drained

boundary. An incremental loading of 80 kPa was applied to each sample and start the consolidation test. The photo of the model test is shown in Fig. 4.19.

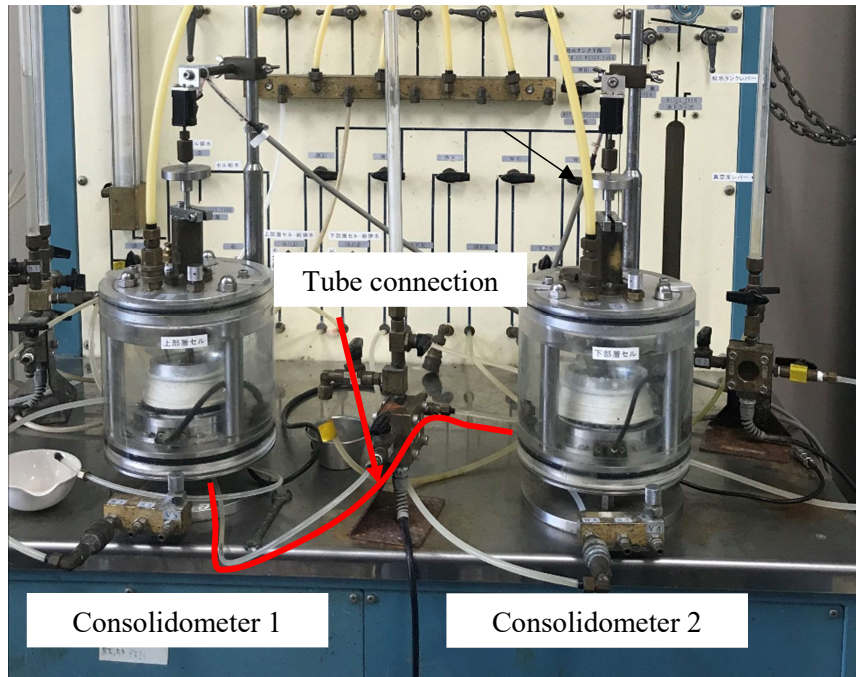


Figure 4.19 Photo of model test for two-soil layer system

4.4.3 Test results

A model test of C-M case was conducted and C-M case refers that the sample of clay located at layer-1 (with drainage) and the sample of mixture located at layer-2.

The excess pore water pressure measured at the bottom of each layer are shown in the Fig. 4.20. The settlement – time (\log) curve for each samples are plotted in Fig. 4.21. It can be seen from the S - $\log t$ curve that the primary consolidation of the sample is finished. The soil layer-2 (mixture sample) started to deform at 13 minute after the beginning of the test. It is believed that the first clay layer had a significant effect of reduction on the rate of consolidation the second layer. The measured pore pressure and settlement will be used to make comparison with FEA results in later section.

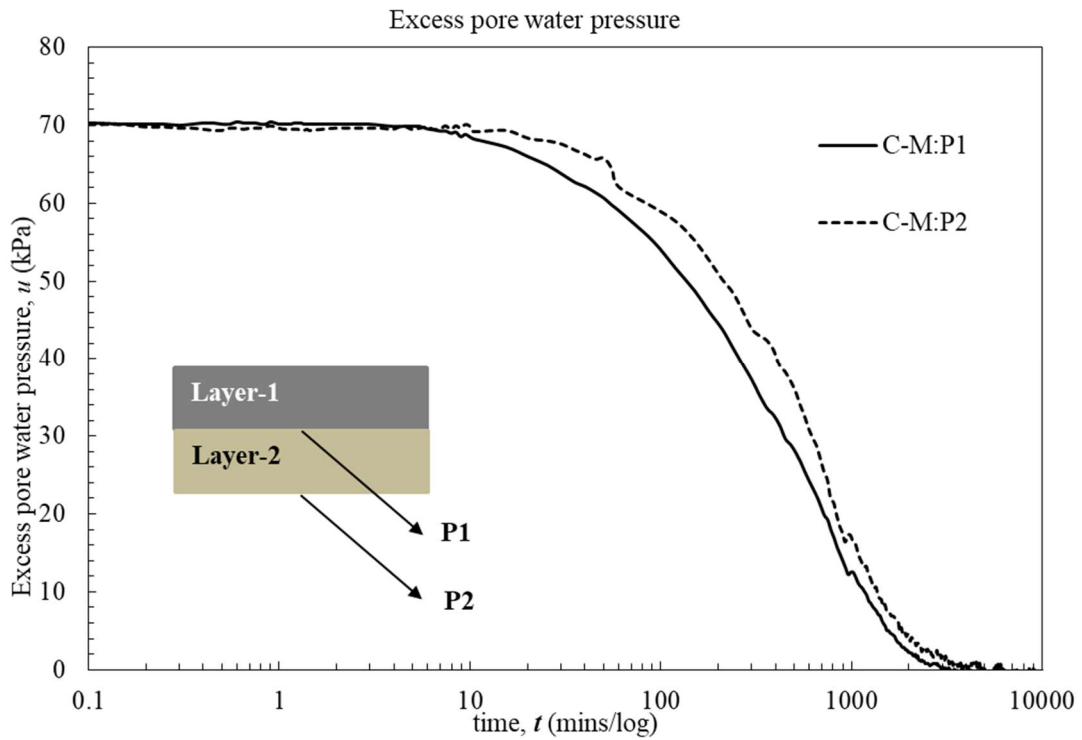


Figure 4.20 Excess pore water pressure measured at the bottom of the soil layer

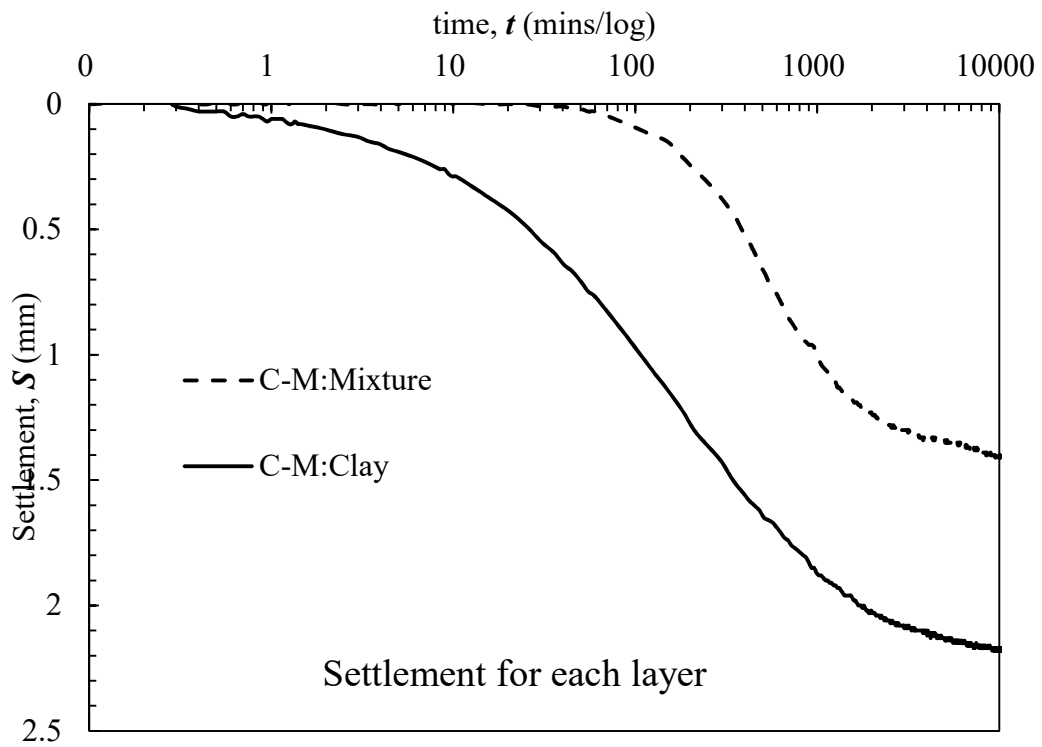


Figure 4.21 Measured settlement for each layers

4.5 Numerical investigation on two-soil layer system

4.5.1 Simulating the test

The model test was simulated by finite element analysis (FEA). The model and mesh used in FEA are shown in Fig. 4.22. Each soil layer has a height of 20 mm and a diameter of 60 mm. The surface of the layer-1 was set to be drained boundary.

The properties of the soils used in FEA are listed in the Table 4.6. The initial void ratio (e_0) was evaluated from the water content measured after the preloading. And the initial permeability (k_{v0}) of both soils were estimated using Taylor's (1948) equation (Fig. 4.18) corresponding to e_0 . Soft soil model (SSM) and Taylor's (1948) equation were adopted in FEA to simulate the consolidation of the model ground.

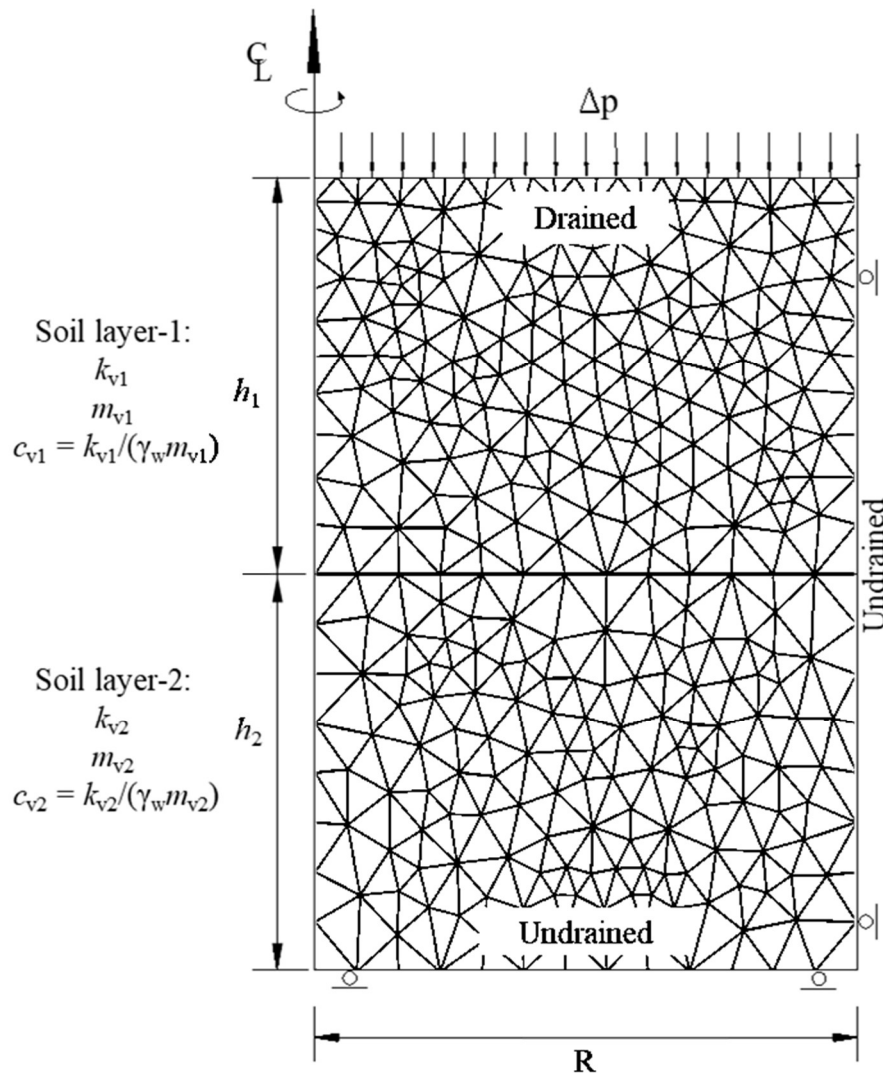


Figure 4.22 The model and mesh used in simulation of model tests

Table 4.6 Properties of soil and loading conditions used in simulation

Case	Soil layer	e_0^*	k_{v0} 10^{-05}m/day	C_c	C_k	p_0 Δp	
						kPa	
C-M	Clay	2.59	2.4	0.69	1.40	20	80
	Mixture	1.43	6.0	0.30	0.72		

* $e_0 = G_s w$, $G_s = 2.67$ is the specific gravity and w is the water content

4.5.2 Simulation results

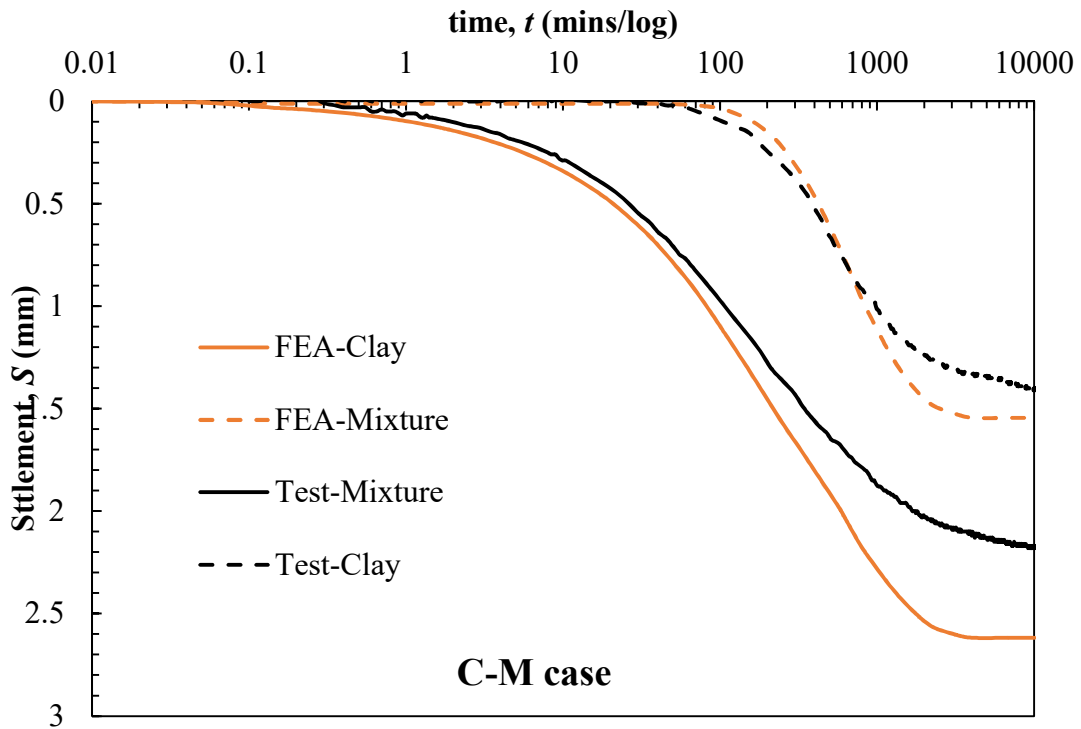


Figure 4.23 Comparison of settlement from test and FEA

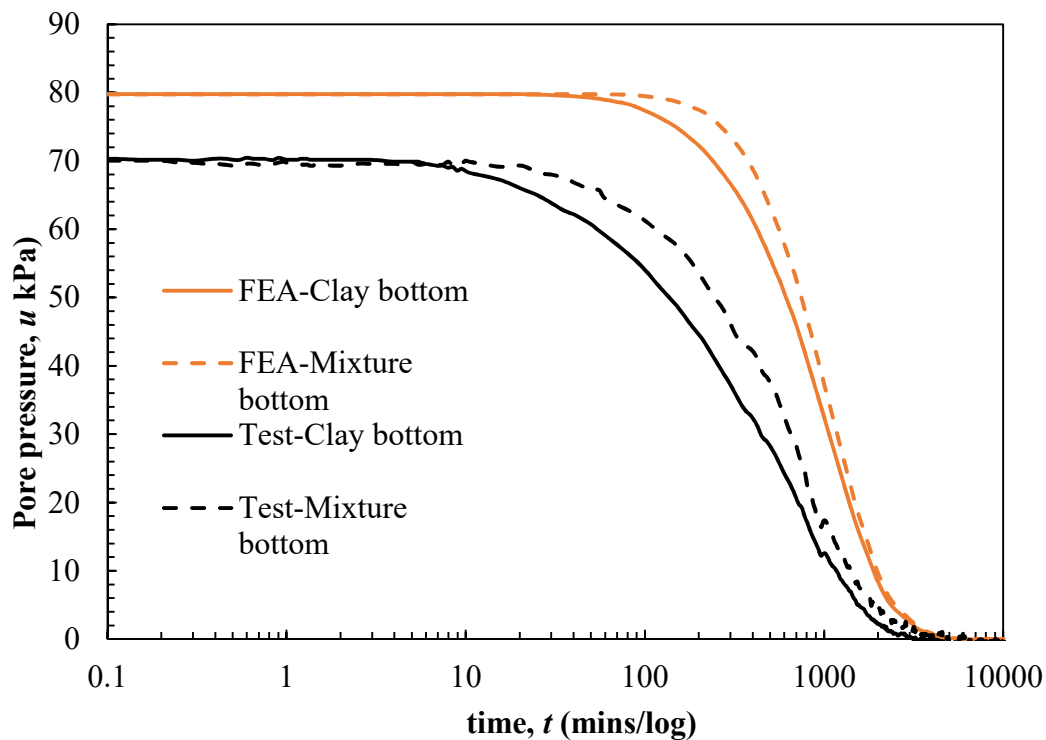


Figure 4.24 Comparison of pore pressure from test and FEA

The comparisons of measured settlement and excess pore water pressure at bottom of soil layer and that from FEA are shown in Fig. 4.23 and Fig. 4.24, respectively. The settlement from FEA and test agreed with each other well, especially for the mixture sample. The FEA also simulated the rate of settlement for both samples very well. The simulated pore pressure is higher than the measured results slightly because the initial maximum value of excess pore pressure (about 80kPa) in FEA is higher than the observed maximum value (70 kPa) in the model test. In the model test, the measured maximum value of excess pore water pressure is lower than the applied stress which maybe due to the unsaturation of the samples. Even through the tendency of pore water pressure from FEA simulated the test results well. As a conclusion, the FEA can give fair simulation of the model tests.

4.5.3 Analysis of the average degree of consolidation

The average degree of consolidation (DOC) was calculated using pore pressures in FEA. And the DOC from FEA was compared with the DOC analyzed by Zhu and Yin's (1999) solution in Fig.4.25. The representative value of permeability (k_v) and coefficient

of volumetric compressibility (m_v) for each layer were evaluated using Eq. (2.26) and Eq. (2.28) at mean effective stress which can be calculated using Eq. (4.2). It is clear the analytical solution over-predict the average DOC of the FEA result. For this C-M case considered in this study, the maximum difference of DOC between the analytical result and FEA result is approximate to 10%.

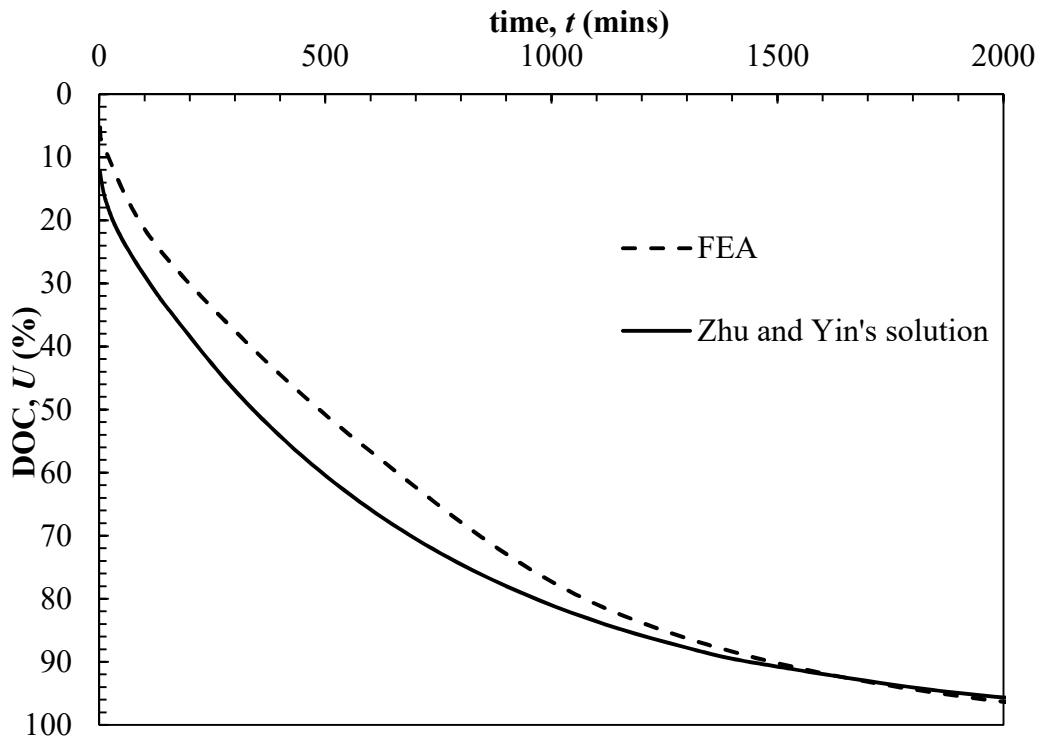


Figure 4.25 Comparison of DOC from FEA and analytical results

4.5.4 Analysis of the average degree of consolidation

4.5.4.1 Cases analyzed

The effect of non-uniform consolidation on the rate of consolidation of two-soil layer system under one-way drainage condition was investigated by finite element analysis (FEA). The model used for FEA is shown as Fig. (4.22). Each soil layer has a height of 1.0 m and a diameter of 2.0 m. The cases simulated were classified in to three series and the parameters used are listed in Tables 4.7, 4.8 and 4.9.

Table 4.7 Parameters used in simulation for Series 1

Case	Layer	C_c	e_0	p'_0 :kPa	Δp :kPa	k_v : 10^{-4} m/day	k_h : 10^{-4} m/day	C_k : (0.4-0.6) e_0										
1	1	0.5	2.5	10	100	1.5	6	60.89										
	2		1.41															
2	1	1.0	2.5	10	100			1.5	6	0.95								
	2		1.5															
3	1	2.0	2.5	10	100					1.5	6	1.00						
	2		1.68															
4	1	0.5	2.5	10	50							1.5	6	0.90				
	2		1.4															
5	1	1.0	2.5	10	150									1.5	6	0.95		
	2		1.53															
6	1	2.0	2.5	10	200											1.5	6	1.03
	2		1.77															
1	1	0.5	2.5	10	100	3	6											0.89
	2		1.41															
2	1	1.0	2.5	10	100			3	6									0.95
	2		1.5															
3	1	2.0	2.5	10	100					3	6							1.00
	2		1.68															
4	1	0.5	2.5	10	50							3	6					0.90
	2		1.4															
5	1	1.0	2.5	10	150									3	6			0.95
	2		1.53															
6	1	2.0	2.5	10	200											3	6	1.03
	2		1.77															
1	1	0.5	2.5	10	100	6	6											0.89
	2		1.41															
2	1	1.0	2.5	10	100			6	6									0.95
	2		1.5															
3	1	2.0	2.5	10	100					6	6							1.00
	2		1.68															
4	1	0.5	2.5	10	50							6	6					0.90
	2		1.4															
5	1	1.0	2.5	10	150									6	6			0.95
	2		1.53															
6	1	2.0	1.77	10	200											6	6	1.03
	2		2.5															
1	1	0.5	1.41	10	100	12	6											0.89
	2		2.5															
2	1	1.0	1.5	10	100			12	6									0.95
	2		2.5															
3	1	2.0	1.68	10	100					12	6							1.00
	2		2.5															
4	1	0.5	1.4	10	50							12	6					0.90
	2		2.5															
5	1	1.0	1.53	10	150									12	6			0.95
	2		2.5															
6	1	2.0	1.77	10	200											12	6	1.03
	2		2.5															

Table 4.8 Parameters used in simulation for Series 2

Case	Layer	C_c	e_0	p'_0 :kPa	Δp :kPa	k_{v1} : 10^{-4} m/day	k_{v2} : 10^{-4} m/day	C_k : (0.4-0.6) e_0
1	$\frac{1}{2}$	1.0	2.5	10	100	1.5	6	1.17
2	$\frac{1}{2}$	1.0	3	10	100			1.14
3	$\frac{1}{2}$	1.0	2	10	100			1.22
4	$\frac{1}{2}$	1.0	2.5	30	100			1.16
5	$\frac{1}{2}$	1.0	2.5	75	100			1.15
6	$\frac{1}{2}$	1.0	2.5	10	50			1.16
7	$\frac{1}{2}$	1.0	2.5	40	150			1.17
8	$\frac{1}{2}$	1.5	2.5	10	100			1.00
9	$\frac{1}{2}$	2.5	3	10	100			1.80
10	$\frac{1}{2}$	1.0	1.5	100	100			1.80
11	$\frac{1}{2}$	1.0	3	10	50			1.16
12	$\frac{1}{2}$	1.1	3	5	120			1.30
1	$\frac{1}{2}$	1.0	2.5	10	100	3	6	1.17
2	$\frac{1}{2}$	1.5	2.5	10	100			1.99
3	$\frac{1}{2}$	1.0	3.0	10	100			1.14
4	$\frac{1}{2}$	1.0	2.0	10	100			1.22
5	$\frac{1}{2}$	1.0	2.5	30	100			1.16
6	$\frac{1}{2}$	1.0	2.5	75	100			1.15
7	$\frac{1}{2}$	1.0	2.5	10	50			1.16
8	$\frac{1}{2}$	1.0	2.3	40	150			1.17
9	$\frac{1}{2}$	1.1	3.0	5	120			1.30
10	$\frac{1}{2}$	1.0	2.5	10	100			1.25
11	$\frac{1}{2}$	1.5	2.5	100	100			1.00

Case	Layer	C_c	e_0	p'_0 :kPa	Δp :kPa	$k_{v1}:10^{-4}$ m/day	$k_{v2}:10^{-4}$ m/day	$C_k: (0.4-0.6)e_0$										
12	1	2.5	3.0	10	100	3	6	1.80										
	2																	
13	1	1.0	1.5	10	100			3	6	0.60								
	2																	
14	1	1.0	3.0	10	100					3	6	1.80						
	2																	
15	1	1.0	2.5	30	100							3	6	1.00				
	2																	
16	1	1.0	2.5	75	100	3	6							1.50				
	2																	
17	1	1.0	2.5	10	50			3	6					1.00				
	2																	
18	1	1.0	2.5	10	150					3	6			1.50				
	2																	
1	1	1.0	2.5	10	100							6	6	1.17				
	2																	
2	1	1.5	2.5	10	100	6	6							1.99				
	2																	
3	1	1.0	1.5	10	100			6	6					1.29				
	2																	
4	1	1.0	3.5	10	100					6	6			1.12				
	2																	
5	1	1.0	2.5	5	100									6	6	1.19		
	2																	
6	1	1.0	2.5	20	100											6	6	1.16
	2																	
7	1	1.0	2.5	30	100													6
	2																	
8	1	1.0	2.5	50	100							6	6					
	2																	
9	1	1.0	2.5	75	100	6	6											
	2																	
10	1	1.0	2.5	100	100			6	6									
	2																	
11	1	1.0	2.5	10	50					6	6							
	2																	
12	1	1.0	2.5	10	150									6	6			
	2																	
13	1	1.0	2.5	10	200											6	6	
	2																	
1	1	1.0	2.5	10	100													12
	2																	
2	1	1.5	2.5	10	100							12	6					
	2																	
3	1	1.0	3.0	10	100	12	6											1.14
	2																	
4	1	1.0	2.0	10	100			12	6			1.22						
	2																	

Case	Layer	C_c	e_0	p'_0 :kPa	Δp :kPa	$k_{v1}:10^{-4}$ m/day	$k_{v2}:10^{-4}$ m/day	$C_k: (0.4-0.6)e_0$																
5	1	1.0	2.5	30	100	12	6	1.16																
	2																							
6	1	1.0	2.5		100			12	6	1.15														
	2																							
7	1	1.0	2.5	10	50					12	6	1.16												
	2																							
8	1	1.0	2.3	40	150							12	6	1.17										
	2																							
9	1	1.1	3.0	5	120									12	6	1.30								
	2																							
10	1	1.0	2.5	10	100											12	6	1.25						
	2																							
11	1	1.5	2.5	100	100													12	6	1.00				
	2																							
12	1	2.5	3.0	10	100															12	6	1.80		
	2																							
13	1	1.0	1.5	10	100																	12	6	0.60
	2																							
14	1	1.0	3.0	10	100	12	6																	1.80
	2																							
15	1	1.0	2.5	30	100			12	6															1.00
	2																							
16	1	1.0	2.5	75	100					12	6													1.50
	2																							
17	1	1.0	2.5	10	50							12	6											1.00
	2																							
18	1	1.0	2.5	10	150									12	6									
	2																							

Table 4.9 Parameters used in simulation for Series 3

Case	Layer	C_c	e_0	p'_0 :kPa	Δp :kPa	$k_v:10^{-4}$ m/day	$k_v:10^{-4}$ m/day	$C_k: (0.4-0.6) e_0$								
1	1	0.5	1.41	10	100	1.5	6	60.89								
	2		2.5													
2	1	1.0	1.5	10	100			1.5	6	0.95						
	2		2.5													
3	1	2.0	1.68	10	100					1.5	6	1.00				
	2		2.5													
4	1	0.5	1.4	10	50							1.5	6	0.90		
	2		2.5													
5	1	1.0	1.53	10	150									1.5	6	0.95
	2		2.5													
6	1	2.0	1.77	10	200	1.5	6									1.03
	2		2.5													
1	1	0.5	1.41	10	100			3	6							0.89
	2		2.5													
2	1	1.0	1.5	10	100					3	6					0.95
	2		2.5													
3	1	2.0	1.68	10	100							3	6			1.00
	2		2.5													
4	1	0.5	1.4	10	50									3	6	0.90
	2		2.5													
5	1	1.0	1.53	10	150	3	6									0.95
	2		2.5													

Case	Layer	C_c	e_0	p'_0 :kPa	Δp :kPa	$k_v:10^{-4}$ m/day	$k_v:10^{-4}$ m/day	$C_k: (0.4-0.6) e_0$										
6	1	2.0	1.77	10	200	3	6	1.03										
	2		2.5															
1	1	0.5	1.41	10	100	6	6	0.89										
	2		2.5															
2	1	1.0	1.5	10	100			6	6	0.95								
	2		2.5															
3	1	2.0	1.68	10	100					6	6	1.00						
	2		2.5															
4	1	0.5	1.4	10	50							6	6	0.90				
	2		2.5															
5	1	1.0	1.53	10	150									6	6	0.95		
	2		2.5															
6	1	2.0	1.77	10	200											6	6	1.03
	2		2.5															
1	1	0.5	1.41	10	100	12	6											0.89
	2		2.5															
2	1	1.0	1.5	10	100			12	6									0.95
	2		2.5															
3	1	2.0	1.68	10	100					12	6							1.00
	2		2.5															
4	1	0.5	1.4	10	50							12	6					0.90
	2		2.5															
5	1	1.0	1.53	10	150									12	6			0.95
	2		2.5															
6	1	2.0	1.77	10	200											12	6	1.03
	2		2.5															

Series 1: the ratio of m_{v1}/m_{v2} was fixed to be 0.67 and the ratio of k_{v1}/k_{v2} vary from 0.25 to 5.

Series 2: the ratio of m_{v1}/m_{v2} was fixed to be 1 and the ratio of k_{v1}/k_{v2} vary from 0.25 to 5.

Series 3: the ratio of m_{v1}/m_{v2} was fixed to be 1.5 and the ratio of k_{v1}/k_{v2} vary from 0.25 to 5.

4.5.4.2 Effect of non-uniform consolidation

The average degree of consolidation (DOC) were calculated using the simulated excess pore water pressures. The consolidation theory proposed by Zhu and Yin (1999) was adopted to analyze the average DOC theoretically. The representative values of k_v and m_v for each layer were evaluated by Eq. (2.26) and (2.28) corresponding to the mean void ratio, e , which was obtained at a mean effective stress estimated using Eq. (4.2). An example comparison of analytical and simulated DOCs is given in Fig. 4.26. Zhu and Yin's (1999) theory over-predicts the average DOC significantly.

For two-soil layer system under one-way drainage condition, the effect of non-uniform consolidation is mainly affected by the soil layer close to the drainage boundary. In order to back-fit the simulated average DOC for a two-soil layer system using Zhu and Yin's solution, we adopt an approach of reducing permeability, $k_{v1-n} = \beta_1 k_{v1}$ of the soil layer-1 (with drainage boundary) in theoretical analysis. The value of β_1 can be obtained when the back-fitted DOC matched with the simulated DOC by FEM at DOC = 50%. Similar to one layer cases, the back-fitted DOC can fit the simulated DOC well before the average DOC = 50%.

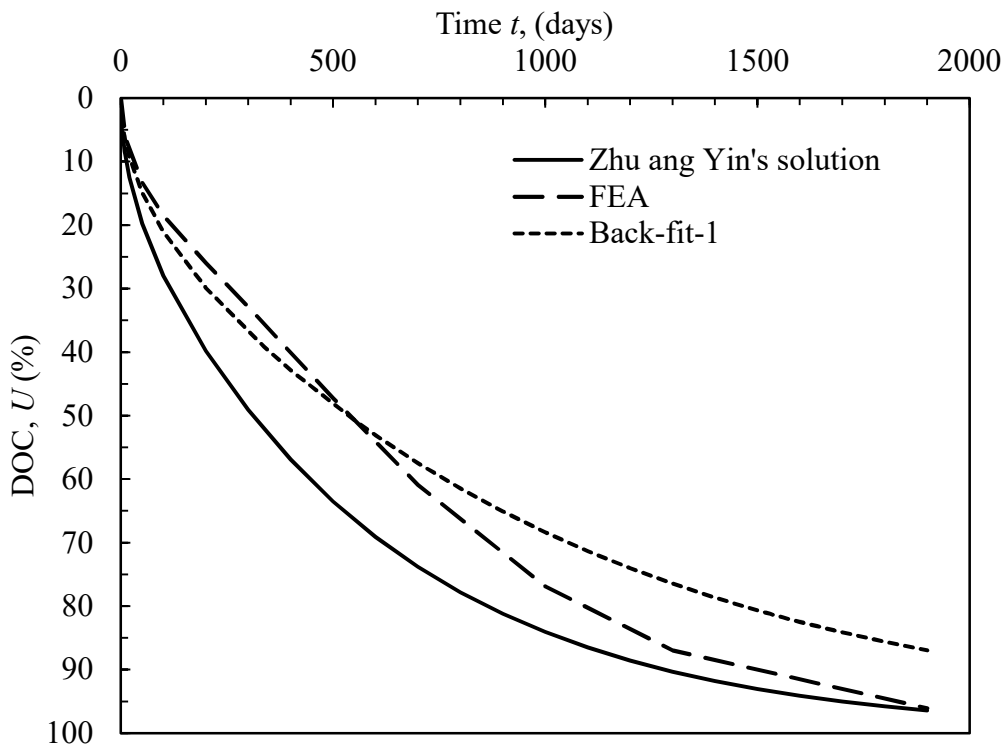


Figure 4.26 Comparison of degree of consolidation

4.5.4.3 $\beta_1 \sim \Delta e_1 / C_k$ relationship

The variation of the back-fitted values of β_1 with $\Delta e_1 / C_k$ for the two series analyzed are shown in Fig. 4.27 to 4.29, respectively. Δe_1 is the reduction of the void ratio of soil layer-1 which contains the drainage boundary. Generally, the value of β_1 decreases with the increase of $\Delta e_1 / C_k$ which indicates the bigger the value of $\Delta e_1 / C_k$, the larger the effect of non-uniform consolidation. For a two-soil layer system, the ratios of k_{v1} / k_{v2} and m_{v1} / m_{v2} will also have significant influences on the rate of consolidation. For a fixed m_{v1} / m_{v2} ,

higher k_{v1}/k_{v2} results in a smaller β_1 . If carefully checking the data in Fig. 4.27 and 4.29, it is found that for a same value of $\Delta e_1/C_k$ and k_{v1}/k_{v2} , the value of β_1 for cases with a lower value of m_{v1}/m_{v2} are larger than that with a higher value of $m_{v1}/m_{v2} = 1.5$. It indicated that compared with the soil in layer-2, the softer the soil in layer-1, the larger the effect of non-uniform consolidation.

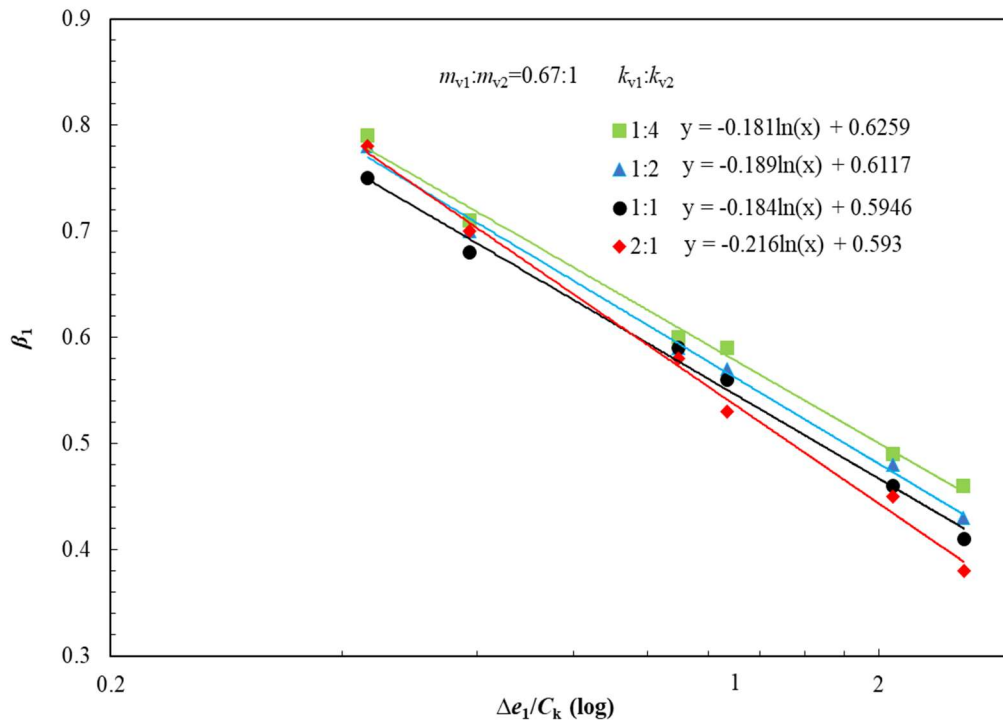


Figure 4.27 Variation of β_1 with $\Delta e_1/C_k$ for $m_{v1}:m_{v2}=0.67$

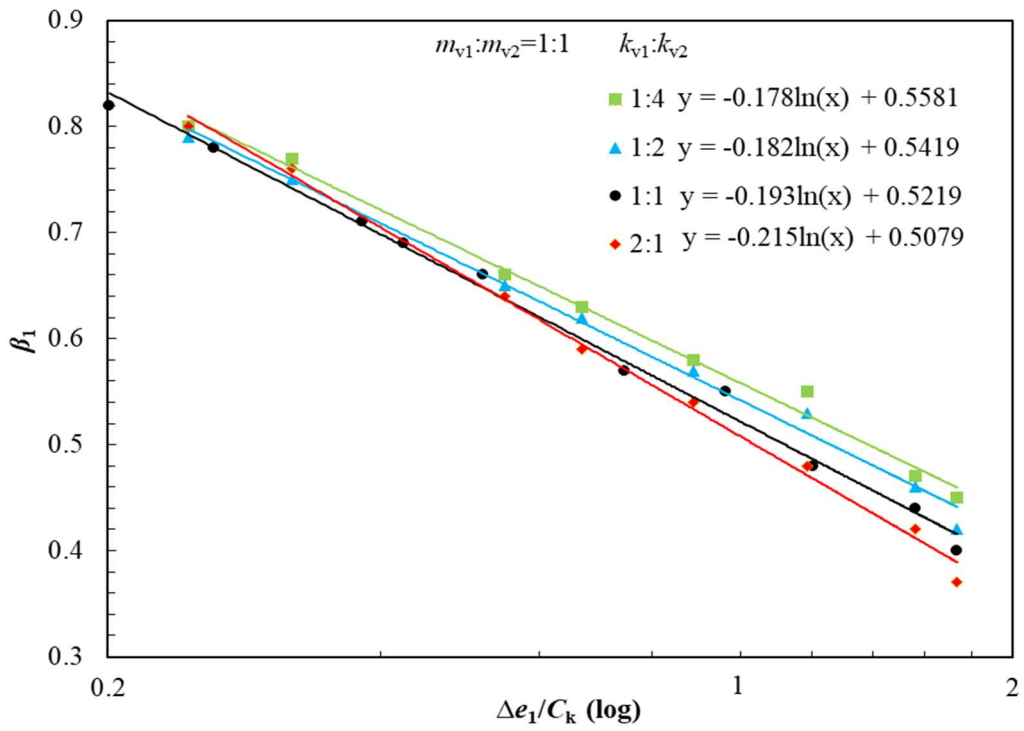


Figure 4.28 Variation of β_1 with $\Delta e_1/C_k$ for $m_{v1}:m_{v2}=1$

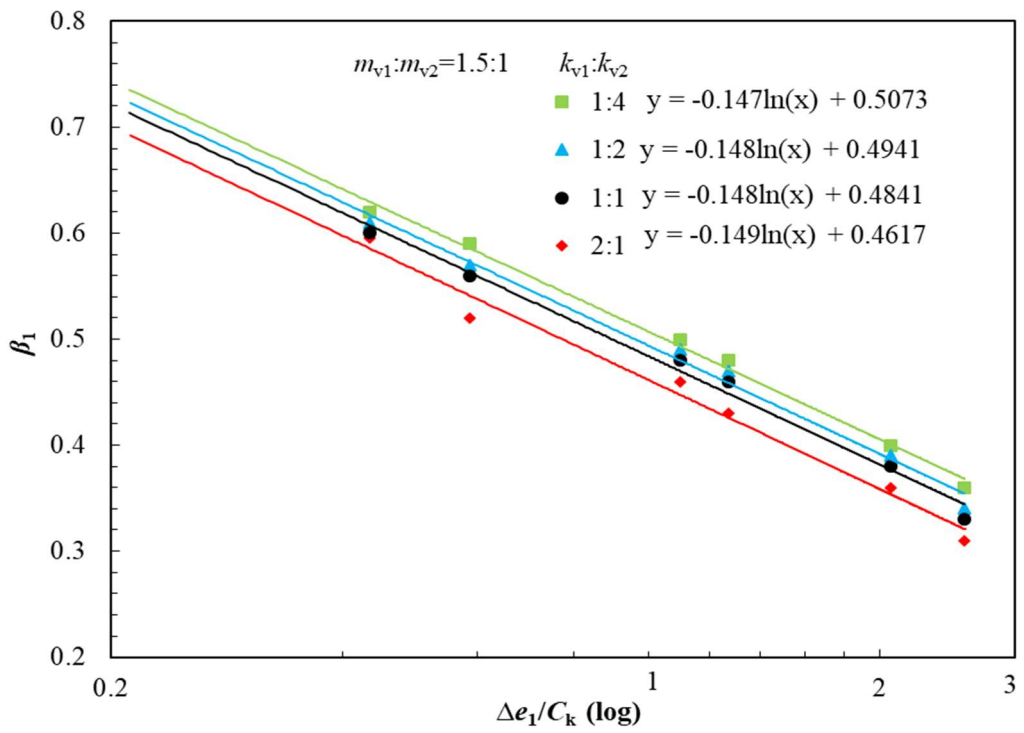


Figure 4.29 Variation of β_1 with $\Delta e_1/C_k$ for $m_{v1}:m_{v2}=1.5$

4.6 Variation of the effect of non-uniform consolidation with DOC

4.6.1 One layer system

The degree of the effect of non-uniform consolidation on the average DOC varies during the consolidation process. Normally it is more significant in the earlier stage of the consolidation and becomes less important at the later stage of the consolidation. As shown in Fig. 4.9, with a constant value of α_1 , the result of Back-fitted-1 evaluated the average DOC well for $\text{DOC} < 50\%$, but underestimated the DOC for $\text{DOC} > 50\%$ comparing with the results of FEA. The same tendency for two-soil-layer system is shown in Fig. (4.26).

To consider the effect of the non-uniform consolidation more precisely, it is proposed that for $\text{DOC} \leq 50\%$ ($T_v \leq 0.2$), using a constant value of $\alpha = \alpha_1$ (from Fig. 4.16), for $\text{DOC} \geq 93\%$ ($T_v \geq 1.0$), $\alpha = 1.0$, and for $50\% < \text{DOC} < 93\%$ ($0.2 < T_v < 1.0$), a linear reduction of α with T_v as shown in Fig. 4.30. The variation of α can be expressed mathematically by the following piecewise function:

$$\alpha = \begin{cases} \alpha_1 = -0.186 \ln \left(\frac{\Delta e}{C_k} \right) + 0.5531 & T_v \leq 0.2 \\ \alpha_1 + \frac{1 - \alpha_1}{0.8} (T_v - 0.2) & 0.2 \leq T_v \leq 1 \\ 1 & T_v \geq 1 \end{cases} \quad (4.5)$$

With the varied value of α , the simulated average DOC of the model test is named as Back-fitted-2 and plotted in Fig. 4.31, which fitted the DOC from the results of FEA well.

The procedure of using the proposed method to consider the effect of non-uniform consolidation in theoretical 1D consolidation analysis is as follows:

- (1) Calculated the value of $\Delta e/C_k$ using soil parameters and stress conditions.
- (2) Obtain the value of α_1 corresponding to the value of $\Delta e/C_k$ from Fig. 4.16.
- (3) Consider variation of α with T_v by Fig. 4.30 or Eq. (4.5).
- (4) Calculate DOC using modified coefficient of consolidation, $\alpha \times c_v$.

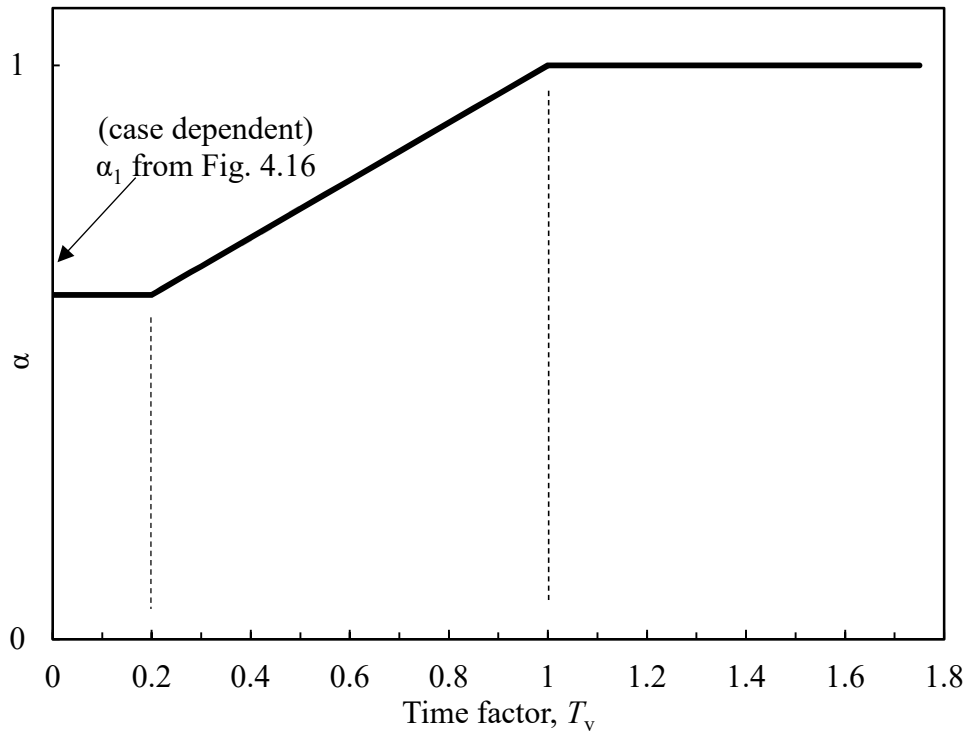


Figure 4.30 Relationship between α and time factor

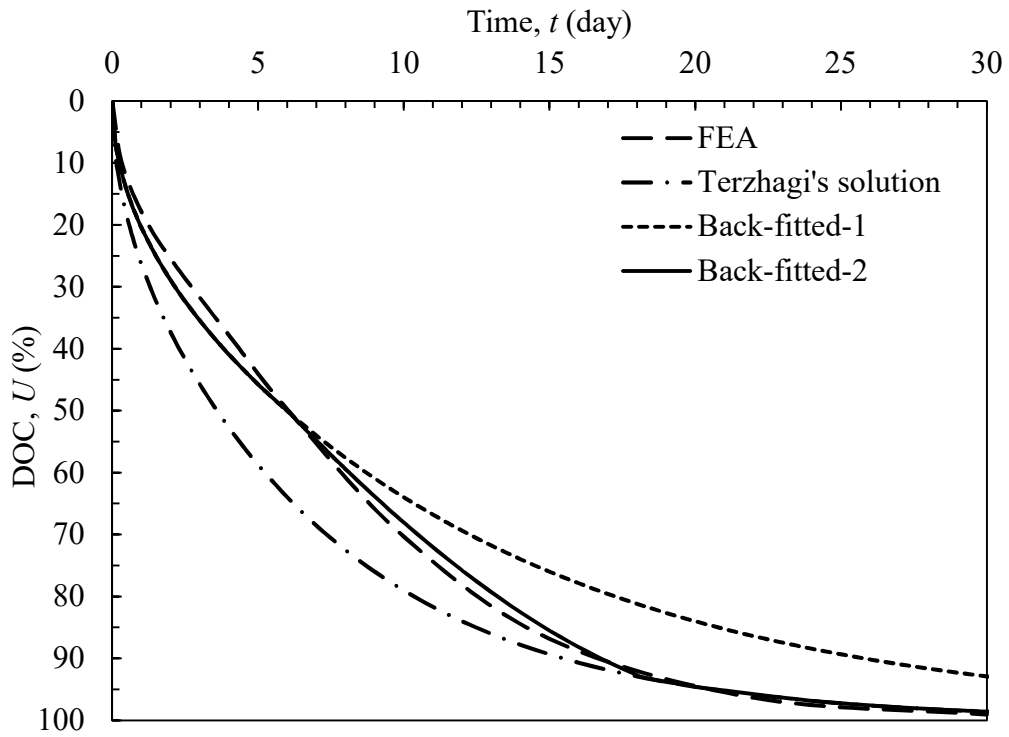


Figure 4.31 Average DOC from FEA and analytical results

4.6.2 Two-layer system

For given values of k_{v1}/k_{v2} and m_{v1}/m_{v2} , as shown in Fig. 4.27 to 4.29, the relationship between β_1 and $\Delta e_1/C_k$ can be expressed as:

$$\beta_1 = -A \ln \left(\frac{\Delta e_1}{C_k} \right) + B \quad (4.6)$$

where A and B can be linked with the values of k_{v1}/k_{v2} . From the results in Fig. 4.27 to Fig. 4.29. For $m_{v1}/m_{v2} = 0.67$, A and B can be calculated as:

$$A = 0.1478 e^{0.0972 \left(\frac{k_{v1}}{k_{v2}} \right)} \quad (4.7)$$

$$B = 0.6005 - 0.017 \ln \left(\frac{k_{v1}}{k_{v2}} \right) \quad (4.8)$$

For $m_{v1}/m_{v2} = 1$, A and B can be calculated as:

$$A = 0.1808 e^{0.0547 \left(\frac{k_{v1}}{k_{v2}} \right)} \quad (4.9)$$

$$B = 0.5236 - 0.025 \ln \left(\frac{k_{v1}}{k_{v2}} \right) \quad (4.10)$$

and for $m_{v1}/m_{v2} = 1.5$,

$$A = 0.1143 e^{0.0295 \left(\frac{k_{v1}}{k_{v2}} \right)} \quad (4.11)$$

$$B = 0.4756 - 0.027 \ln \left(\frac{k_{v1}}{k_{v2}} \right) \quad (4.12)$$

The numerical simulations was conducted with only limited values of m_{v1}/m_{v2} from 0.67 to 1.5, while it may not present all the cases. For a given value of k_{v1}/k_{v2} , β_1 can be obtained by Eq. (4.6) corresponding to m_{v1}/m_{v2} is 0.67 to 1.5. Then a simple interpolation or extrapolation is needed to calculate the value of β_1 for any other values of m_{v1}/m_{v2} .

The degree of the effect of non-uniform consolidation on the average DOC is not constant during the consolidation process. As shown in Fig. 4.26, with a constant value of β_1 , the result of Back-fitted-1 underestimated the DOC for $DOC > 50\%$ comparing with the results of FEA. The variation of effect of non-uniform consolidation on the rate of consolidation should be considered. Similar with one layer system, a piecewise function is proposed to calculated the final value of β :

$$\beta = \begin{cases} -A \ln \left(\frac{\Delta e_1}{C_k} \right) + B & T_v \leq T_{v50} \\ \beta_1 + \frac{1 - \beta_1}{(1 - T_{v50})} (T_v - T_{v50}) & T_{v50} \leq T_v \leq 1 \\ 1 & T_v \geq 1 \end{cases} \quad (4.13)$$

where T_{v50} is the time factor corresponding to $\text{DOC} = 50\%$. If using a varied k_{v1} in Zhu and Yin's solution (Eq. (2.15)), the eigen-values, λ_n will also be changed corresponding to a different value of k_{v1} . For simplicity, the eigen-value of λ_n is assumed to be constant. It has been checked that the errors involved is small. Considering the variation of the effect of non-uniform consolidation with the DOC, the back-estimated result of DOC, designated as Back-fitted-2 are plotted in Fig. 4.32 and the back-fitted DOC can match the results of FEA well.

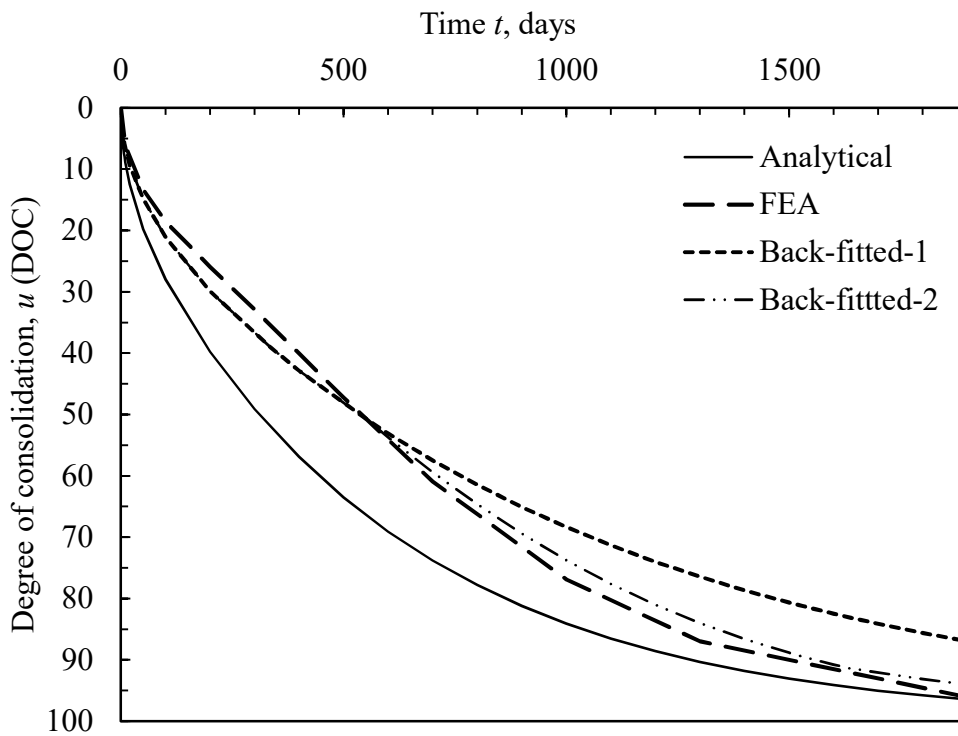


Figure 4.32 Comparison of average degree of consolidation

The procedure of using the proposed method to consider the effect of non-uniform consolidation in theoretical 1D consolidation analysis of a two-soil layer system is as follows:

- (1) Calculated the value of $\Delta e_1/C_k$ using soil parameters and stress conditions of layer-1.
- (2) Obtain the value of β_1 corresponding to the value of $\Delta e_1/C_k$ from Eq. (4.6). Consider variation of β with T_v by Eq. (4.13).
- (3) Calculate DOC using modified coefficient of permeability, $k_{v1-n} = \beta k_{v1}$.

4.7 Application of proposed method

4.7.1 One layer system

Three cases reported by Watabe et al. (2007), Davis and Raymond (1965) and Lekha (2003) respectively were analyzed by Terzhghi's solution and proposed method. The summary of the three cases are as follows:

- (1) Case of Watabe et al. (2007):

A one-dimensional consolidation test was conducted using a sample with a total thickness of 100 mm. The soil of the sample was undisturbed Ma12 clay from the seabed of Kansai International Airport at depth of 63 m. The sample consists of five inner-connected subspecimens and each one has a thickness of 20 mm. The subspecimen had an initial void ratio, $e_0 = 2.18$, compression index, $C_c = 1.05$. The sample was pre-consolidated under 39 kPa for 24 h and then under 291 kPa for 7 days. Last, the applied load was increased to 904 kPa to conduct long-term consolidation test. The vertical strain during long-term consolidation was 15%. The value of c_v evaluated from measured results of the test was also given in the reported case. The change of the reduction of the void ratio during long-term consolidation, $\Delta e = 0.44$ was estimated based on the e -log(p') curve and the vertical strain. And the value of C_k is assumed to be $0.5 e_0$. According to Fig. 4.16, the value of α_1 can be obtained. The main parameters used are listed in Table 4.10.

The DOC was analysed by Terzaghi's solution and proposed method. The variation of the effect of non-uniform consolidation with DOC was considered in proposed method. The analytical results are compared with measured average DOC in Fig. 4.33. It clearly shows that the proposed method resulted in a much better simulation of the measured results.

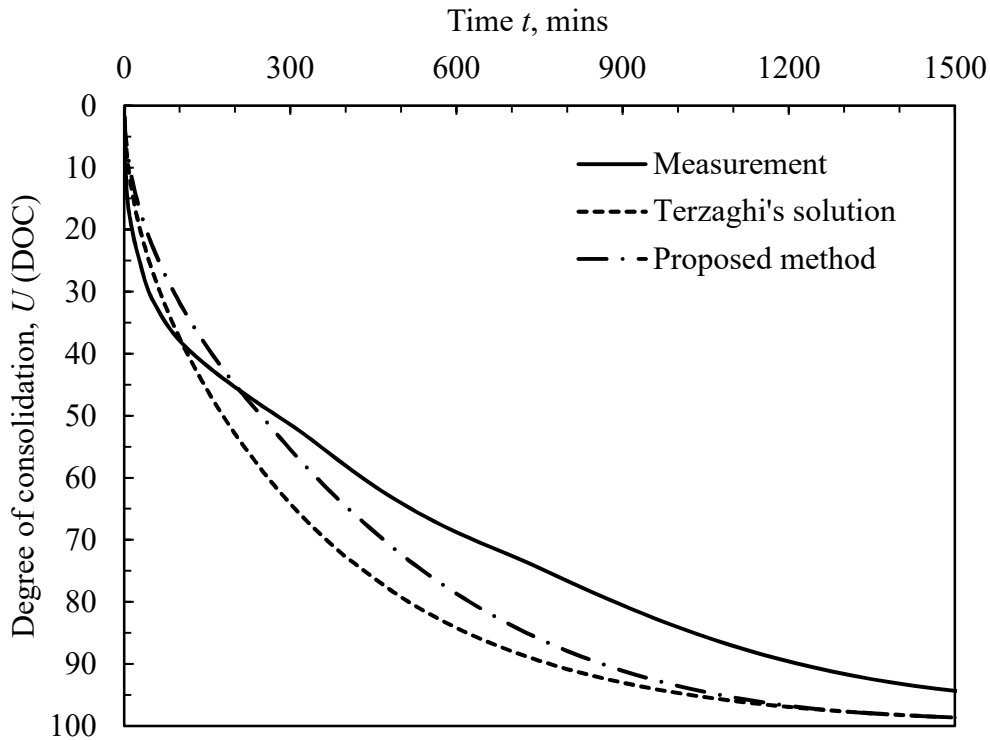


Figure 4.33 Comparison of average DOC for case of Watabe et al. (2007)

(2) Case of Davis and Raymond (1965)

One modified conventional incremental loading oedometer test with pore water pressure of the bottom measured was conducted by Davis and Raymond (1965). The soil used in the test is remould Port Kembla clay. The applied stress was from 12 kPa to 188 kPa and the value of $\Delta e = 0.762$ was measured in the test. The value of c_v and the volume of the dry soil particles (v_s) of the sample was given. The initial void ratio, e_0 corresponding to 12 kPa was calculated according to v_s . Assume the value of C_k to be 0.5 e_0 in this case, then the value of $\alpha_1 = 0.57$ was obtained from Fig. 4.16. The main parameters used are listed in Table 4.10.

By Terzaghi's theory and proposed method, the average DOC was analysed. The variation of the effect of non-uniform consolidation with DOC was considered in proposed method. While the pore pressured measured at the bottom is the maximum value along the height of the sample which can not be a representative of average pore water pressure. Here, the distribution of the pore pressure with height was assumed to be hyperbolic and

the average pore pressure was estimated as, $u = \frac{2}{3} u_{\max}$. The analytical results and measured results are compared in Fig. 4.34.

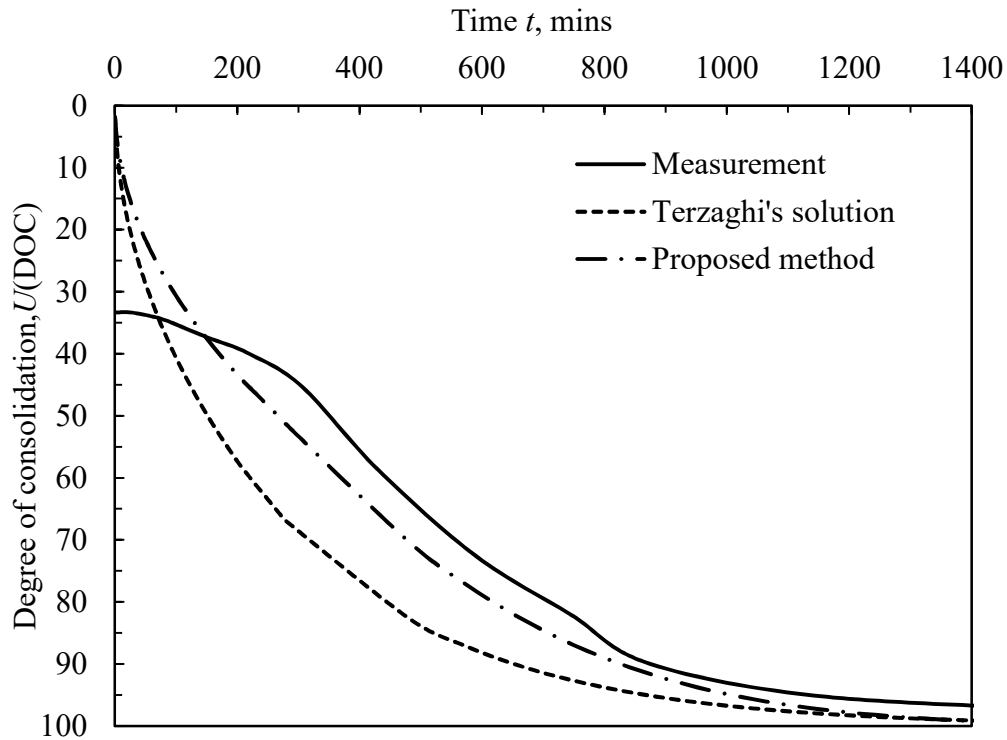


Figure 4.34 Comparison of average DOC for case of Davis and Raymond (1965)

(3) Case of Lekha et al. (2003)

Conventional IL oedometer test was conducted following the loading step of 25-50-100-200-400-800 kPa using calcium bentonite. The calcium bentonite had a value of compression index, $C_c = 0.8$ and $C_k = 0.84$. For the loading step from 200 kPa to 400 kPa, the value of c_v was given and from e - $\log(p')$ curve a reduction of void ratio, $\Delta e = 0.24$ was estimated. Then the value of α_1 can be obtained from Fig. 4.16. The main parameters used are listed in Table 4.10.

The average DOC was calculated by Terzaghi's solution and proposed method. The variation of the effect of non-uniform consolidation with DOC was considered in proposed method. The average DOC of the test was estimated through the settlement-time curve and compared with analytical results in Fig. 4.26.

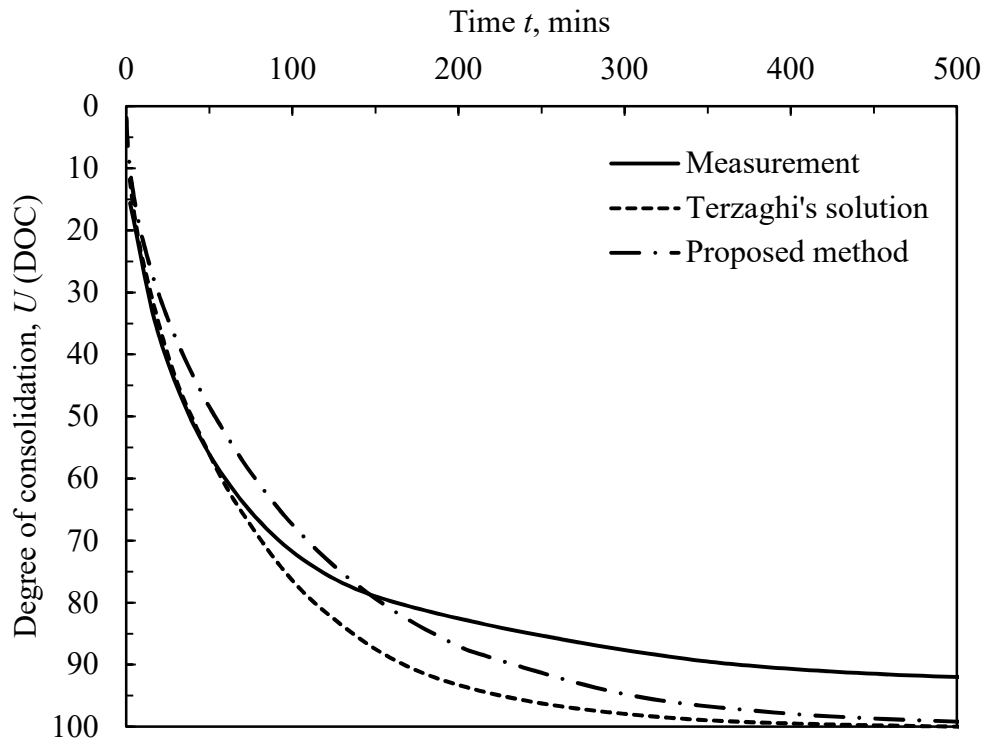


Figure 4.35 Comparison of average DOC for case of Lehka (2003)

Defining D_1 is the maximum different between DOC from Terzaghi's solution and the measurements, and D_2 is the maximum difference between DOC from the proposed method and the measurements. The results of D_1 and D_2 are shown in Table 4.10. The maximum differences of average DOC for the three cases considered were reduced significantly with proposed method. It came to a conclusion that the proposed method can give a good prediction of the average DOC.

Table 4.10: Parameters used for the cases analyzed

<p>Watabe et al.(2007) Undisturbed Ma12 clay</p>	<p>load range: 291-904 kPa c_v: 11.1 mm²/min, test result Δe: 0.44, evaluated from strain C_k: 1.09, evaluated as $0.5e_0$ α_1: 0.72 D_1: 20% D_2: 8% (0.4 D_1)</p>
<p>Davis and Ramond (1965) Remoulded Port Kembla</p>	<p>load range: 12-188 kPa c_v: 0.52 mm²/min, test result Δe: 0.762, test result C_k: 0.92, evaluated as $0.5e_0$ α_1: 0.57 D_1: 20%, measured DOC was evaluated from u_{max} D_2: 7% (0.35D_1)</p>
<p>Lekha et al.(2003) Remoulded calcium bentonite</p>	<p>load range: 200-400 kPa c_v: 0.47 mm²/min, test result Δe: 0.24, evaluated from e-log (p') curve C_k: 0.84, test result α_1: 0.79 D_1: 15% D_2: 7% (0.47D_1)</p>

4.7.2 Two-soil layer system

The proposed methods were applied to two assumed cases of numerical experiments. and the parameters used for the two cases are listed in Table 4.11. The solutions of Zhu and Yin (1999) is also adopted to analysis the average degree of consolidation for these two cases. The results of average DOC from FEA and analytical solutions are compared. In analytical solutions, the representative values of k_v and m_v for each layer were

calculated using Eq. (2.26) and Eq. (2.28) corresponding to the mean consolidation stress. From the proposed method, the value of β for case 1 and case 2 are 0.632 and 0.537 when matching DOC of FEA at 50%, respectively. The comparison of the degree of consolidation from different methods are plotted in Fig. 4.36 and 4.37 for case 1 and case 2, respectively. The variation of β with average DOC was considered by Eq. (4.13). The results from Zhu and Yin (1999) over predict the average DOC significantly. Even there are some discrepancies, it can be seen that the analytical results using the proposed method can predict the DOC very well.

Table 4.11 Parameters used in FEA and theoretical analysis

No.	Layer	C_c	e_0	p'_0 :kPa	Δp :kPa	$k_v:10^{-4}$ m/day	H :m	$C_k: 0.5 e_0$	β (matching 50%)
1	1	1.1	3.5	10	100	4.0	1.0	1.75	0.632
	2	0.7	1.3			6.0	1.0	0.65	
2	1	0.6	1.0	30	100	15.0	1.0	0.50	0.537
	2	1.2	3.8			6.0	1.0	1.90	

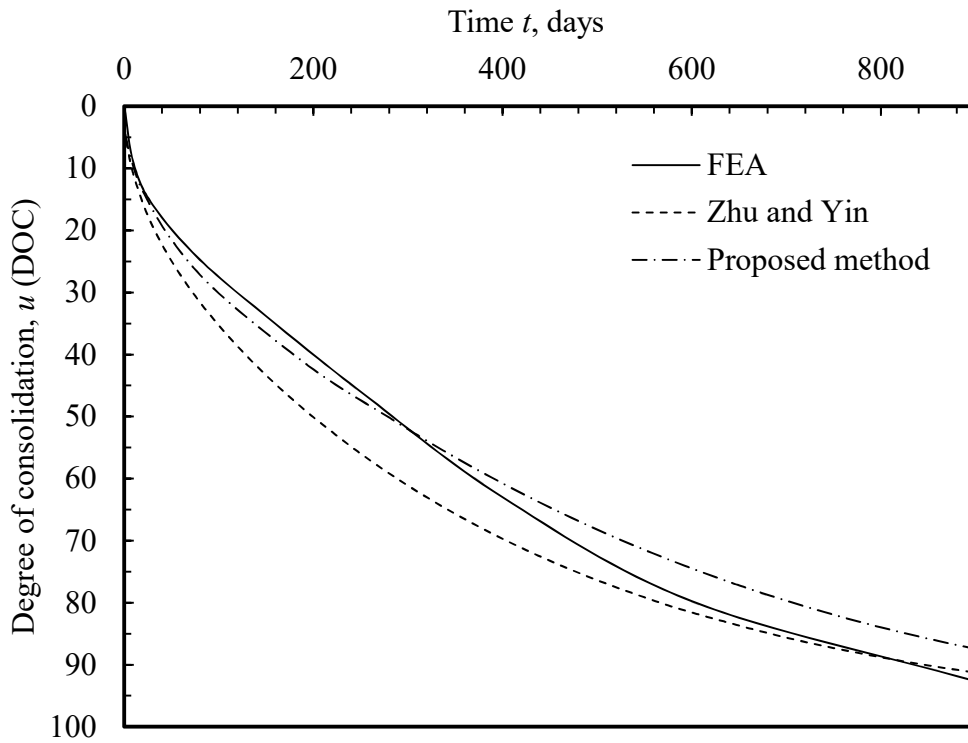


Figure 4.36 Comparison of DOC from different methods for case 1

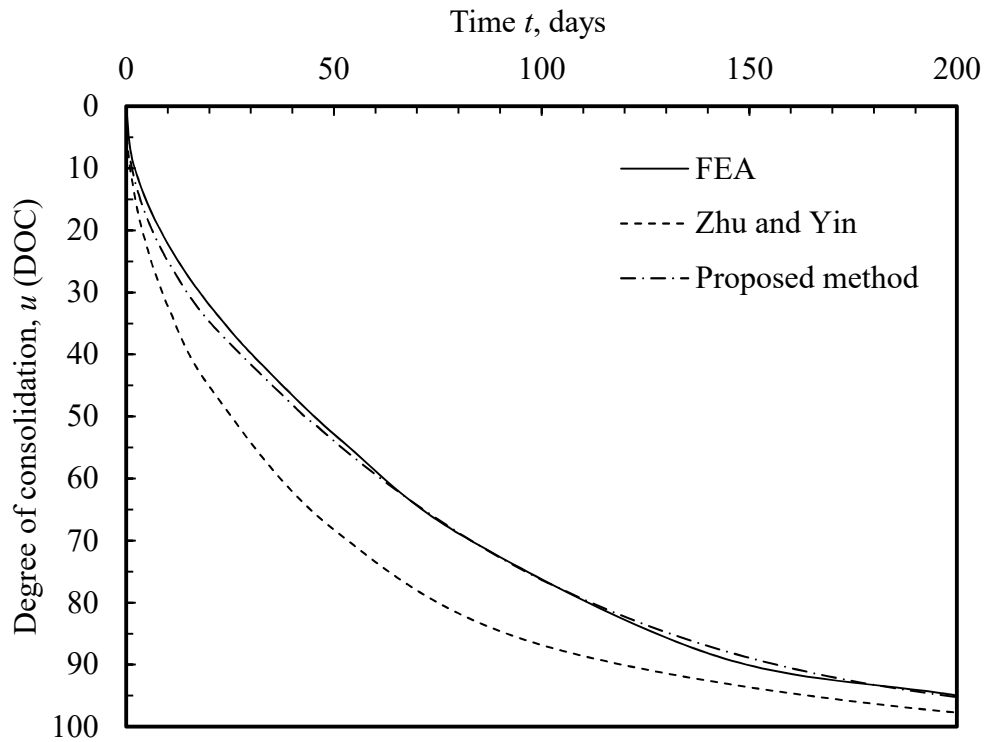


Figure 4.37 Comparison of DOC from different methods for case 2

4.8 Summary

The effects of non-uniform consolidation on the rate of consolidation of one soil layer system and two soil-layer system under one-dimensional (1D) condition were investigated through laboratory tests and finite element analysis (FEA). Based on the results of the tests and the FEA, the following conclusions can be drawn.

4.8.1 One layer system

- (1) For a 1D consolidation problem of one soil layer system, during the consolidation process DOC within a domain is not uniform, especially at the earlier stages of the consolidation. The zone near the drainage boundary always has a higher DOC than that in a zone away from the drainage boundary before DOC reaches 100%. The phenomenon of the non-uniform consolidation has a considerable effect on the rate of consolidation but the existing analytical theories do not consider it.

- (2) A laboratory 1D consolidation test was conducted and analyzed. By comparing the results of the test and the FEA, which directly considers the effect of non-uniform consolidation, with the analytical results, the effect of the non-uniform consolidation on average DOC has been confirmed.
- (3) Based on the results of the FEA, a method for considering the effect of the non-uniform consolidation into 1D theoretical consolidation analysis has been proposed. Using a modified coefficient of consolidation evaluated by the proposed method, the settlement as well as the average DOC versus time curves of the model test can be simulated well by Terzaghi's 1D consolidation theory.

4.8.2 Two-soil layer system

- (1) For a two-soil layer system with one-way drainage boundary condition, the non-uniform consolidation has a significant effect on the rate of the consolidation which was not considered by previous theories.
- (2) Numerical investigations were conducted to study the factors influencing the effect of the non-uniform consolidation on the rate of consolidation of the whole soil domain. A method was proposed to predict the DOC for a two-soil-layer system considering the effect of non-uniform consolidation. The method adopts a modified permeability, k_{v1} , of the soil layer with drainage boundary. It has been demonstrated that the average DOC of the two-soil layer system obtained by FEA can be predicted well using the proposed method.

CHAPTER FIVE

CONCLUSIONS AND RECOMMENDATIONS

5.1 Conclusions

The effect of non-uniform consolidation on the rate of consolidation for prefabricated vertical drain (PVD) induced consolidation and one-dimensional (1D) consolidation, including one soil layer system and two-soil layer system, was investigated by laboratory tests and finite element analysis (FEA). The factors influencing the effect of non-uniform consolidation are (a) initial void ratio (e_0), (b) compression index (C_c), (c) loading conditions and (d) the rate of variation of permeability with void ratio. And they were studied and evaluated quantitatively. Then the methods are proposed to predict the average degree of consolidation (DOC) considering the effect of non-uniform consolidation.

5.1.1 Effect of non-uniform consolidation on the rate of consolidation

- (1) For PVD induced consolidation:
 - (a) From large laboratory model tests, the variation of the void ratio and permeability in the horizontal radial distance have be studied. The test results indicated that the consolidation in the zone near the PVD is much faster than that in the zone near the periphery of a PVD unit cell (a PVD and its influencing zone), especially in the earlier stage of consolidation. By analyzing the results of laboratory tests and FEA, the effect of non-uniform consolidation on the average DOC of the whole soil domain was confirmed.
 - (b) The concept of equivalent ‘smear’ effect, $(k_h/k_s)_e$ (k_h and k_s are the horizontal permeability in the undisturbed and smear zone of a PVD unit cell) has been proposed to consider the effect of non-uniform consolidation. From the results of FEA, it is found that the basic soil properties and loading conditions have a significant influence on the effect of non-uniform consolidation. There is a good relationship between $(k_h/k_s)_e$ and the term, $\Delta e/C_k$. Δe is the stress increment induced

reduction of void ratio, and C_k is a constant in Taylor's permeability (k)-void ratio (e) relationship.

(2) For 1D consolidation:

- (a) Based on the results of laboratory test and FEA, it has been confirmed that the non-uniform consolidation has a considerable effect on the rate of consolidation. The effect is more significant in the earlier stage of consolidation.
- (b) For consolidation of a one soil layer system, the effect of non-uniform consolidation results in a reduction of coefficient of consolidation with a reduction factor, α . The value of α has been related to the term $\Delta e/C_k$.
- (c) For consolidation of a two-soil layer system under one-way drainage, the basic soil properties and loading stress in layer-1 which contains the drainage boundary, the ratios of k_{v1}/k_{v2} and m_{v1}/m_{v2} (k_{v1} , k_{v2} , m_{v1} and m_{v2} are permeability and coefficient of volumetric compressibility of the two soil layers and the subscript '1' means the layer contains the drainage) are all influencing the degree of effect of non-uniform consolidation. The relationship between the permeability reduction factor, β and $\Delta e_1/C_k$ (Δe_1 is the stress induced reduction of void ratio in soil layer containing the drainage boundary) for different ratios of k_{v1}/k_{v2} and m_{v1}/m_{v2} are established.

5.1.2 Proposed method to predict the average degree of consolidation

(1) For PVD induced consolidation:

Based on the results of laboratory tests and FEA, a method has been proposed to predict the average degree of consolidation (DOC) for PVD induced consolidation considering the effect of non-uniform consolidation. The effect of non-uniform consolidation is expressed by an concept of equivalent 'smear' effect, $(k_h/k_s)_e$ which is a function of $(k_h/k_s)_{e0}$ and D_e/d_w , and $(k_h/k_s)_{e0}$ can be quantified by the term $\Delta e/C_k$ as shown in Fig. 5.1. The variation of $(k_h/k_s)_e$ with DOC was also considered in the proposed method.

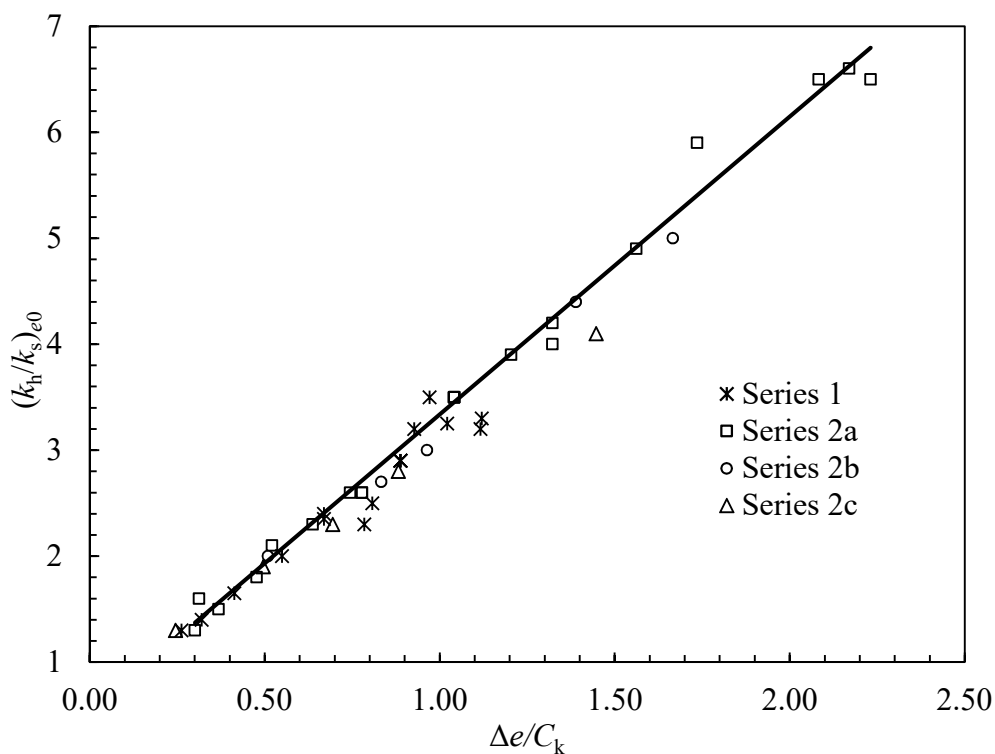


Fig. 5.1 Relationship between $(k_h/k_s)_{e0}$ and $\Delta e/C_k$ (Fig. 3.22 bis)

(2) For 1D consolidation of one soil layer system:

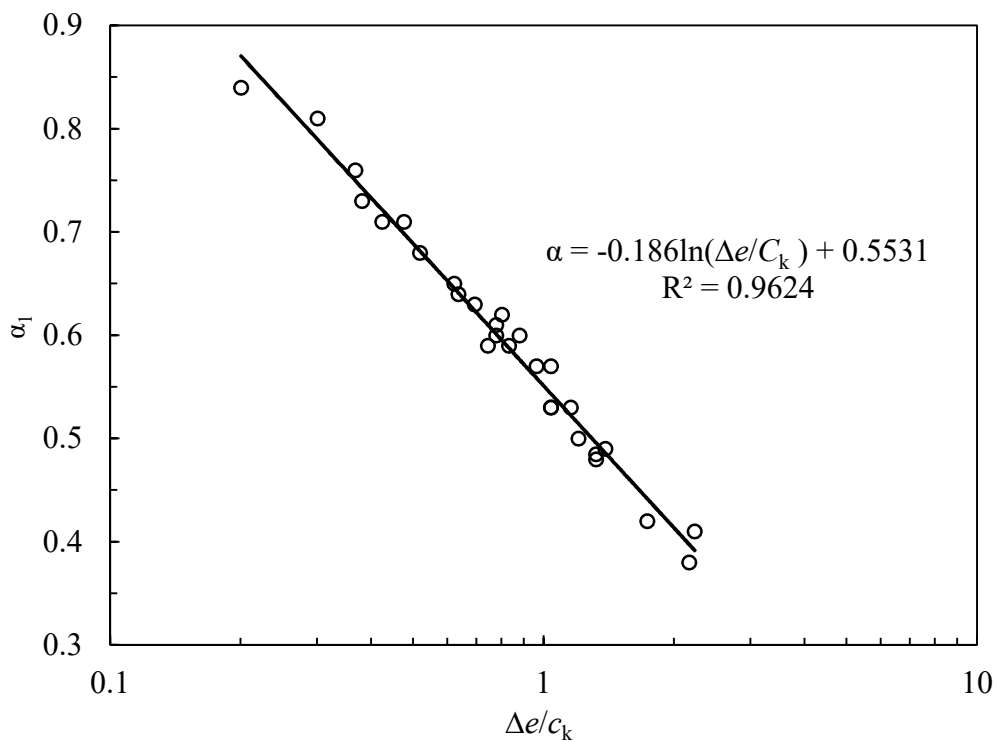


Figure 5.2 Relationship between α_1 and $\Delta e/C_k$ (4.16 bis)

A method has been proposed to evaluate the average DOC for 1D consolidation of a one soil layer system considering the effect of non-uniform consolidation from the laboratory test and FEA results. A reduction factor, α has been proposed in the method to estimate the degree of effect of non-uniform consolidation. The value of α can be evaluated by α_1 which is related with the term $\Delta e/C_k$ using Fig. 5.2 considering the variation of α with DOC.

(3) For 1D consolidation of a two-soil layer system:

Based on the results of FEA, a method was proposed to analysis the DOC for 1D consolidation of a two-soil layer system considering the effect of non-uniform consolidation. The two-soil layers in the system have the same thickness. Under one-way drainage, the effect of the non-uniform consolidation was linked with a reduction factor (β) on the permeability in soil layer with drainage boundary. The relationship of β and $\Delta e_1/C_k$ was expressed by Eq. (5.1).

$$\beta_1 = -A \ln \left(\frac{\Delta e_1}{C_k} \right) + B \quad (5.1)(4.6 \text{ bis})$$

where A and B are parameters linked with the ratios of k_{v1}/k_{v2} and m_{v1}/m_{v2} . The variation of effect of consolidation with the DOC was also considered in the proposed method.

5.2 Recommendations

The present study has proposed methods to consider the effect of non-uniform consolidation in theoretical analysis of average degree of consolidation. Some recommendations and suggestions for future study in this area are as follows:

The proposed methods are based on laboratory model tests under surcharge loading. While for a PVD improved soil with vacuum pressure, which is anisotropic consolidation pressure, whether the equivalent ‘smear’ effect induced by the vacuum pressure is the same as that of surcharge load is not clear yet, and further study on this aspect is needed.

REFERENCES

- Abu-Hejleh, A. N., Znidarčić, D. and Barnes, B. L. (1996). Consolidation characteristics of phosphatic clays. *Journal of geotechnical engineering*, **122**(4): 295-301.
- Akagi, T. (1977). Effect of mandrel-driven sand drains on strength. *Proceedings 10th International Conference on Soil Mechanics and Foundation Engineering*, Tokyo, **1**: 3-6.
- Barron, R. A. (1948). Consolidation of fine-grained soils by drain wells. *Trans. ASCE*, **113**: (2346): 718–742.
- Basak, P. and Madhav, M. R. (1978). Analytical solutions of sand drain problems. *Journal of the Geotechnical Engineering Division*, **104**(1): 129-135.
- Basu, D. and Prezzi, M. (2007). Effect of the smear and transition zones around prefabricated vertical drains installed in a triangular pattern on the rate of soil consolidation. *International Journal of Geomechanics*, **7**(1): 34-43.
- Bergado, D. T., Asakami, H., Alfaro, M. C. and Balasubramaniam, A. S. (1991). Smear effects of vertical drains on soft Bangkok clay. *Journal of Geotechnical Engineering*, **117**(10): 1509-1530.
- Bergado, D. T., Balasubramaniam, A. S., R Jonathan Fannin, R. J. and Holtz. R. D. (2002). Prefabricated vertical drains (PVDs) in soft Bangkok clay: a case study of the new Bangkok International Airport project. *Canadian Geotechnical Journal*, **39**(2): 304-315.
- Berilgen, S. A., Berilgen, M. M. and Ozaydin, I. K. (2006). Compression and permeability relationships in high water content clays. *Applied Clay Science*, **31**(3): 249-261.
- Carrier, W. D. and Bechman, J. F. (1984). Correlations between index tests and the properties of remoulded clays. *Geotechnique*, **34** (2): 211–228.
- Carrillo, N. (1942). Simple two and three dimensional cases in the theory of consolidation of soils. *Journal of Mathematics and Physics*, **21**(1): 1-5.
- Casagrande, A., and Fadum, R.F. (1940). Notes on soil testing for engineering purposes. *Soil Mechanics Series No. 8*, Publication No. 268, Harvard Univ., Cambridge, Mass., 37.

- Chai, J. C. and Miura, N. (1999). Investigation of factors affecting vertical drain behavior. *J. Geotech. Geoenviron. Engng*, ASCE, **125**(3): 216–226.
- Chai, J. C., Miura, N. and Nomura, T. (2004). Effect of hydraulic radius on long-term drainage capacity of geosynthetic drains. *Geotextiles and Geomembranes*, **22**(1-2): 3-16.
- Chai, J. C., Hong, Z. S. and Shen, S. L. (2010). Vacuum-drain consolidation induced pressure distribution and ground deformation. *Geotextiles and Geomembranes*, **28**(6): 525-535.
- Chai, J. C. and Nguyen D. Q. (2013). Geocomposite induced consolidation of clayey soils under stepwise loads. *Geotextiles and Geomembranes* **37**: 99-108.
- Chai, J. C., Horpibulsuk, S., Shen, S. L. and Carter, J. P. (2014). Consolidation analysis of clayey deposits under vacuum pressure with horizontal drains. *Geotextiles and Geomembranes*, **42**(5): 437-444.
- Chai, J. C., Jia, R., Nie, J. X., Aiga, K., Negami, T. and Hino, T. (2015). 1D deformation induced permeability and microstructural anisotropy of Ariake clays. *Geomechanics and Engineering*, **8**(1): 81-95.
- Chai, J. C., Rondonuwu, S. G. (2015). Surcharge loading rate for minimizing lateral displacement of PVD improved deposit with vacuum pressure. *Geotextiles and Geomembranes*, **43**(6): 558-566.
- Chai, J.C., Shen, S. L., Zhu, H. H. and Zhang, X.-L. (2004). Land subsidence due to groundwater drawdown in Shanghai. *Geotechnique*, **54**(2): 143-147.
- Davis, E. H. and Raymond, G. P. (1965). A non-linear theory of consolidation. *Geotechnique*, **15**(2): 161-173.
- Deng, Y. B., Xie, K. H. and Lu, M. M. (2013). Consolidation by vertical drains when the discharge capacity varies with depth and time. *Computers and Geotechnics*, **48**: 1-8.
- Dolinar, B. (2009). Predicting the hydraulic conductivity of saturated clays using plasticity-value correlations. *Applied Clay Science*, **45**: 90–94
- Fellenius, B. H. and Castonguay N. G. (1985). *The efficiency of band shaped drains: a full scale laboratory study*. Report to National Research Council and the Industrial Research Assistance Programme, 54.

- Fox, P. J. and Berles, J. D. (1997). CS2: A PIECEWISE-LINEAR MODEL FOR LARGE STRAIN CONSOLIDATION. *International Journal for Numerical and Analytical Methods in Geomechanics*, **21**(7): 453-475.
- Geng, X., Indraratna, B., Rujikiatkamjorn, C. and Kelly, R. (2012). Non-linear analysis of soft ground consolidation at the Ballina by-pass. *11th Australia - New Zealand Conference on Geomechanics: Ground Engineering in a Changing World*, 197-202.
- Ghandeharioon, A., Indraratna, B. and Rujikiatkamjorn, C. (2011). Laboratory and finite-element investigation of soil disturbance associated with the installation of mandrel-driven prefabricated vertical drains. *Journal of Geotechnical and Geoenvironmental Engineering*, **138**(3): 295-308.
- Gibson, R. E., England, R. E. and Hussey, M. J. L. (1967). The theory of one-dimensional consolidation of saturated clays, I. Finite Non-Linear Consolidation of Thin Homogeneous Layers. *Geotechnique*, **17**(3): 261-273.
- Gibson, R. E., Schiffman, R. L. and Cargill, K. W. (1981). The theory of one-dimensional consolidation of saturated clays, II. Finite nonlinear consolidation of thick homogeneous layers. *Canadian Geotechnical J.*, **18**(2): 280-293.
- Griffiths, D.V and Huang, J. (2010). One-dimensional consolidation theories for layered soil and coupled and uncoupled solutions by the finite-element method. *Geotechnique*, **60**(9): 709-713.
- Guo, S.-H. and Teng, Y.-F. (2015). Generalized Consolidation Theory for Anisotropic Saturated Soils. *International Journal of Geomechanics ASCE*, **16**(3): 06015009.
- Hansbo, S. (1977). *Geodrains in theory and practice*. Geotechnical Report from Terrafigo, Stockholm.
- Hansbo, S. (1979). Consolidation of Clay by Band-Shaped Vertical Drains. *Ground Engineering*, **12**(5): 16–25.
- Hansbo, S. (1981). Consolidation of fine-grained soils by prefabricated drains. *Proceedings of the 10th international conference on soil mechanics and foundation engineering*, Stockholm, **3**: 677–682. Rotterdam, the Netherlands: Balkema.

- Hansbo, S. (1987). Design aspects of vertical drains and lime column installations. *Proceeding 9th Southeast Asian Geotechnical Conference*, Southeast Asian Geotechnical Society, Bangkok, Thailand, **2**: 8-1–8-12.
- Holtz, R. D. and Holm, G. (1973). Excavation and sampling around some sand drains SkaEdeby, Sweden. *Proceeding Specialty Conference on Performance on Earth and Earth supported Structure*, Purdue University, **1**: 435-464.
- Holtz, R. D., Jamiolkowski, M., Lancellotta, R. and Pedroni, S. (1988). Behavior of bent prefabricated vertical drains. *Proceeding 12th International Conference Soil Mechanics and Foundation Engineering*, Rio De Janeiro, 1657-1660.
- Holtz, R. D., Jamiolkowski, M., Lancellotta, R. and Pedroni, S. (1991). *Prefabricated vertical drains: design and performance*, CIRIA ground engineering report: ground improvement. UK, Butterworth-Heinemann Ltd. 118.
- Hird, C. C. and Moseley, V. J. (2000). Model study of seepage in smear zones around vertical drains in layered soil. *Géotechnique*, **50**(1): 89–97.
- Huerta, A., Kriegsmann, G. A. and Krizek, R. J. (1988). Permeability and compressibility of slurries from seepage-induced consolidation. *Journal of Geotechnical Engineering*, **114**(5): 614-627.
- Imai, G. (1979). Development of a new consolidation test procedure using seepage force. *Soils and Foundations*, **19**(3): 45-60.
- Imai, G., & Tang, Y. (1992). A constitutive equation of one-dimensional consolidation derived from inter-connected tests. *Soils and Foundations*, **32**(2): 83-96.
- Indraratna, B. and Redana, I. W. (1998). Laboratory determination of smear zone due to vertical drain installation. *Journal of Geotechnical and Geoenvironmental Engineering*, **124**(2): 180-184.
- Indraratna, B. and Redana, I. W. (2000). Numerical modeling of vertical drains with smear and well resistance installed in soft clay. *Canadian Geotechnical Journal*, **37**(1): 132-145.
- Indraratna, B., Sathananthan, I., Bamunawita, C. and Balasubramaniam, A. S. (2005). Theoretical and numerical perspectives and field observations for the design and

- performance evaluation of embankments constructed on soft marine clay. *Elsevier Geo-Engineering Book Series*, 3: 51-89.
- Indraratna, B., Perera, D., Rujikiatkamjorn C. and Kelly, R. (2015). Soil disturbance analysis due to vertical drain installation. *Proceedings of the ICE - Geotechnical Engineering*, **168**(3): 236–246.
- Jamiolkowski, M. and Lancellotta, R. (1981). Consolidation by vertical drains: Uncertainties involved in prediction of settlement rates. *Proceedings 10th International Conference on Soil Mechanics and Foundation Engineering*, Balkema, Rotterdam, The Netherlands, **4**: 593-595.
- JSA (Japanese Standard Association) (2000). JIS A 1217. *Test method for consolidation of soils*. JSA, Tokyo. (in Japanese)
- JSA (2000b) JIS A 1227. *Test method for one-dimensional consolidation properties of soils using constant rate of strain loading*. JSA, Tokyo. (in Japanese)
- Kim, H. J., Lee, K. H., Jamin, J. C. and Mission, J. L. C. (2014). Stochastic cost optimization of ground improvement with prefabricated vertical drains and surcharge preloading, *Geomech. Eng., Int. J.*, **7**(5): 525-537.
- Karim, M. R. and Lo, S. C. (2015). Estimation of the hydraulic conductivity of soils improved with vertical drains. *Computers and Geotechnics*, **63**: 299-305.
- Karunaratne, G. (2011). Prefabricated and electrical vertical drains for consolidation of soft clay. *Geotextiles and Geomembranes*, **29**(4): 391-401.
- Lei, G. H., Zheng, Q., Ng, C. W. W., Chiu, C. F. and Xu. B. (2015). An analytical solution for consolidation with vertical drains under multi-ramp loading. *Géotechnique* **65**(7): 531–547.
- Lekha, K. R., Krishnaswamy, N. R. and Basak, P. (1998). Consolidation of clay by sand drain under time-dependent loading. *Journal of geotechnical and geoenvironmental engineering*, **124**(1): 91-94.
- Leroueil, S., Bouclin, G., Tavenas, F., Bergeron, L. and Rochelle, P. L. (1990). Permeability anisotropy of natural clays as a function of strain. *Canadian Geotechnical Journal*, **27**(6): 568–579.

- Lu, M. M., Wang, S. Y., Sloan, S. W., Indraratna, B. and Xie, K. H. (2015). Nonlinear radial consolidation of vertical drains under a general time-variable loading. *International Journal for Numerical and Analytical Methods in Geomechanics*, **39**(1): 51-62.
- Madhav, R., Park, Y. M., and Miura, N. (1993). Modelling and study of smear zones around band shaped drains. *Soils and Found.*, **33**(4): 135–147.
- Mesri, G. and Rokhsar A. (1974). Theory of consolidation of clays. *Journal of Geotechnical Engineering ASCE*, **100**(8): 889-904.
- Mesri, G. and Khan, A. Q. (2012). Ground Improvement Using Vacuum Loading Together with Vertical Drains. *Journal of Geotechnical and Geoenvironmental Engineering*, **138**(6): 680-689.
- Nagaraj, T. S., Pandian, N. S., Narasimha Raju, P. S. R. (1993). Stress state–permeability relationships for fine-grained soils. *Geotechnique*, **43**(2): 333–336.
- Oliveira, P. V. (2013). A formula to predict the effect of the variable discharge capacity of prefabricated vertical drains. *Geosynthetics International*, **20**(6): 408-420.
- Parsa-Pajouh, A., Fatahi, B., Vincent, P. and Khabbaz, H. (2014). Analyzing consolidation data to predict smear zone characteristics induced by vertical drain installation for soft soil improvement. *Geomechanics and Engineering*, **7**(1): 105-131.
- PLAXIS 2D-Version (8.2) (2012). *Plaxis material model manual*. Delft University of Technology & PLAXIS bv, Netherlands.
- Pothiraksanon, C., Bergado, D. T. and Abuel-Naga, H. M. (2010). Full-scale embankment consolidation test using prefabricated vertical thermal drains. *Soils and Foundations*, **50**(5): 599-608.
- Pyrah, I. C. (1996). One-dimensional consolidation of layered soils. *Géotechnique*, **46** (3): 555–560.
- Redana, I. W. (1999). *Effectiveness of vertical drains in soft clay with special reference to smear effect*. PhD Thesis, University of Wollongong, Australia.
- Rixner, J. J., Kraemer, S. R. and Smith, A. D. (1986). *Prefabricated vertical drains. Vol. II: Summary of Research Effort*, Federal Highway Administration Research Report No. FHWA/RD-86/169, Washington, DC, USA, 171.

- Roscoe K. H., Burland J. B., Heyman J., Leckie F. A. . On the generalized stress–strain behaviour of 'wet' clay. *Engineering plasticity*, 1968, Cambridge: 535–609.
- Rujikiatkamjorn, C., Ardana, M. D. W., Indraratna, B. and Leroueil, S. (2013). Conceptual model describing smear zone caused by mandrel action. *Géotechnique*, **63**(16): 1377–1388.
- Samarasinghe, A. M., Huang, Y. H. and Drnevich, V. P. (1982). Permeability and consolidation of normally consolidated soils. *Journal of Geotechnical Engineering ASCE*, **108**(6): 835–850.
- Sathananthan, I. and Indraratna, B. (2006). Laboratory evaluation of smear zone and correlation between permeability and moisture content. *J. Geotech. Geoenviron. Engng ASCE*, **132**(7): 942–945.
- Schiffman, R. L. (1958). Consolidation of soil under time-dependent loading and varying permeability. *In Highway Research Board Proceedings*, **37**.
- Sharma, J. S., and Xiao, D. (2000). Characterization of a smear zone around vertical drains by large-scale laboratory tests. *Canadian Geotechnical Journal*, **37** (6): 1265–1271.
- Shen, S. L., Chai, J. C., Hong, Z. S. and Cai, F. X. (2005). Analysis of field performance of embankments on soft clay deposit with and without PVD-improvement. *Geotextiles and Geomembranes*, **23**(6): 463-485.
- Stickland, A. D., Scales, P. J. and Styles, J. R (2005). Comparison of Geotechnical Engineering Consolidation and Physical Science Filtration Testing Techniques for Soils and Suspensions. *Geotechnical Testing Journal*, **28**(6): 596-604.
- Tanaka, H. (2005) Consolidation behavior of natural soil around p_c values –Inter-connected oedometer test. *Soils and Foundations*, **45**(3): 97-105.
- Tavenas F, Jean P, Leblond P and Leroueil S. (1983a). The permeability of natural soft clays. Part I: Methods of laboratory measurement. *Canadian Geotechnical Journal*, **20**(4): 629–644.
- Tavenas F, Jean P, Leblond P and Leroueil S. (1983b). The permeability of natural soft clays. Part II: Permeability characteristics. *Canadian Geotechnical Journal*, **20**(4): 645–660.

- Taylor, D.W. (1948). *Fundamentals of Soil Mechanics*. John Wiley and Sons Inc., New York.
- Terzaghi, K. (1923) Die berechnung der durchlässigkeitsziffer des tones aus dem verlauf der hydrodynamischen spannungserscheinungen. *Sitzungsberichte der Akademie der Wissenschaften in Wien, Mathematisch-Naturwissenschaftliche Klasse, Abteilung IIa*, 132: 105-124.
- Watabe, Y., Udaka, K., Kobayashi, M., Tabata, T. and Emura, T. (2008). Effects of friction and thickness on long-term consolidation behavior of Osaka Bay clays. *Soils and foundations*, **48**(4): 547-561.
- Xie, K. H., Leo, C J. (2004). Analytical solutions of one-dimensional large strain consolidation of saturated and homogeneous clays. *Computers and Geotechnics*, **31**(4): 301-314.
- Xie, K-H, Xie, X-Y, Wen J. (2002) A study on one-dimensional nonlinear consolidation of double-layered soil. *Computers and Geotechnics*, **29**(2): 151-168.
- Xu, F. & Chai, J. C. (2014). Lateral displacement of PVD-improved deposit under embankment loading. *Geosynthetics International*, **21**(5): 286–300.
- Xu, F. (2015). *Method for Predicting Lateral Displacement of PVD-improved Deposits under Embankment Loading*. PhD Thesis, Saga University, Japan
- Yoshikuni, H. and Nakanodo, H. (1974). Consolidation of soils by vertical drain wells with finite permeability. *Soils and Foundations*, **14**(2): 35-46.
- Zhu, G. & Yin, J. H. (1999). Consolidation of double soil layers under depth-dependent ramp load. *Géotechnique*, **49**(3): 415–421.
- Zeng, L. L., Hong, Z. S., Cai, Y. Q. and Han, J. (2011). Change of hydraulic conductivity during compression of undisturbed and remolded clays. *Applied Clay Science*, **51**(1): 86-93.
- Zhuang, Y. C, Xie, K. H. and Li, X. B. (2005). Nonlinear analysis of consolidation with variable compressibility and permeability. *Journal of Zhejiang University-SCIENCE A*, **6**(3): 181-187.